NATIONAL TRANSPORTATION SAFETY BOARD

Office of Research and Engineering
Materials Laboratory Division
Washington, D.C. 20594

March 5, 2004

MATERIALS LABORATORY FACTUAL REPORT Report No. 03-078

A. ACCIDENT

Place : Miami, Florida
Date : May 25, 2003
Vehicle : Cruise ship S/S Norway
NTSB No. : DCA03MM032
Investigator : Robert Ford

B. COMPONENTS EXAMINED

Header sections from boiler 23 from the cruise ship S/S Norway operated by Norwegian Cruise Lines (NCL). The sections examined were as follows (see Figure 9):

Section 1: fracture at forward end of the lower longitudinal repair weld
Section 2: mating fracture to Section 1 on the liberated piece of header
Section 3: center section of fracture adjacent to the repair weld on the upper longitudinal weld on the liberated piece
Section 4: non-fractured region of lower longitudinal weld without repair welds
Section 5: center section of the fracture adjacent to the repair weld on the lower longitudinal weld
Section 6: mating fracture to Section 3
Sections 7 and 8: fracture along the upper longitudinal repair weld in vicinity of transverse outer housing support welds (on outer diameter surface).

C. DETAILS OF THE EXAMINATION

1. On-Site Examination

On-site examinations were conducted from June 3rd through June 6th, approximately 9 to 12 days after the accident. From the on-site examination it was observed that a massive steam release occurred from the header of boiler 23 in the aft boiler room, where a large section of the header was liberated. A view of the S/S Norway boiler arrangement can be seen in the schematics in Figure 1.

The boiler is composed of three separate drums that are interconnected with tubes to exchange heat with the firebox to produce steam. The largest drum at the top of the boiler is the steam drum. The intermediate drum is the water drum (also known as the mud drum) and the smallest diameter drum is the header. The header is approximately 29 inches in diameter.[1] The header (and the other drums) are manufactured by joining two half cylinders with longitudinal welds and then welding on hemispherical caps on either end with circumferential welds. The two half cylinders are of different thickness. The thick-walled portion of the header is referred to as the tube sheet, while the thin-walled region is

referred to as the wrapper sheet. During new-make manufacture the tube sheet is tapered down to where it meets the wrapper sheet and the two are welded together at the bottom of the tapered region. The surfaces may or may not be machined to original contour following welding. The Penhoet boilers were manufactured by Chantiers de L'Atlantique in France and since the boiler company is no longer in business not all documents and manufacturing details could be obtained. The operating pressure of the boilers is approximately 900 psi or 62 bar.

Header 23

The middle images in Figure 2 show the fracture area on the header of boiler 23. The wrapper sheet fractured at the lower longitudinal weld for a length of approximately 8 feet and along the upper longitudinal weld for approximately 11 feet. Shear ligaments connected the two fractured regions along the welds. A view of the liberated and deformed portion of the header can be seen in the top image in Figure 4. The fracture surfaces of interest were cleaned by use of mineral spirits and a nylon brush prior to examination. Immediately following examination and documentation the fracture surfaces were covered with white grease for preservation.

The fracture along the lower longitudinal weld extended along the edge of what appeared to be a weld repair region (lower four images in Figure 2, upper left image Figure 3, and middle image in Figure 3). The presence of repair welds on the ship's boilers was confirmed by examination of documents.[2] The documents indicate that cracks were observed in the original equipment manufacturer (OEM) longitudinal welds in the headers, water drums, and steam drums of all four of the ship's boilers, with the first detection occurring in December 1970. The documents further indicate that the boiler drums were periodically monitored by visual and NDT methods and cracks that were detected were removed by grinding. When cracks extended below the minimum allowable wall thickness they were ground off and the walls were built back up by weld repairs. The welding procedure was created by Deutsche Babcock, approved by the classification society (Bureau Veritas), and welding was performed by Lloyd Werft or its subcontractor at the shipyard. Weld repairs were performed while the ship was in drydock in Bremerhaven, Germany in both 1987 and 1990. Specific documents indicate that the OEM welds on the header of boiler 23 were weld repaired in 1990.[a]

The top schematic in Figure 2 shows the location where the fracturing occurred along the repair welds (orange regions in schematic). The repair welds were superimposed on the original longitudinal welds. The cylindrical portion of the header (the tube and wrapper sheets) is approximately 13.0 feet long, and the entire header including hemispherical caps is approximately 16.5 feet long. The repair welds were approximately 1.5 inches wide extending along almost the entire length of the original longitudinal weld seams, except 1 to 2 feet at both ends (top images in Figure 3).

Visual examination of the fracture surface on the tube sheet side of the lower longitudinal weld revealed the presence of pre-existing cracks (dark areas of fracture surface), which

[a] The other areas that were weld repaired included the steam drum and header of boiler 21 in 1987 and the header of boiler 22 in 1990. The header of boiler 21 was re-welded in 1990 as well.

extended from the inner diameter (ID) surface and propagated through approximately 60% of the wall thickness toward the outer diameter (OD) surface (middle image in Figure 3). The pre-existing crack region was nearly continuous throughout the length of the lower longitudinal fracture. However, at both ends of this fracture, additional isolated thumbnail-shaped regions indicative of fatigue were observed (lower images in Figure 2). The weld repair region contained both longitudinal and transverse cracks. The transverse cracks were between 0.5 and 2 inches long (middle image in Figure 3).

The upper longitudinal fracture was approximately 11 feet long and was adjacent to the upper side of the longitudinal repair weld. This fracture also contained pre-existing cracking that was very similar to the pre-existing cracking on the lower longitudinal fracture, with initiation from the ID surface. However, the pre-existing cracking on the upper longitudinal fracture extended through only approximately 40% of the wall thickness toward the OD (lower right image in Figure 3). The wrapper sheet adjacent to the liberated section of the header was bowed outward toward starboard on the forward side (lower left image in Figure 3). The OD surface at the fracture locations of both the upper and lower weld was locally deformed outward.

A view of the liberated section of the header can be observed in the top image in Figure 4. This section was found intact, but contained areas of heavy damage from collision with other objects and had a transverse tear near the middle of the lower longitudinal weld. A higher magnification view of a portion of the fracture surface of the upper longitudinal weld can be seen in the lower image in Figure 4. This section shows the presence of the pre-existing cracks (dark region of the fracture). It also shows the presence of copper nuggets covering the fracture surface near the ID side (described in more detail later).

Examination of the header support feet revealed that both were lifted off their bases. The forward foot was approximately 6 inches off the base and the aft foot was approximately 5.5 inches off the base (upper left images in Figures 5 and 6). The aft foot had transverse slots and the forward foot had oblique slots (upper right images in Figures 5 and 6, respectively). The bolts on the bases were found to contain the nuts, washers, and sleeves (lower images in Figures 5 and 6). All washers were deformed upward consistent with the feet separating upward from the base. The floor plating below the ruptured area of the header was found to have been bent downward, likely a result of the steam release.

Headers 21, 22, and 24

Visual examination of the interior of the headers from the other three boilers revealed that header 22 also showed the presence of repair welds (built-up regions along the OEM weld) in the lower longitudinal weld. One weld repair region was approximately 16 inches long in-line with tubes 7-10 from the forward end. The other repair area was approximately 12 inches long in-line with tubes 5-7 from the aft end (upper image in Figure 7). Both repair welds showed visual cracking in both the transverse and longitudinal directions (middle image in Figure 7). Repair welds were not found on the upper longitudinal weld of this header, but the inside diameter surface showed the presence of circular and linear blisters/pits near this weld (lower image in Figure 7).

The headers from boilers 21 and 24 did not show evidence of repair welds visually (lack of built-up regions), though documentation showed that welding was performed on header 21 twice, in 1987 and 1990.[2] According to documentation, header 24 was never weld repaired. The internal surface of header 21 showed significant corrosion blisters, which, when flaked off, revealed internal rusting consistent with oxygen corrosion (right images in Figure 8). Header 24 showed significant flash-rusting (red rust or hematite) and also a visible water line toward the top of the drum (upper left image in Figure 8). Discussions with boiler water experts and literature indicated that marine boiler interiors are usually passivated so that the ID surface has a protective black layer of magnetite (Fe_3O_4) and not a red rust layer of hematite (Fe_20_3). These sources indicated that water chemistry is the main factor that affects the amount of magnetite present and hence the propensity for corrosion.[3]

2. Non-destructive testing of other boilers

A follow-up visit to the ship was performed June 23 through 25, 2003 for non-destructive testing (NDT) to determine if cracking was present along the longitudinal welds of the other boiler drums. The method of inspection involved screening the entire length of the welds for the presence of cracks by fluorescent magnetic particle inspection (MT) and performing an ultrasonic inspection (UT) for assessment of crack depth of any areas with indications from the MT testing. MT was initially performed since it was easier to perform than UT, and limited time was available. The work, procedure, and results are described in report FS-03-239 generated by Engineering and Inspections Unlimited, Inc. [4]

3. Laboratory Examination

Eight sections were removed from the header of ruptured boiler 23 for examination in NTSB's materials laboratory in Washington, D.C. The fracture surfaces of these sections were coated in grease before shipment in order to preserve fractographic features. The top schematic in Figure 9 shows the locations from which the sections were taken, while the lower image is an overall view of the sections after initial ultrasonic cleaning in grease solvent and brushing the samples with a nylon brush and methanol to remove the grease. Further cleaning was done with a nylon brush in a warm Alconox solution followed by ultrasonic cleaning in acetone as necessary.

3.1 Section 4- Lower longitudinal OEM weld

Section 4 was through the OEM portion of the lower longitudinal weld. Optical examination of Section 4 revealed that some portions of the ID surface had been ground at the original weld location, reducing the wall thickness in the weld area below other areas of the wrapper sheet (compare the top two images in Figure 10). The ID surface contained grinding marks in areas of reduced thickness and had overall general pitting, even on areas with grinding. Preferential longitudinal pitting and cracks were also observed on the ID surface on the portion of the weld with minimal grinding (lower right image in Figure 10). At the position where the grinding had removed the most material, the wall thickness was approximately 0.788 inch, which is below the minimum allowed thickness of 20.3 millimeters (0.799 inch) before weld repair is required[5]. In areas not affected by grinding,

the wrapper sheet was approximately 0.940 inch thick, close to the specified nominal thickness of 24 millimeters (0.945 inch).

Examination of an etched transverse metallographic section through Section 4 showed that the original weld was comprised of an initial weld pass on the ID surface, followed by at least two weld passes from the OD surface (images in Figure 11). The weld was approximately 0.4 inch wide at the ID surface and 1 inch wide at the OD surface. The weld morphology is consistent with the use of a submerged arc-welding process (SAW).

Cracking was observed on the ID in both the wrapper sheet and the OEM weld region. The most significant cracking was at the weld interface up to 0.1 inch deep. In the wrapper sheet pitting/cracking was up to approximately 0.05 inch deep.

3.2 Sections 1 & 2- Lower longitudinal weld at forward end of the fracture

Sections 1 and 2 were from the forward end of the fracture in the lower longitudinal weld. The fractures on these sections mated with each other over most of the section lengths. Optical examination of Sections 1 and 2 revealed that the fracture propagated along the starboard side of the weld repair region (wrapper sheet side). The fracture was comprised of cracks on multiple longitudinal planes joining up to form a larger crack front (top image in Figure 12).

Optical examination of the fracture surface of Section 2 (from the large liberated piece) revealed pre-existing cracking up to a maximum depth of approximately 0.55 inch in a section approximately 0.933 inch thick, measured from an area of the wrapper sheet removed from the fracture (middle image in Figure 12). At the fracture location the overstress region was necked down, reducing the fracture thickness to 0.7-0.8 inch. The fracture in the pre-existing region was dark and intersected the interior surface at a 90-degree angle. On the ID side of the fracture multiple copper-colored nuggets were observed. The nuggets were between approximately 0.070 and 0.190 inch in length (yellow arrows in the middle image in Figure 12). Additional smaller smeared areas were observed on the fracture adjacent to the ID surface. A thin layer of smeared material with a similar copper color was observed on the fracture surface of Section 2, in the region that was all shear (between the lower and upper longitudinal welds at a location not shown in the middle Image in Figure 12, but indicated by the red arrow slightly off the photograph). Close-up views of the fracture and weld repair region in Section 1 can be seen in the lower images in Figure 12.

A transverse metallographic mount through both Sections 1 and 2 confirmed the presence of a repair weld above the original weld. The repair weld was approximately 1.5 inch wide, 0.3 inch thick, and contained a heat-affected zone (HAZ) approximately 0.050 inch wide (right images in Figure 13). The repair weld was centered above the original weld and was made by at least 20 separate weld passes. The morphology of the repair weld beads was consistent with the use of a shielded metal arc welding (SMAW) process, as specified in the approved weld procedure by use of SMAW electrodes.[2] The use of multiple weld

passes and the language of the repair procedure indicates that a temper bead welding[b] technique was employed without the use of a post-weld heat treatment (PWHT).

Cracking/pitting was observed on the transverse cross sections in the wrapper sheet up to 0.1 inch deep (bottom left image in Figure 13) and in the center of the repair weld up to 0.15 inch deep (right images in Figure 13). The fracture itself was through the starboard side of the repair weld approximately 0.1 inch away from the weld interface with the wrapper sheet (lower images in Figure 13).

Baseline micrographs of the tube sheet, wrapper sheet, and original weld can be seen in Figure 14 at varying magnifications. Both sheets show a banded structure consisting of ferrite layers (white regions) and pearlite layers (a mixture of ferrite and lamellar cementite which appears dark). The original weld appeared to have a lower volume fraction of pearlite compared to either sheet. Additional micrographs of the OEM weld HAZ, repair weld, and associated HAZ can be seen in the images in Figure 15. The original weld did not appear to show a HAZ at the interface with the wrapper sheet (top right image in Figure 15), whereas a HAZ approximately 0.010 inch thick is present at the weld interface with the tube sheet (top left image in Figure 15). The HAZ from the repair weld was approximately 0.050 inch thick (lower right image in Figure 13). The repair weld itself showed a columnar microstructure with a Widmanstatten morphology indicative of rapid cooling.

Examination of the microstructure in the tube sheet, wrapper sheet, and welds at high magnification did not show the presence of significant amounts of carbide precipitation at grain boundaries or grain boundary voiding indicative of creep damage.

From the metallographic mount it could be observed that the fracture initiated at the base of very large corrosion pits and then propagated through the repair weld and wrapper sheet in a transgranular manner (images in Figure 16). Additional large pits with crack-like features connecting them were observed in the wrapper sheet adjacent to the repair weld (top image in Figure 17) and in the repair weld itself (lower image in Figure 17).

Copper Deposits Found on Section 2

The yellow arrows in Figure 12 indicated the copper colored nuggets were found on the fracture surface of Section 2. A small section of the nugget, identified as Piece A in Figure 12, was removed from the fracture by light hand forces, ground slightly in one area and examined in the SEM as shown in the top image in Figure 18. The piece was rounded on the interior side of the crack (side visible in Figure 18). The side exposed to the ID surface was flat. Energy dispersive spectroscopy (EDS) identified the material as being almost pure copper with the addition of small amounts of iron, silicon, and calcium, likely from debris on the surface of the nugget (EDS 1- Figure 19).

A metallographic mount was made by polishing into the ID face of the sample (the flattest surface). The microstructure was duplexed and banded, consistent with highly wrought

[b] Temper bead welding is a welding technique that is used when PWHT can't be performed or is impractical. This technique uses successive weld passes of varying size and with varying heat input to refine and temper the grain structure of the previous weld bead or layer.

material (lower image in Figure 18). X-ray fluorescence spectroscopy (XRF) compositional analysis[c] confirmed that it was almost pure copper (XRF1- Figure 19).

SEM examination and EDS analysis of selected areas on the fracture surface of Section 2 revealed that on the interior of the fracture (away from either the ID or OD surfaces) and at some of the locations along the ID surface deposits of almost pure copper were observed (lighter gray areas in Figure 20, EDS 3 in Figure 21). Deposits rich in lead (white regions in Figure 20- EDS 2 in Figure 21) were observed on top of portions of the copper deposits and, in some areas, directly on the fracture surface adjacent to the copper deposits. The lead and copper regions were separate and EDS analysis of multiple areas did not show any location where the copper and lead were mixed together. In the interior of the fracture the deposits appeared smeared on to the fracture. An overall EDS analysis of one of the interior smeared areas showed the presence of lead and copper, though still separate materials (lower image in Figure 20, EDS 4 in Figure 21).

3.3 Section 5- Lower longitudinal weld at middle of fracture

Section 5 was from the approximate middle of the length of the fracture along the lower longitudinal weld. The fracture on this section propagated along the starboard side of the repair weld (top image in Figure 22). The fracture was comprised of cracks on multiple longitudinal planes joining up to form a larger crack front. The fracture surface showed pre-existing cracks with multiple origins initiating from the ID surface and continuing to a depth between approximately 0.45-0.55 inch, in a section approximately 0.940 inch thick in the wrapper sheet removed from the fracture (lower image in Figure 22). At the fracture location the wrapper sheet was reduced to 0.8-0.85 inch thick by necking.

SEM examination of the fracture surface revealed that the fracture near the ID surface was pitted (left and lower right images in Figure 23). From the pits thumbnail shaped fatigue arrest marks were observed propagating toward the OD. The arrest marks extended to a depth of approximately 0.1 inch. The fracture continued in a flat, transgranular manner to the final fatigue depth of approximately 0.45 to 0.55 inch. Beyond that point rough features with ductile dimples indicative of tensile overstress were observed. All along the fatigue fracture secondary micro-cracking was observed (left and top right images in Figure 23). SEM examination of the interior of one of the corrosion pits is shown in the top image in Figure 24. Within the pit very small circular deposits less than 0.0002 inch in diameter were observed (white spots). Compositional analysis of the white spots showed that they were composed primarily of copper, with the addition of iron, likely from the base metal (EDS 5- Figure 24). The fracture surface composition was primarily composed of iron, with traces of calcium, sulfur, phosphorus, silicon, aluminum, zinc, and oxygen (EDS 6- Figure 24).

A transverse metallographic section through Section 5 confirmed the presence of a repair weld region on the original weld. The repair weld was slightly off-center of the OEM weld (images in Figure 25), compared to the location shown in Section 1 (images in Figure 13). In this mount longitudinal cracking was observed on the tube sheet (port) side of the repair weld to a depth of approximately 0.15 inch and in the center of the repair weld to a depth of

[c] Work performed at Federal Bureau of Investigations (FBI) materials laboratory in Quantico, Virginia.

0.060 inch. The fracture propagated through the starboard side of the repair weld and in the wrapper sheet.

The back side of the metallographic mount was ground parallel to the face shown in Figure 25 until a flat plane through the mounted piece was created. This allowed macro-hardness measurements to be taken with metal-to-metal contact between the section and the hardness machine anvil. An average hardness of HRB 87 was obtained in the tube sheet, HRB 92 in the wrapper sheet, HRB 80 in the original OEM weld, HRB 97 in the repair weld, and HRB 106[d] in the repair weld HAZ. The hardness locations on the mount can be seen in the lower image in Figure 25. Since the original material specification was not known a hardness comparison could not be made with a specification. However, the hardness readings are typical for low carbon steel of the current composition (shown later).

A longitudinal micrograph through the weld repair in Section 5 showed that in a 2 inch long section six transverse cracks were observed, with an average spacing of approximately 0.33 inch (images in Figure 26). At this location the transverse cracks ranged in depth from 0.12 to 0.2 inches. Two of the six cracks extended beyond the repair weld into the tube sheet. The cracks were perpendicular to the surface with significant pitting near the ID surface. When one of the cracks was opened up in the laboratory a dark thumbnail was observed. These features are consistent with fatigue cracks.

The results of quantitative compositional analysis by spark testing performed by Stork Laboratories of the thin plate (wrapper sheet), thick plate (tube sheet), original weld, and weld build-up (repair weld) are shown in Appendix A. The original manufacturing drawings stating the material specification requirements were not available for review. However, documentation showed the material to be 19Mn5[6] or NF A36-205 A52.[7] According to international conversions these steels are similar to European specification DIN 17155 steel and ASTM A516 grade 70 steel. Table 1 below summarizes some of the results from the chemical analysis along with the requirements of some pressure vessel steel specifications.

Table 1: Compositional analysis of samples.

*depending on thickness	Chemical composition (percent)						
	Carbon	**Manganese**	**Phosphorus**	**Sulfur**	**Silicon**	**Molybdenum**	**Chromium**
Tube Sheet	0.21	1.12	0.025	0.03	0.23	0.46	0.09
Wrapper Sheet	0.2	1.26	0.014	0.02	0.19	0.66	0.11
Original Weld	0.08	1.3	0.021	0.025	0.42	0.18	0.04
Repair Weld	0.06	1.23	0.016	0.005	0.32	0.51	0.03
19Mn5	0.17-0.22	1.00-1.30	0.04 max	0.04 max	0.30-0.60	-	0.3 max
A516- Grade 70	0.28/0.30* max	0.79-1.3	0.035 max	0.035 max	0.13-0.45	-	
A302- Grade A	0.20/0.25* max	0.87-1.41	0.035 max	0.035 max	0.13-0.45	0.41-0.64	

The tube and wrapper sheet appear to meet the compositional requirements of 19Mn5 or A516 grade 70 steel, except for the presence of elevated levels of molybdenum. Neither specification calls for the presence of molybdenum. According to specification A516 the

[d] The reading may not be entirely accurate as the HRB scale is only valid up to HRB 100. The appropriate scale (HRC) would have created too large of an indent in such a localized area.

maximum allowable amount of molybdenum is 0.12% for the heat analysis and 0.13% for the product analysis.[8] A search of material specifications shows that the tube and wrapper sheet compositions most closely match A302 grade A steel. Molybdenum is a potent alloying element for increasing the hardenability[e] of an alloy. The weld material cannot be compared since these specifications are intended for wrought material. The consumable electrodes used for the repair welds were SH Schwarz 3,[2] which are comparable to E7018 low hydrogen electrodes. Also, from the compositional analysis, it was found that no significant hydrogen was present in any of the samples (all had levels below 2 parts per million).

3.4 Sections 3 and 6- Upper longitudinal weld at middle of fracture

Sections 3 and 6 were from the approximate middle of the length of the fracture along the upper longitudinal weld. Optical examination of these sections revealed that the fracture propagated along the starboard side of the repair weld (closest to the tube sheet). The fracture was comprised of cracks on multiple longitudinal planes joining up to form a larger crack front (top image in Figure 27).

On the fracture surface copper nuggets were observed on the ID side of the fracture of Section 3 and were not observed on the mating fracture surface of Section 6 (see yellow arrows in Figure 27). The copper nuggets were present on-scene during the field investigation as shown in the lower image in Figure 4. However, they were not noticed initially, but were discovered during the detailed examination in the laboratory. Review of the photographs of the fracture surfaces from the on-scene examination did not reveal any additional nuggets in other areas than the ones on Sections 2 and Section 3. Reportedly, no copper nuggets were observed in the drums of the other boilers.[f] Only fine particulates were observed from mechanically cleaning the drum interiors, a fraction of which was copper in color.

Examination of mating fracture surfaces (Sections 3 and 6) revealed pre-existing cracking with multiple origins from the ID surface to a depth of between approximately 0.3 and 0.4 inch in a section approximately 0.954 inch thick in the wrapper sheet removed from the fracture (middle and lower images in Figure 27 and images in Figure 28). The wrapper sheet width was necked down to a thickness of approximately 0.65 inch at the fracture. One area adjacent to the repair weld on the wrapper sheet side of the weld was reduced by grinding to a thickness of approximately 0.81 inch (measurement not completely accurate due to some necking present at this location). This thickness is above the minimum thickness of 20.3 millimeters (0.799 inch) allowed before weld repair is required.[5]

SEM examination of both fracture halves revealed that the cracking initiated at the ID surfaces at the base of very large corrosion pits (images in Figure 29 and 30). From these regions visible semi-circular fatigue arrest marks were observed to a depth of

[e] Hardenability is a metallurgical term describing the ease of forming martensite in a ferrous alloy in the structure when quenched from above the upper critical temperature. The higher the hardenability the easier it is to form martensite (a strong, hard, brittle phase in steel).
[f] Discussions with metallurgist retained by NCL to participate in the party investigation. The metallurgist visited the ship on behalf of NCL while it was in drydock for repairs in Bremerhaven, Germany on October 27-29, 2003.

approximately 0.14 inch. The fracture continued in fatigue to a depth between approximately 0.3 and 0.4 inch, before transitioning to tensile overstress.

A transverse metallographic mount though both Sections 3 and 6 confirmed the presence of a repair weld on the upper longitudinal weld (images in Figure 31). The repair weld was not centered relative to the original weld. Grinding had reduced the thickness of the wrapper sheet down to approximately 0.78 inch on the side of the repair weld further from the tube sheet. This thickness is below the minimum thickness of 20.3 millimeters (0.799 inch) allowed before weld repair is required.[5] The weld repair was formed from at least 20 separate passes. The fracture surface was found to have extended through the weld/tube sheet interface and propagated down the middle of the original OEM weld.

Copper Deposits Found on Section 3

On Section 3 (from the liberated portion of the header) semi-continuous copper nuggets were observed along a 2.5 inch region of the fracture on the ID surface (upper and lower images in Figure 32). These nuggets can be seen in the photographs in Figure 27, on the cross section in Figure 31, and in closer views in Figure 32. On the ID surface the nuggets were flat, flush with the ID surface of the header, and contained transverse marks consistent with grinding marks (middle left image in Figure 32). On the ID surface smaller amounts of copper were observed inside some of the corrosion pits adjacent to the large copper nuggets found on the fracture surface (middle left image in Figure 32). On the interior side the copper nuggets were rounded and contained longitudinal cracks (middle right and lower images in Figure 32). When both fracture halves were put together it appeared that the nuggets matched the fracture contours very closely (upper image in Figure 32). The nuggets were up to approximately 0.1 inch wide and were up to approximately 0.09 inch deep into the crack. SEM examination confirmed that the nuggets were rounded on the interior side and contained many longitudinal cracks throughout (upper images in Figure 33). These nuggets were confirmed by EDS analysis to be composed of almost pure copper (EDS 8- Figure 33). An EDS spectrum of the base metal is shown in EDS 7 in Figure 33. Optical and SEM examination of a transverse cross-sectional metallographic mount through the copper nugget on the fracture of Section 3 (Figure 31) showed a banded, wrought structure, which contained many longitudinal cracks on the interior side adjacent to the fracture surface (images in Figure 34).

Figure 35 summarizes the location where all copper nuggets were observed on the fracture surfaces of the sections removed from the header along the upper and lower longitudinal welds, in addition to lead on the lower longitudinal weld (see blue arrows).

3.5 Sections 7 and 8- Upper longitudinal weld near outer wall support welds.

Sections 7 and 8 were from the upper longitudinal weld on the liberated piece of the header. The liberated piece of the header at sections 7 and 8 was also fractured from vertical structural plates (outer housing supports) that had been welded to the OD surface of the header at these sections, as shown by the green bars in Figure 9. The examination of these sections was limited to optical examination after cleaning. The longitudinal fractures on these sections showed similar fatigue cracking initiating from the base of pits

on the ID surface. No evidence of copper nuggets was found visually. The ID surface of these samples contained many transverse cracks in the wrapper sheet in a region removed from the repair weld. However, the samples were bent toward the OD surface, where the large vertical welds from the outer housing supports were located (green boxes shown in Figure 9).

4. Laboratory Experiments

Experimental setup: An attempt was made in the laboratory to replicate the overall look, microstructure, composition, and hardness of the copper nuggets observed on the fracture surfaces of the upper and lower longitudinal welds. To this end copper wire and copper refrigeration line (both almost pure copper) were forced into simulated cracks formed by using a band-saw and inserting cuts in the surface. The overall look, microstructure, and hardness were documented and compared to what was found on the accident pieces. Various methods were used to introduce the copper into the simulated cracks as follows:

- copper wire was hammered into the crack (test 1)
- the base metal was pre-heated with an oxy-acetylene torch and then copper wire was melted-in (test 2)
- copper wire was hammered-in and then both the base metal and copper were heated, but without melting the copper (test 3)
- the base metal was pre-heated with an oxy-acetylene torch, copper wire was melted-in, and when the copper cooled it was hammered further into the crack (test 4)
- the base metal was pre-heated with an oxy-acetylene torch, copper wire was melted-in, and then the copper was hammered while hot (test 5)
- refrigeration line was hammered-in and ground flush (test 6)

A view of how the copper was hammered into the cracks and ground is visible in Figure 36. Views of how the copper looked inside the crack after the first five tests were performed are visible in Figure 37 (after opening up the simulated cracks). Laydown metallographic mounts of the copper from the first five tests are shown in Figure 38, along with the structure from Piece A for comparison. A view of the copper refrigeration line from test 6 (after removing it from the simulated crack) can be seen in Figure 39, while a longitudinal metallographic mount through the material can be seen in Figure 40 at varying magnifications.

Rockwell B hardness measurements (converted from Knoop readings) taken from the metallographic mounts of all six tests and the copper nugget (Piece A) from Section 2 on the ship are shown in Table 2 below.

Table 2: Hardness Readings

	Hardness (HRB)
S/S Norway Piece #2	73
Electrical Wire	
baseline (worked)	<43
worked (test 1)	56
worked + heat (test 3)	<<43
cast (test 2)	<<43
cast + work cool (test 4)	56
cast + work hot (test 5)	<<43
Refrigeration line	
baseline (worked)	<43
worked (test 6)	65-72
worked + heated	49-60

Experimental Results:

The macroscopic features,[g] microstructure,[h] and hardness from the copper nuggets on the ship hardware were compared to the findings from the laboratory experiment. The results of the comparison are as follows:

1) The cast (melted) copper wire (tests 2, 4, and 5 in Figure 37) showed rounded internal features, but had splatter on the crack interior that was not found on the samples from the ship. Examination of the micrographs showed that the cast structure showed internal porosity and much larger, strain free grains (test 2, 4, and 5 on Figure 38) compared to the wrought structure on the S/S Norway (lower right image in Figure 38). The cast structures did not appear to match the structure of the copper nuggets.
2) Comparison of the wrought structure produced by hammering the copper into the simulated crack showed that the macroscopic features of the copper from test 1 and 3 were not very rounded and no evidence of the longitudinal cracking was observed. The microstructure of the worked wire (test 1) was much closer in appearance to the ship sample than the cast structure. No internal porosity was observed and the grains were finer and were more worked than the cast structure. However, no significant banding was observed and the structure was not worked enough to say they were similar (Figure 38). The worked structure that was then heated (test 3) showed large, strain-free, recrystallized grains adjacent to the smaller worked grains. The structures from test 1 and test 3 did not match the structure on the S/S Norway (Figure 38), though the structure from test 1 was closer in appearance than that produced by casting.
3) To produce a higher level of work in the structure, copper refrigeration line was hammered into a simulated crack (test 6). When this was done the copper internal to the crack showed some rounded features and some longitudinal cracking (images in Figure 39) similar to what was observed on the S/S Norway nuggets, though to a lesser extent. Examination of the structure showed that the highly worked areas of the tube appeared to show significant banding, was

[g] The ship nugget macroscopic features can be seen in Figures 32 and 33
[h] The ship nugget microstructures can be seen in the lower image in Figure 18 and in Figure 34.

duplexed, and had highly worked grains similar in appearance to the ship sample (Figure 40).

4) When both the copper wire and refrigeration line were worked into the cracks (not cast), the copper never filled a significant portion of the crack; it only filled approximately 10-30% of the crack depth (see middle image in Figure 36, middle left and top left images in Figure 37, and top image in Figure 39). The copper nuggets on the ship only extended to a maximum depth of approximately 0.090 inch, in a cracked area that extended to a depth of 0.4 inch (Section 3) or 0.55 inch deep (Section 2) at the time of the fracture. The copper experiments in the laboratory filled the simulated cracks to a similar degree as was observed on the ship nuggets.
5) The hardness measurements from Table 2 showed that the copper nuggets on the fracture surface were highly worked with a hardness of HRB 73. Hardness measurements from the six tests showed that the cast copper never exceeded HRB 56. The copper wire as-received was soft with a hardness of less than HRB 43, however, when hammered into the crack it elevated to HRB 56. The refrigeration line was also soft in the as-received condition (less than HRB 43), but it was worked up to HRB 72, similar to the S/S Norway nugget.

William R. Rossey Jr.
Materials Engineer

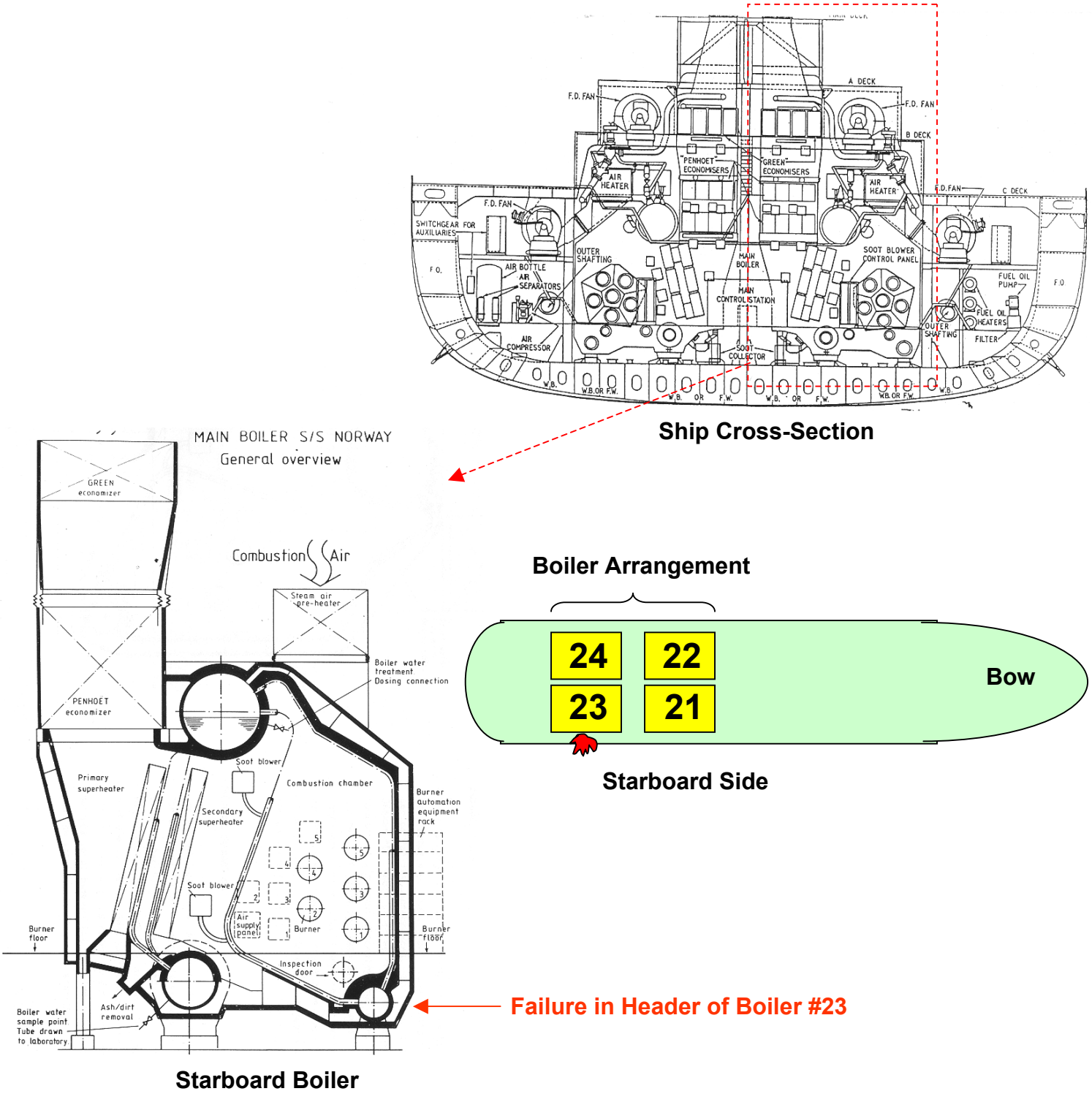

Figure 1: Cross-sectional schematic of the ship in the boiler area (top right image), of a boiler (lower left image) and a top-down view of the boiler arrangement in the ship (lower right image).

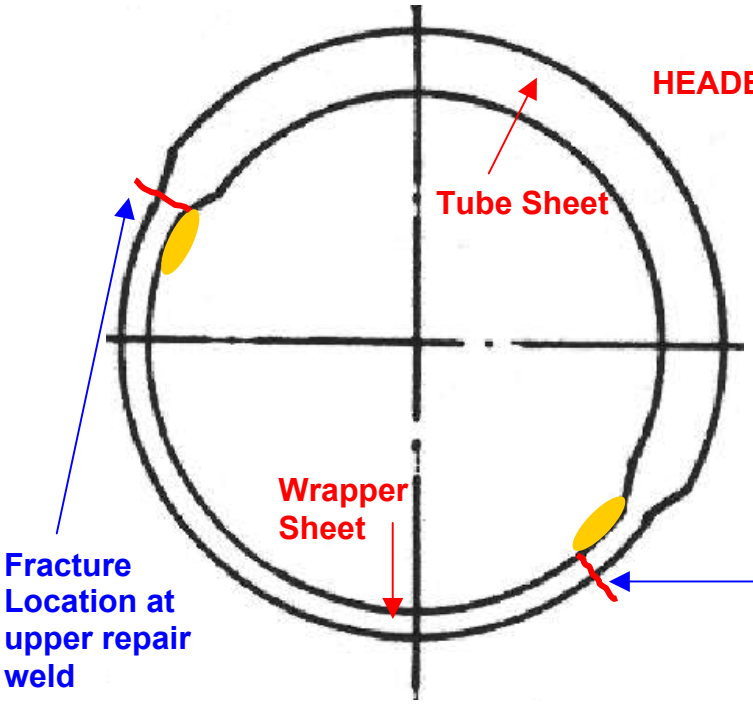

Figure 2: Overall views of the fractured header from boiler 23 (middle two images). The upper schematic shows the location of fracturing along the longitudinal welds. The lower two images show the fracture surface of the lower longitudinal weld at two different locations.

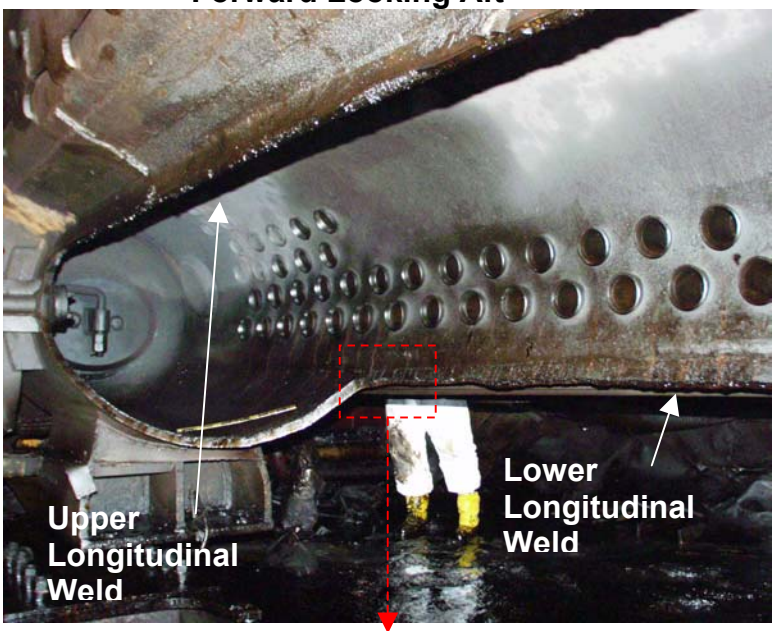

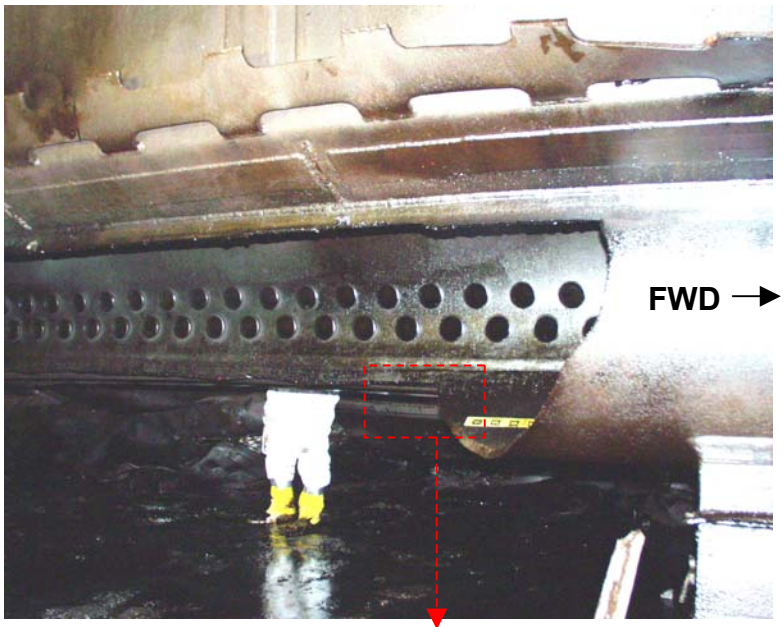

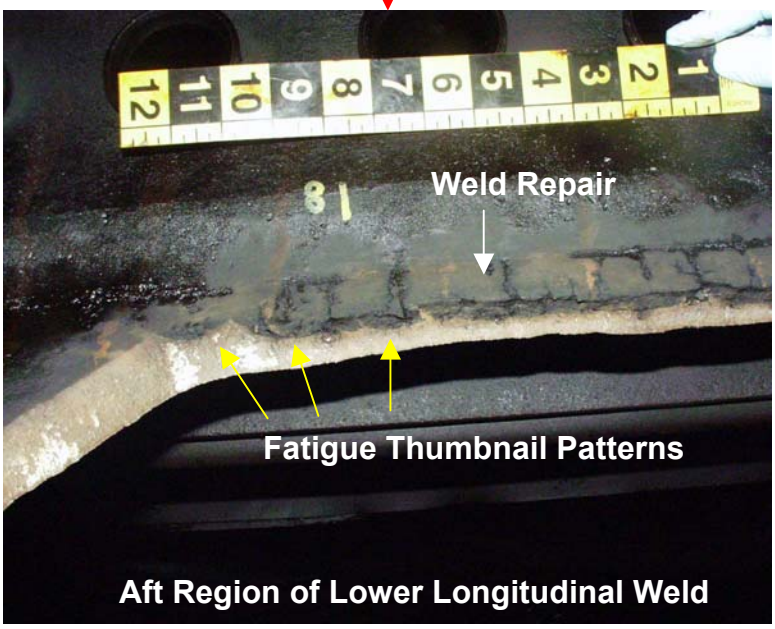

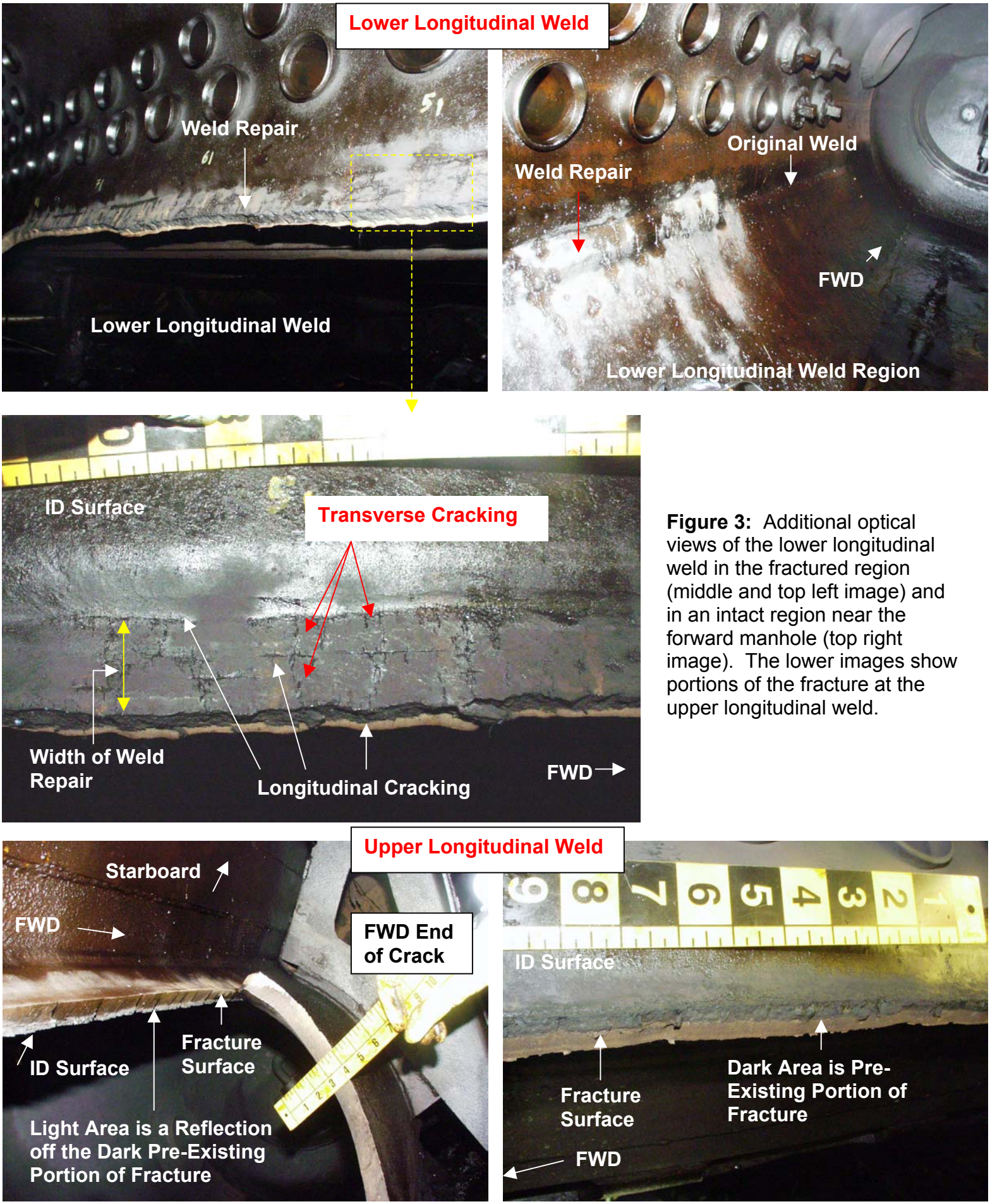

Figure 3: Additional optical views of the lower longitudinal weld in the fractured region (middle and top left image) and in an intact region near the forward manhole (top right image). The lower images show portions of the fracture at the upper longitudinal weld.

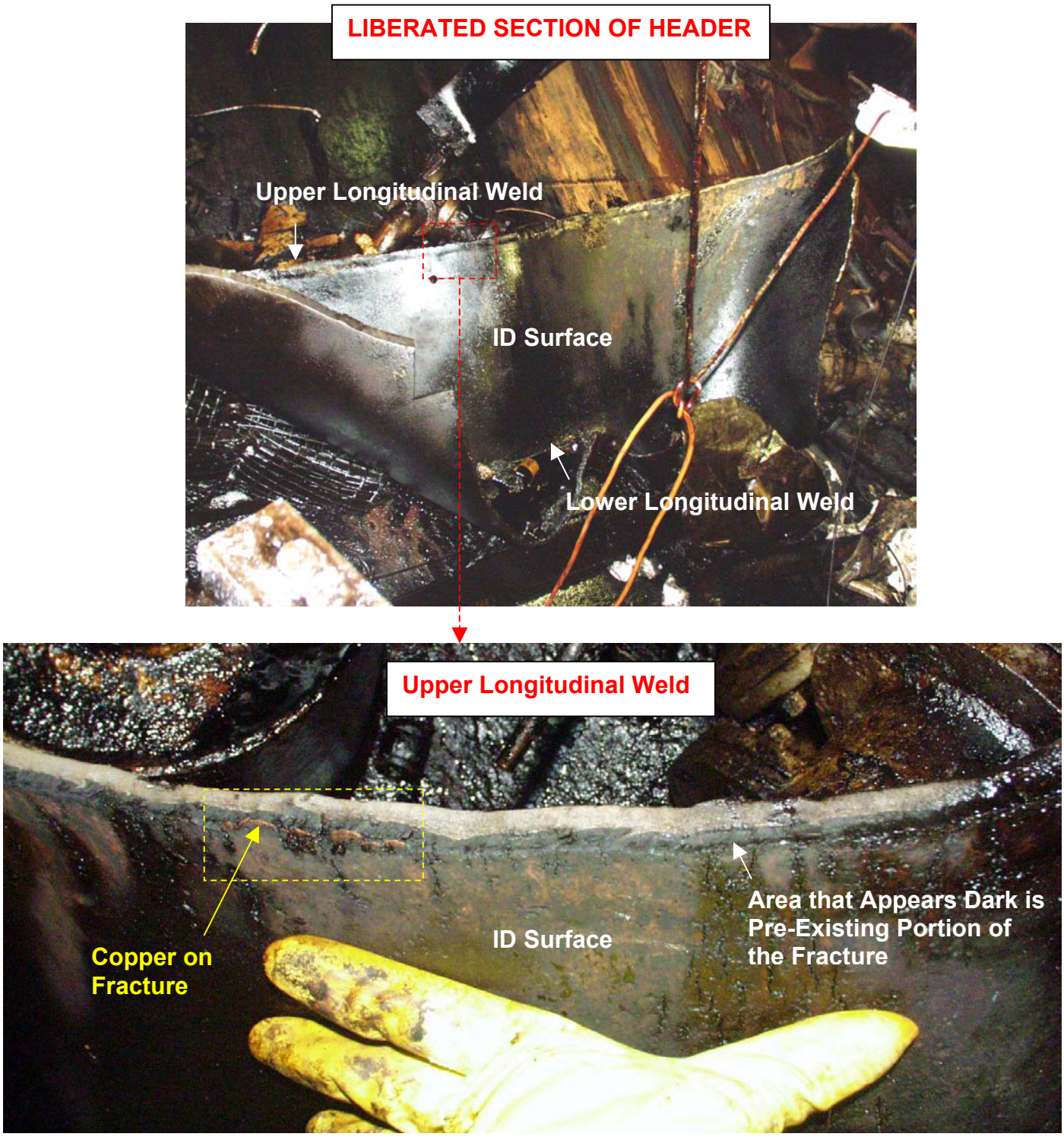

Figure 4: Overall view of the liberated section of the header (top image) and higher magnification view of a portion of the fracture surface of the upper longitudinal weld (lower image).

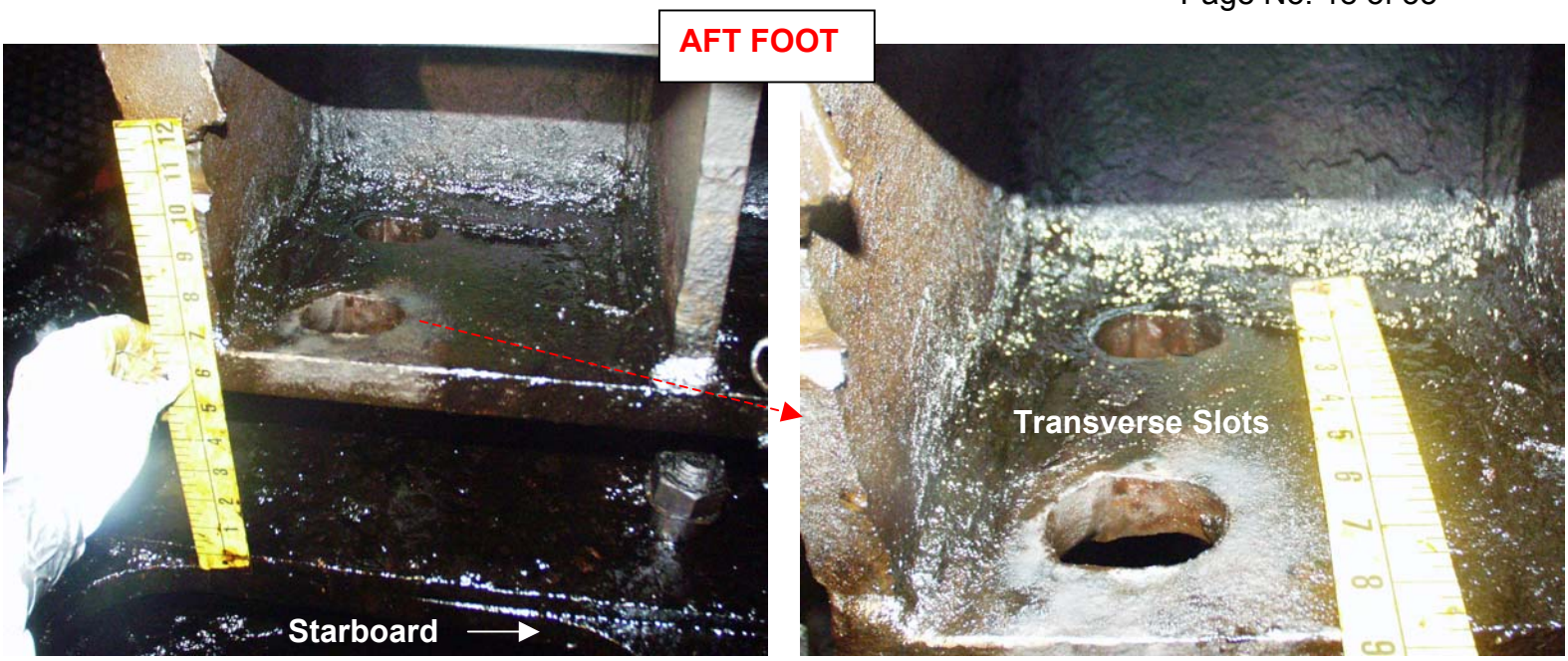

Forward Looking Aft

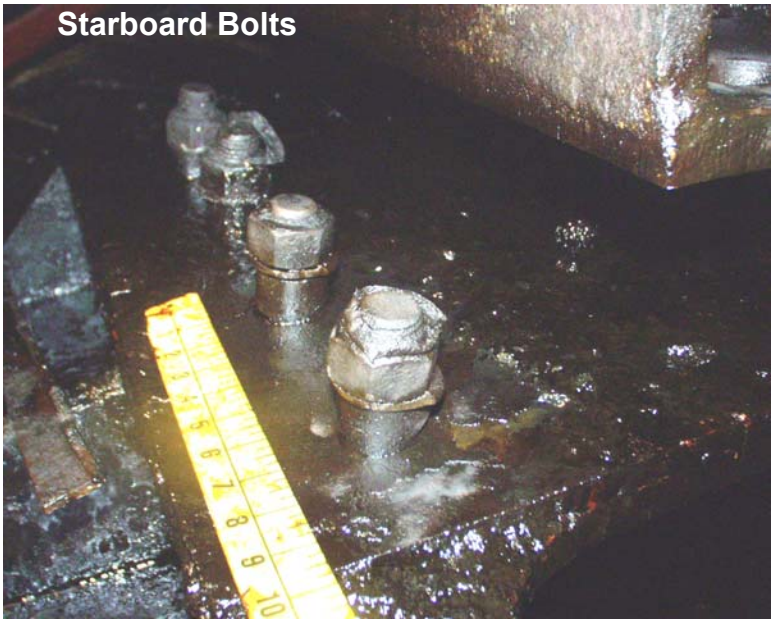

Forward Looking Aft

Figure 5: Views of the aft support foot slots (top two images) and starboard bolts (lower image) for header 23.

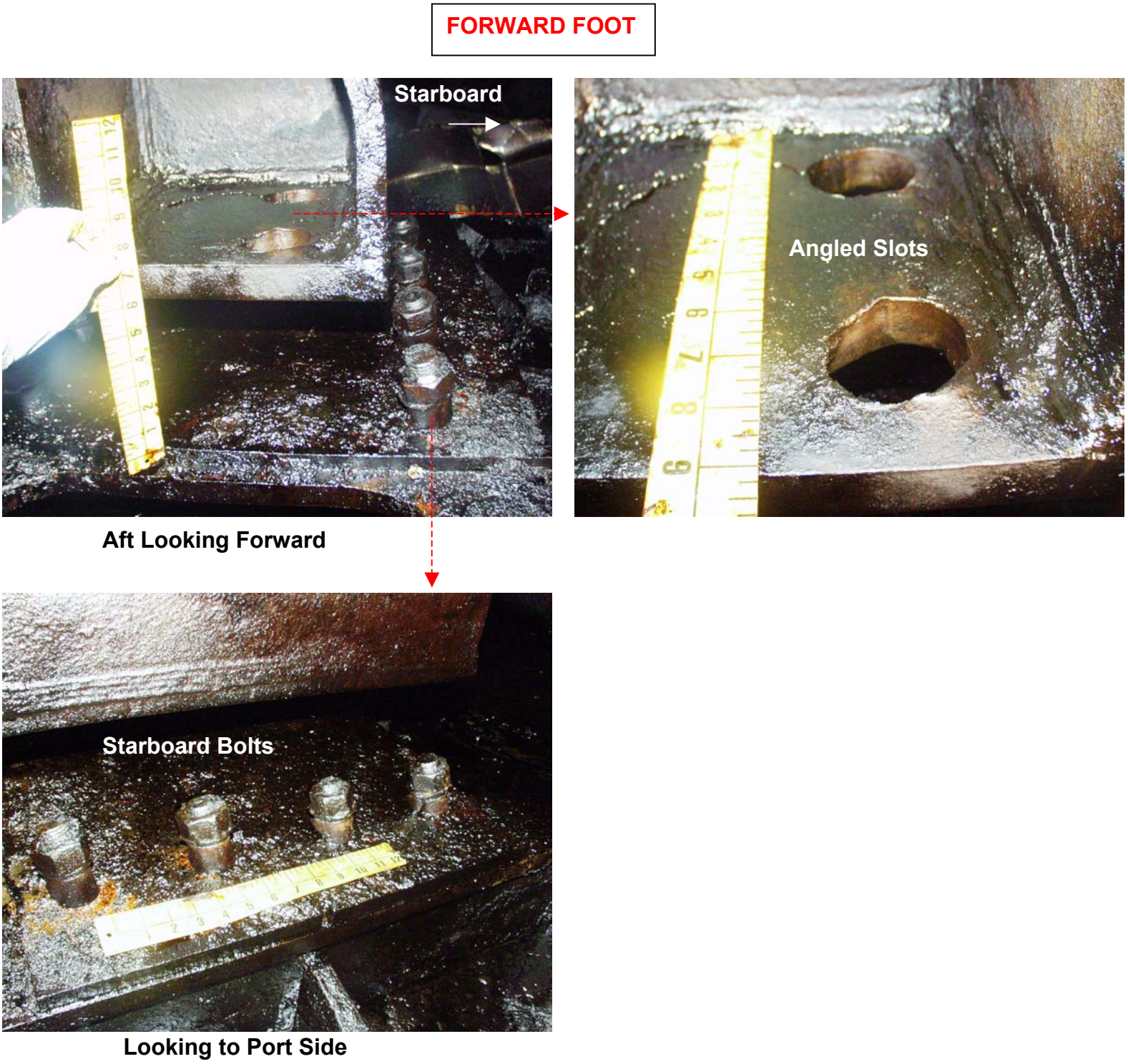

Figure 6: Views of the forward support foot slots (top two images) and starboard bolts (lower image) for header 23.

HEADER FROM BOILER #22

Figure 7: Views of selected areas of the interior of header 22.

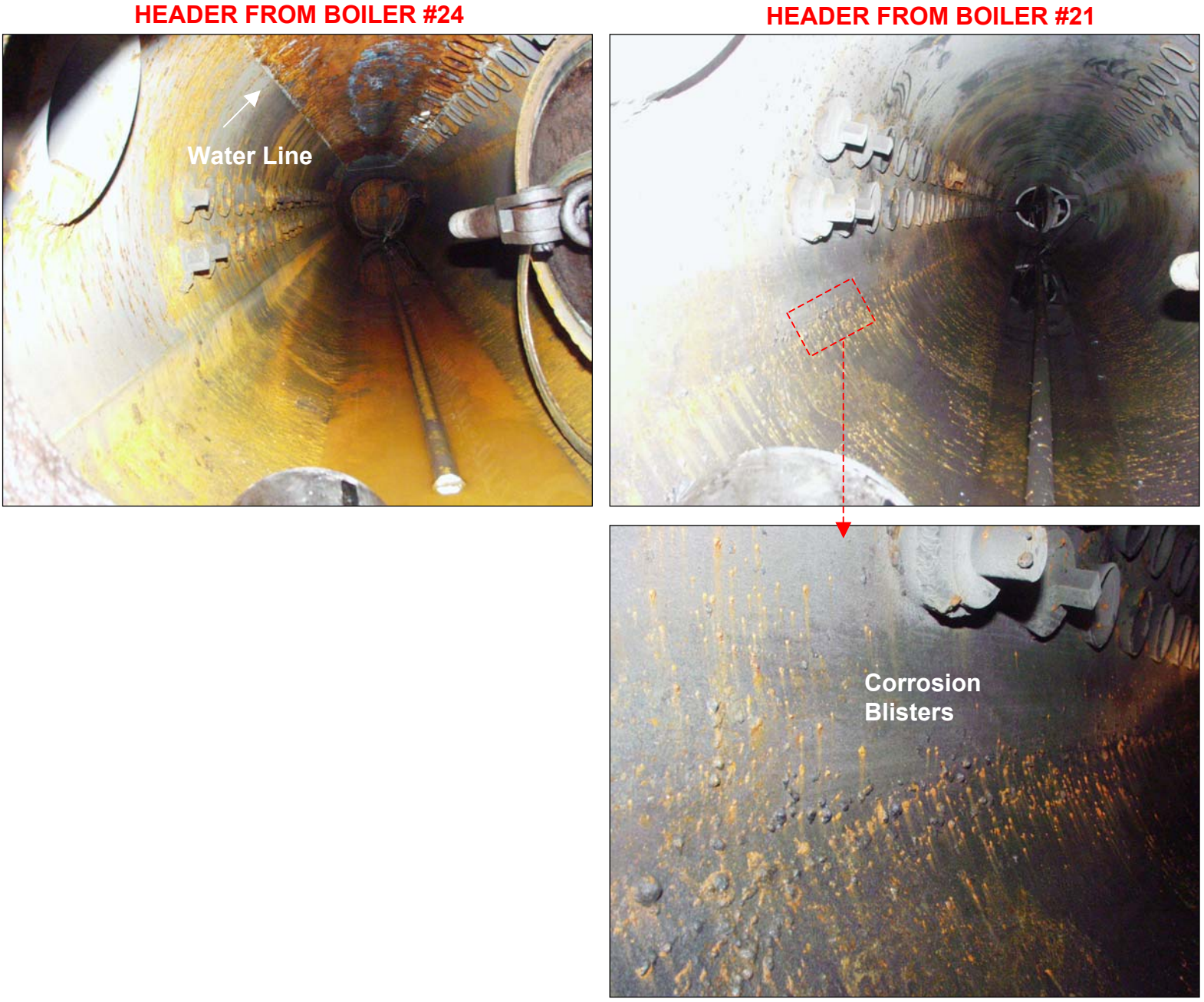

Figure 8: Views of selected areas of the interior of headers 21 and 24.

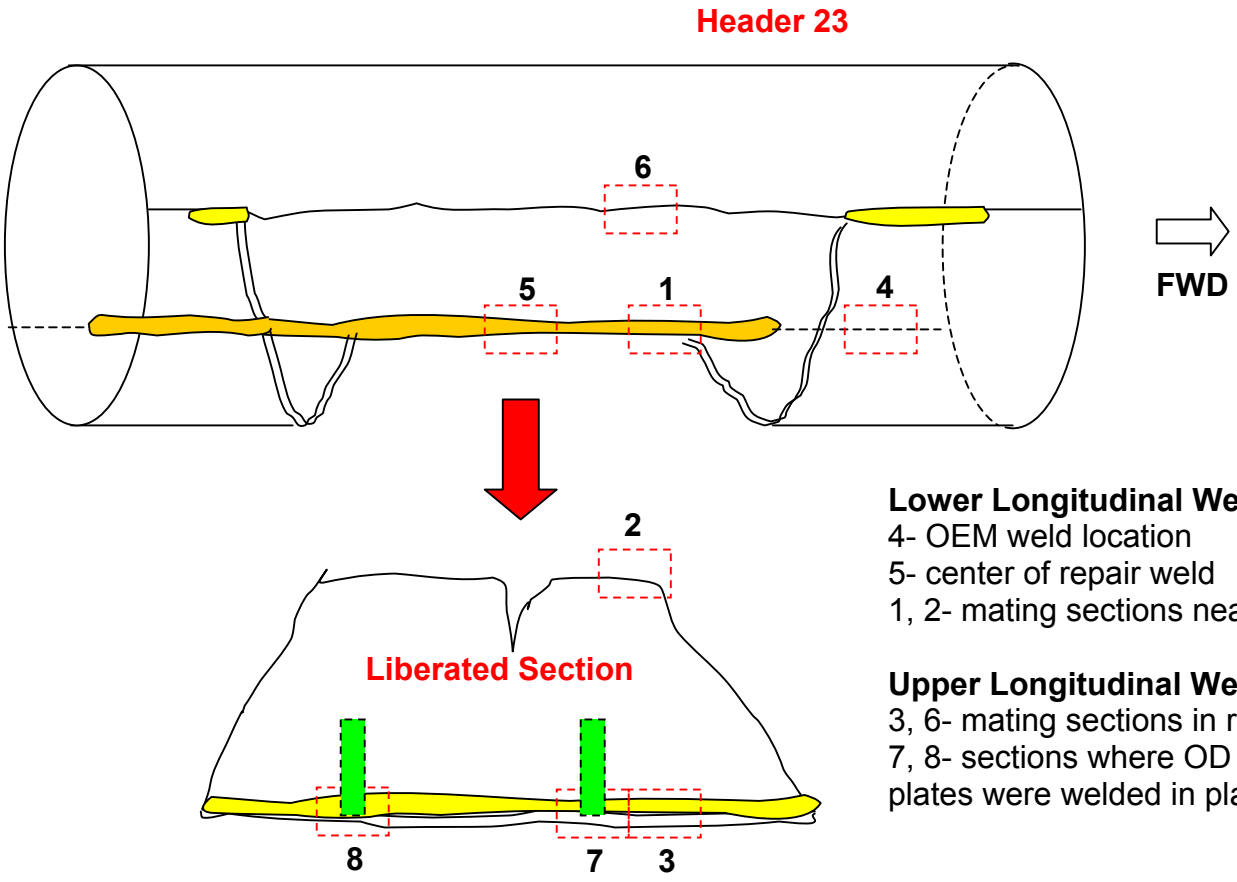

Lower Longitudinal Weld
4- OEM weld location
5- center of repair weld
1, 2- mating sections near end of repair weld

Upper Longitudinal Weld
3, 6- mating sections in repair weld
7, 8- sections where OD vertical structural plates were welded in place (green boxes)

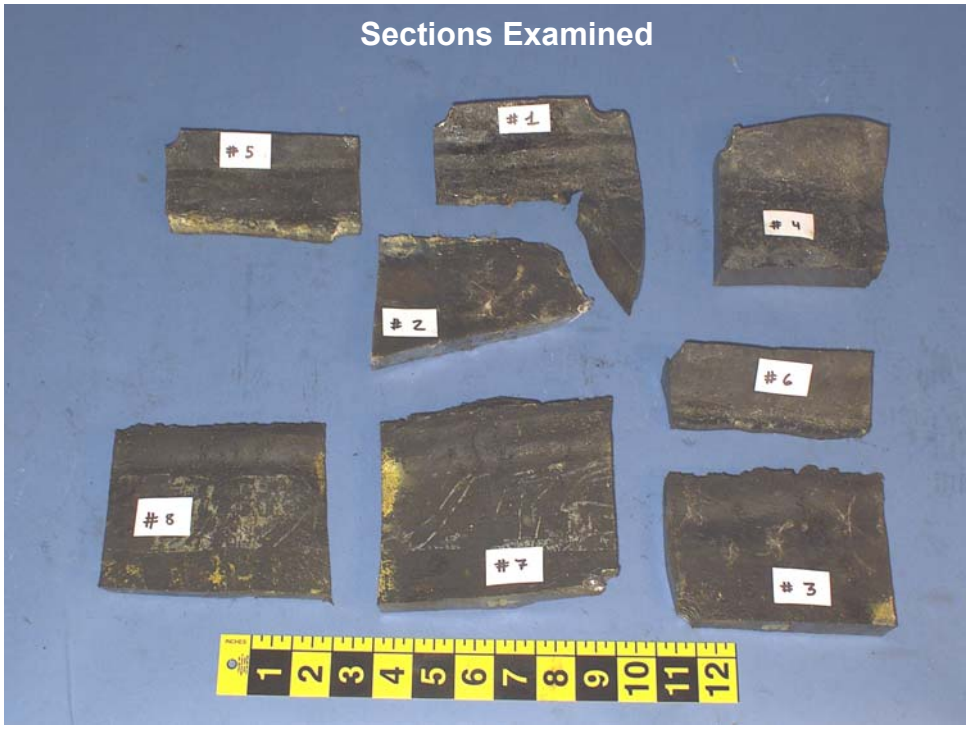

Figure 9: The upper image is a schematic of the fractured header from boiler 23. The numbered regions identify the sections removed from the header for analysis, which can be seen in the lower image.

SECTION 4-OEM Weld Region

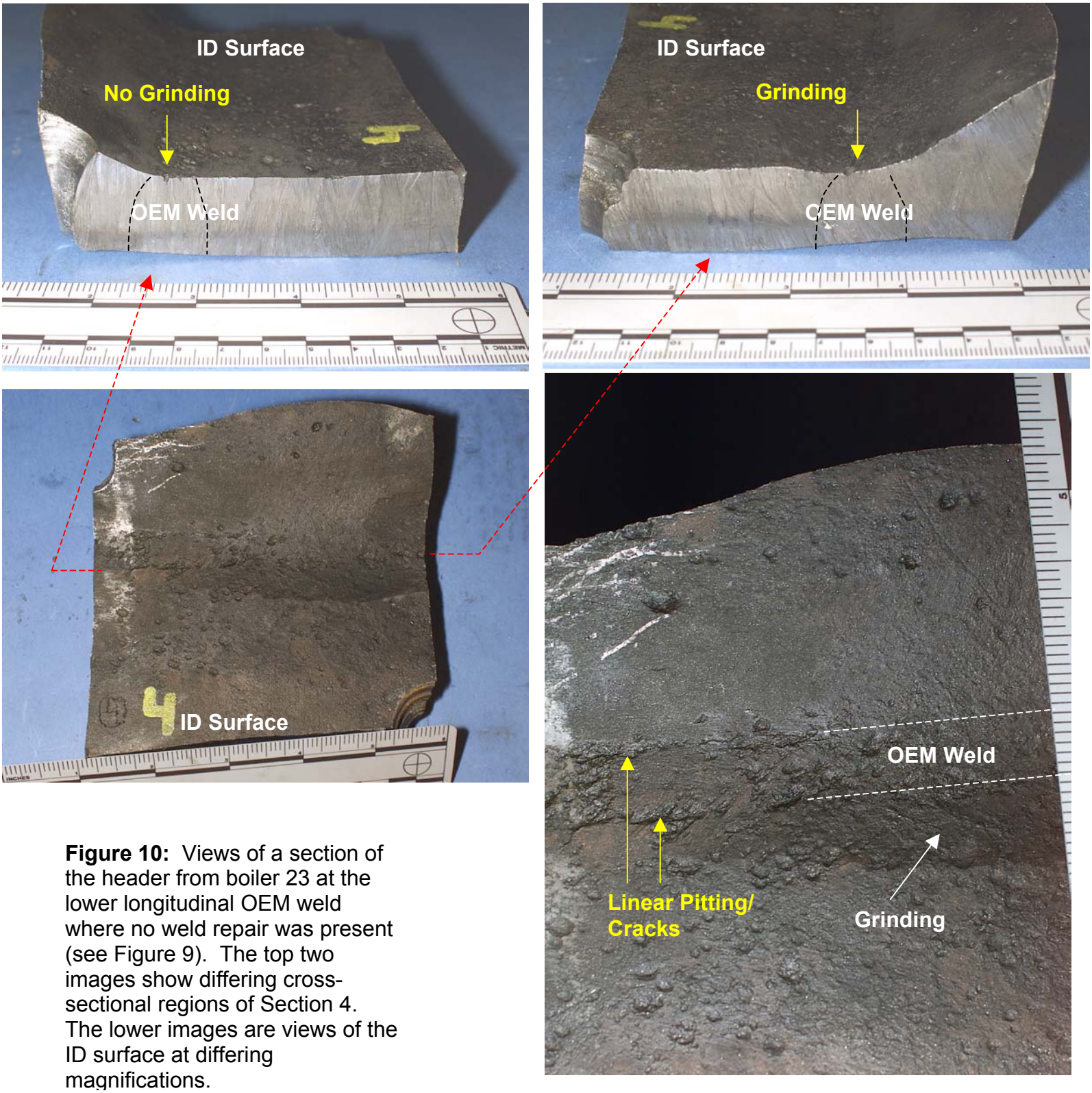

Figure 10: Views of a section of the header from boiler 23 at the lower longitudinal OEM weld where no weld repair was present (see Figure 9). The top two images show differing cross-sectional regions of Section 4. The lower images are views of the ID surface at differing magnifications.

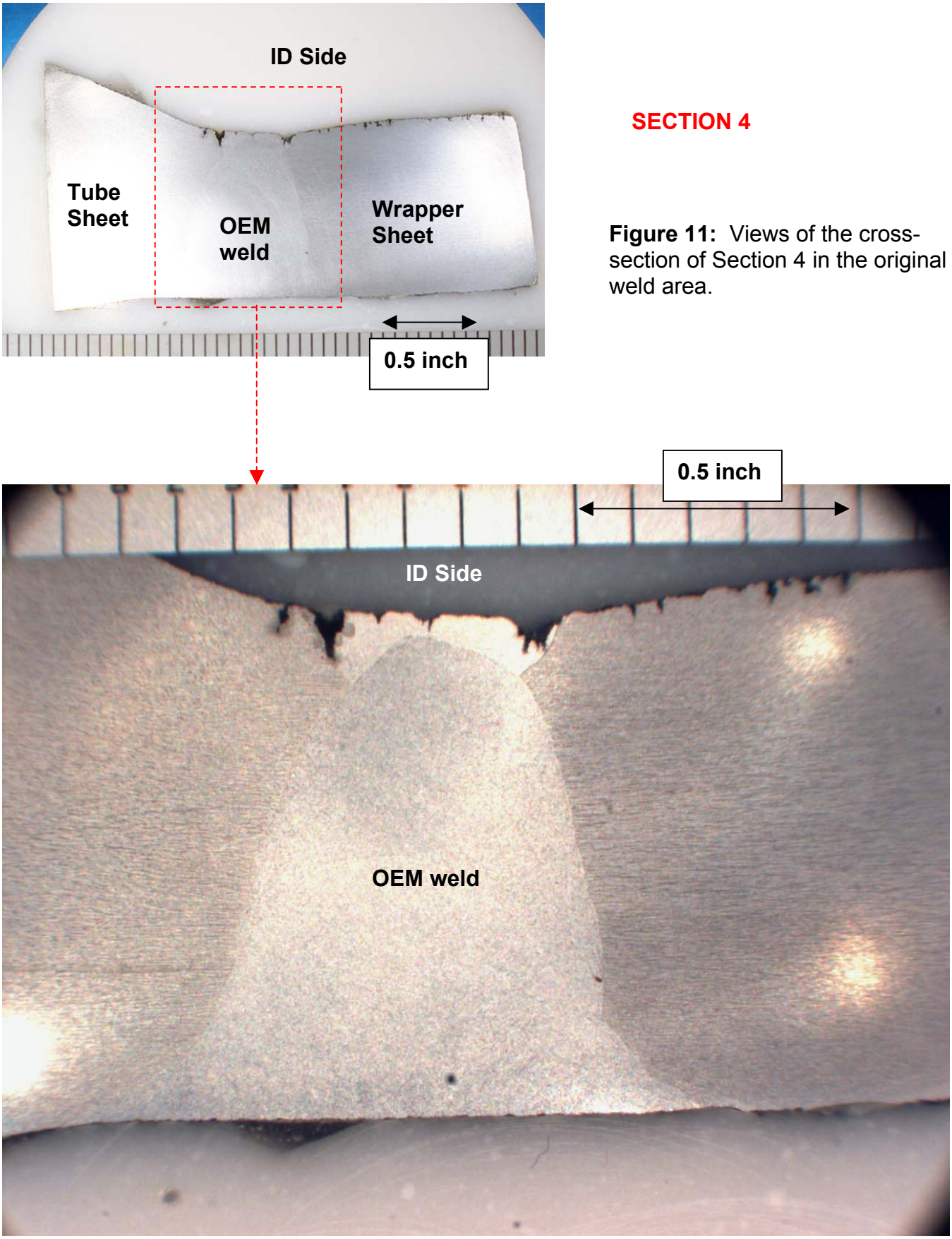

SECTION 4

Figure 11: Views of the cross-section of Section 4 in the original weld area.

SECTIONS 1 & 2

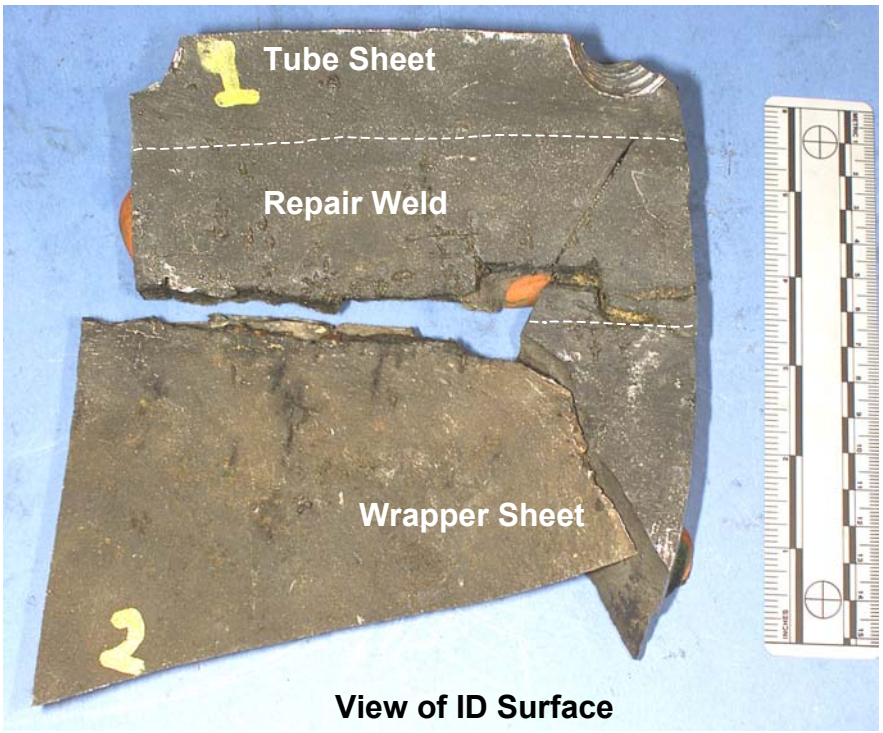

Figure 12: Views of Sections 1 and 2 near the forward end of the fracture at the lower longitudinal weld in the repair region. SEM views of Areas 1-3 are shown in Figures 18 and 20.

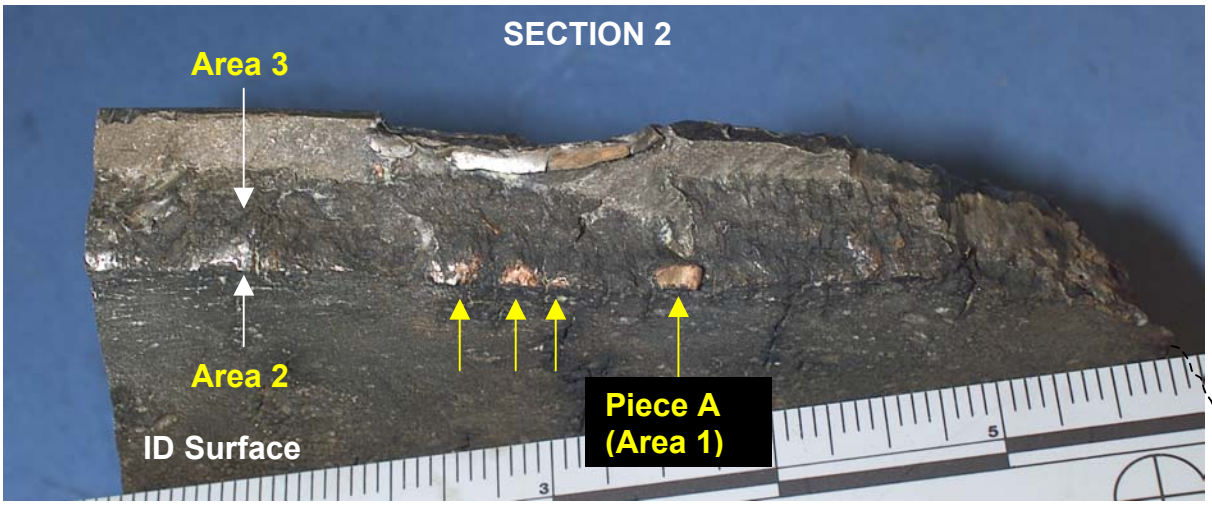

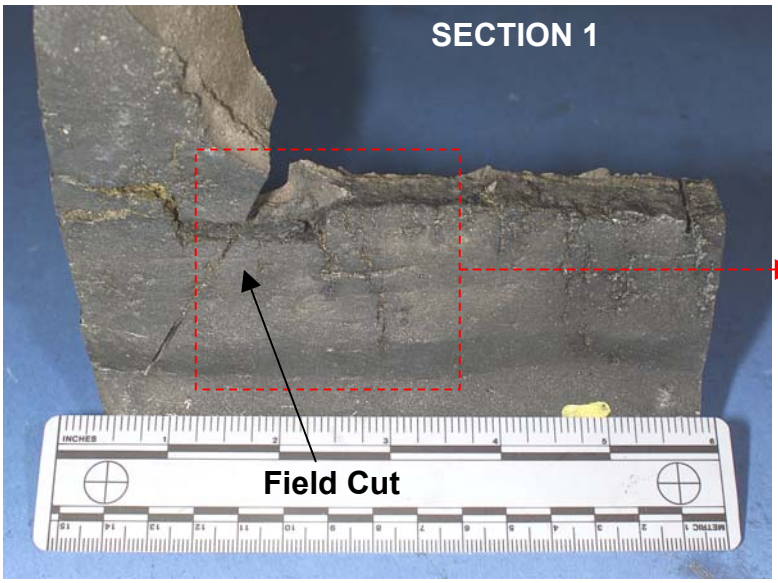

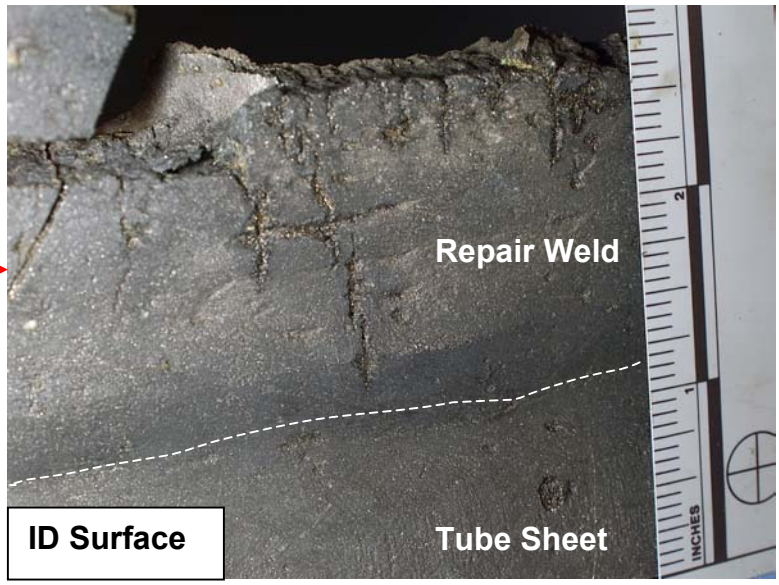

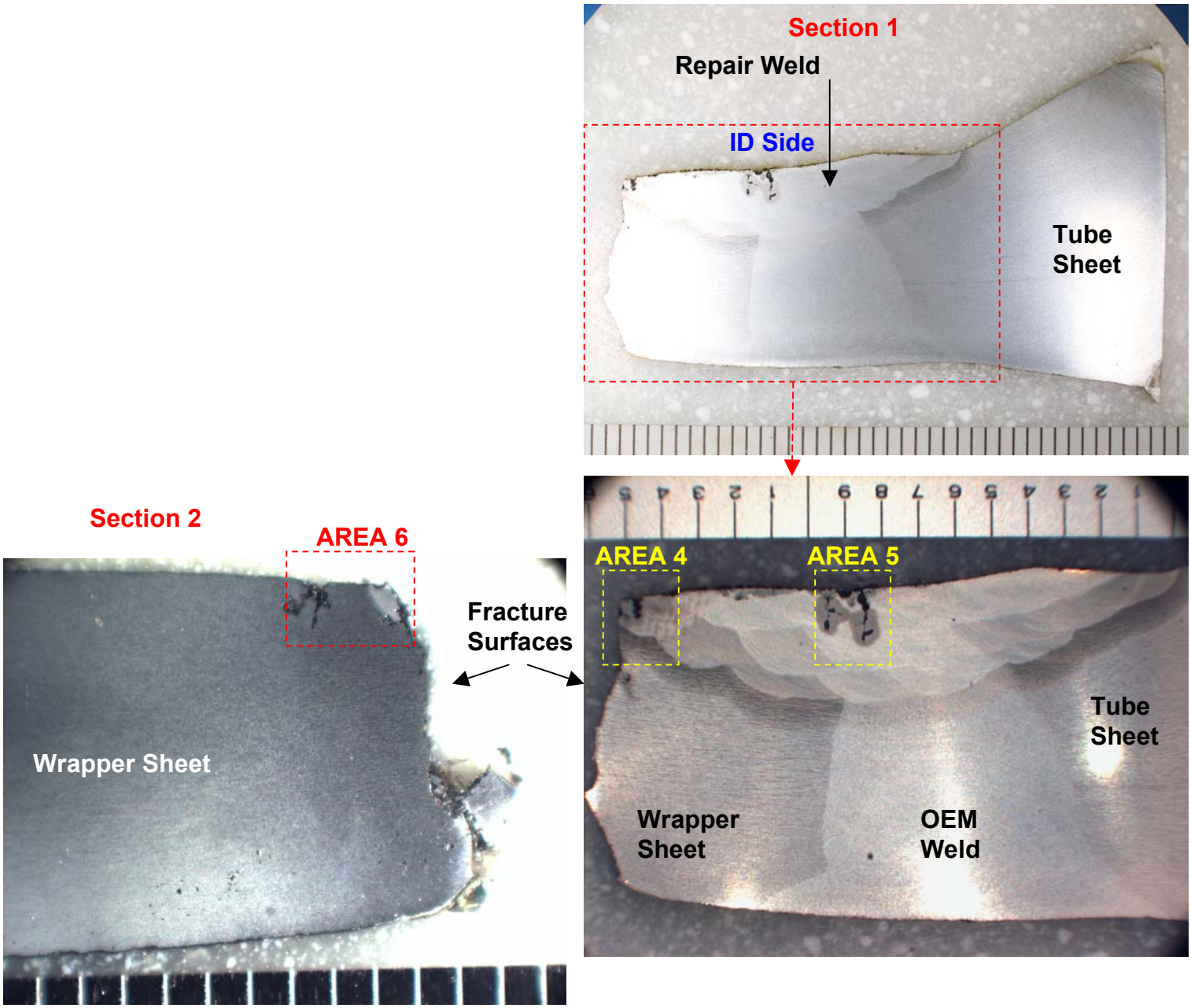

Figure 13: Cross-sectional mounts at varying magnifications of mating Sections 1 and 2 in the lower longitudinal weld.

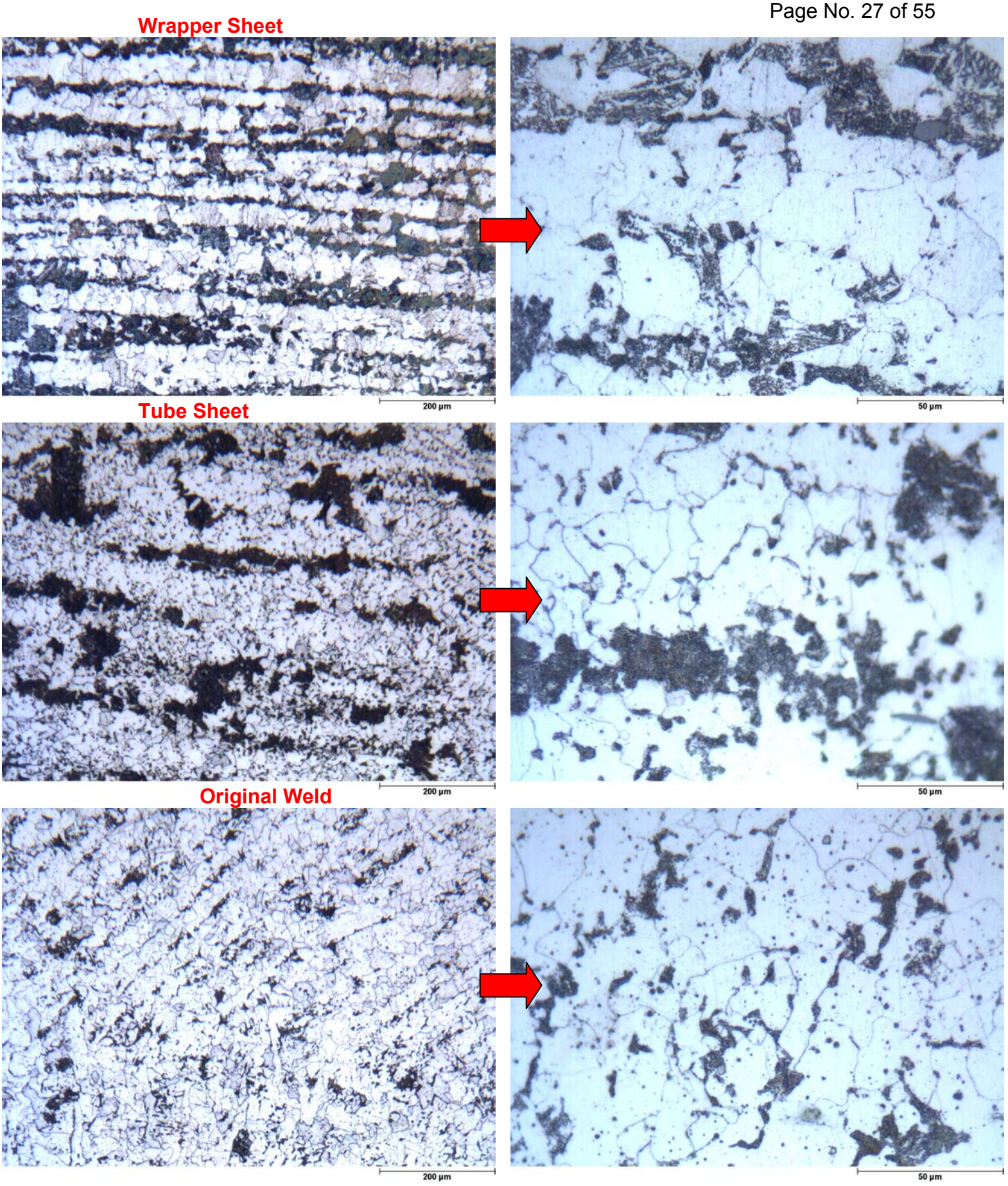

Figure 14: Microstructures at varying magnifications of the wrapper sheet, tube sheet, and original weld.

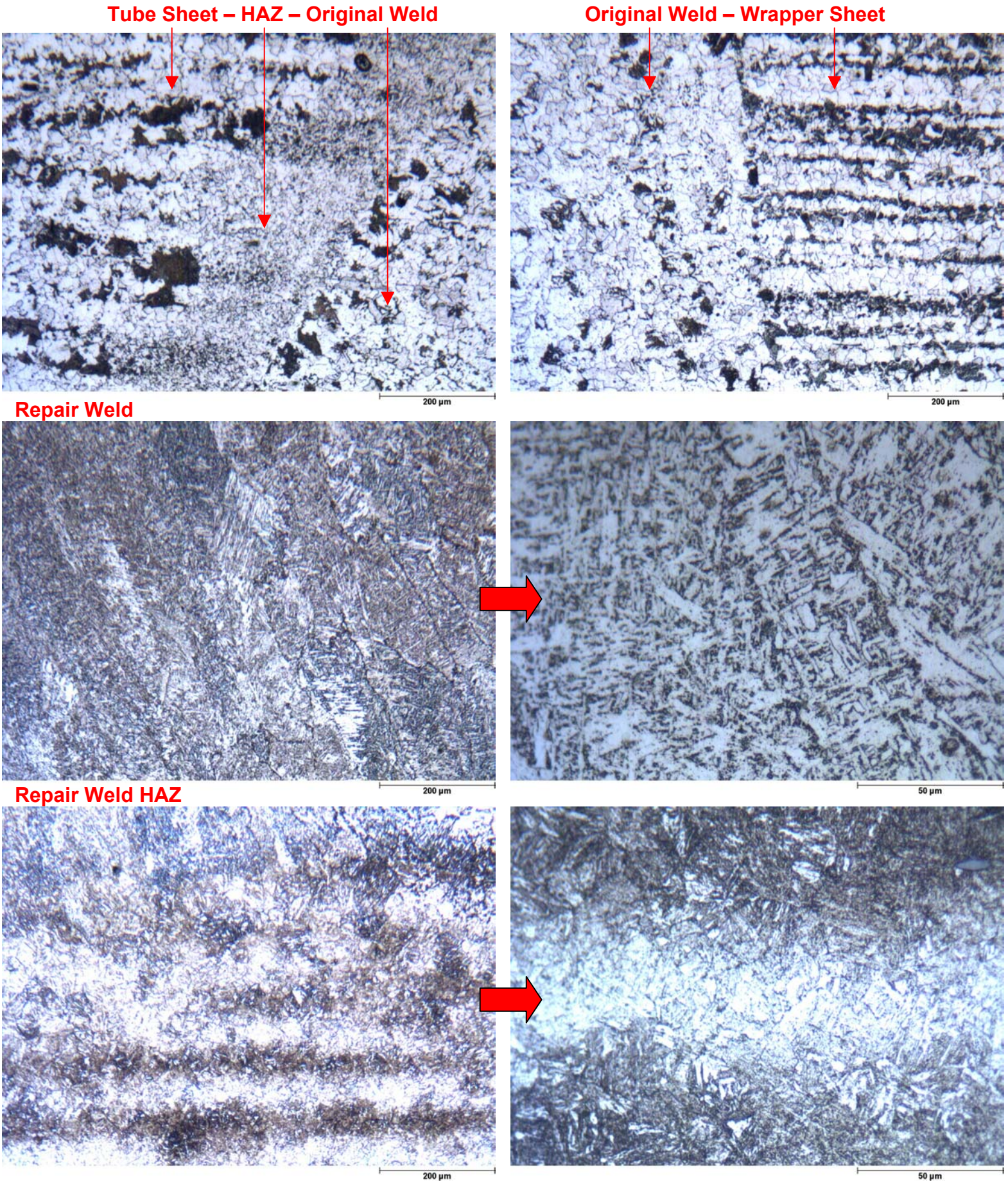

Figure 15: Microstructures of the original weld HAZ, the repair weld, and the repair weld HAZ.

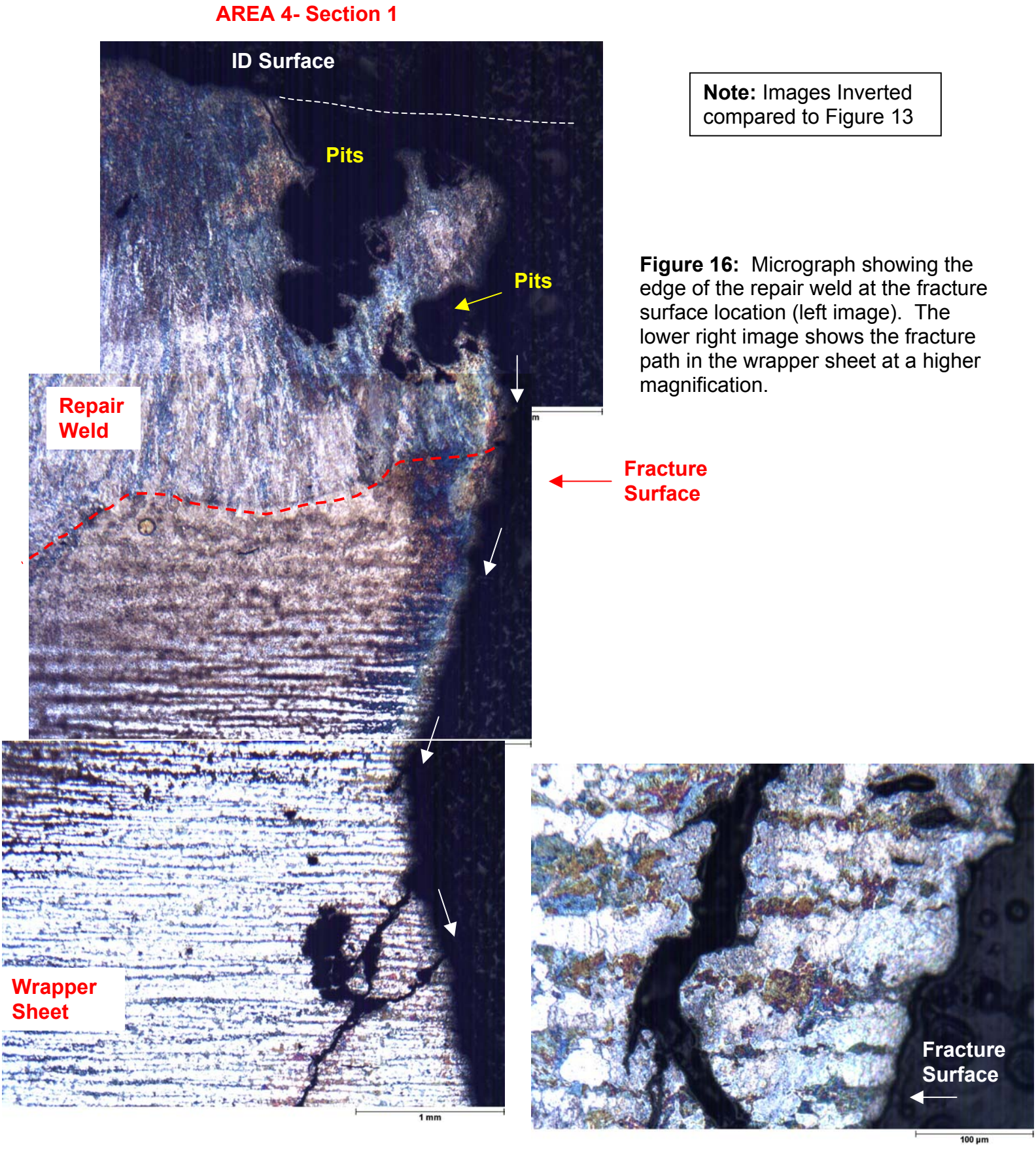

Note: Images Inverted compared to Figure 13

Figure 16: Micrograph showing the edge of the repair weld at the fracture surface location (left image). The lower right image shows the fracture path in the wrapper sheet at a higher magnification.

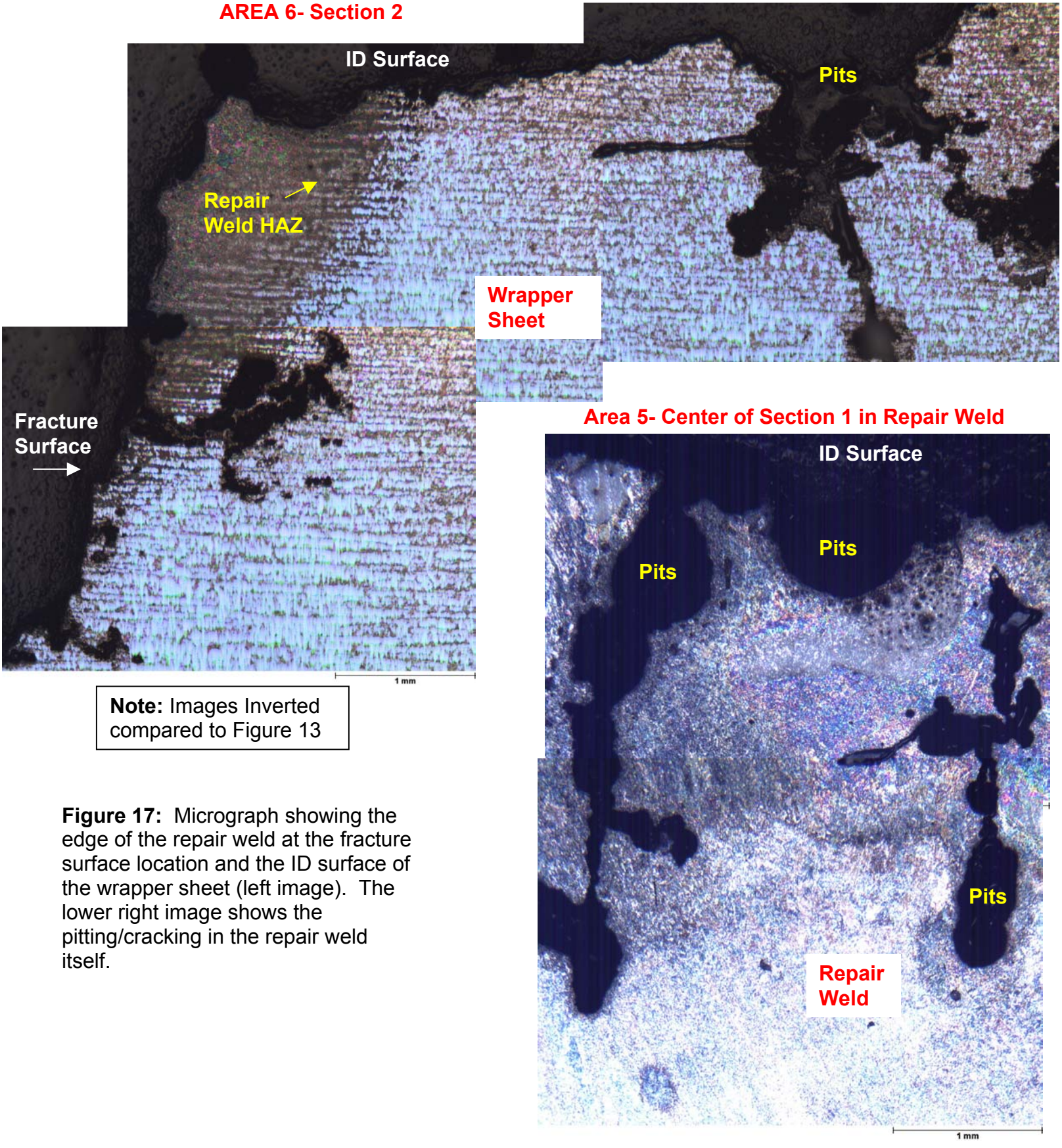

Note: Images Inverted compared to Figure 13

Figure 17: Micrograph showing the edge of the repair weld at the fracture surface location and the ID surface of the wrapper sheet (left image). The lower right image shows the pitting/cracking in the repair weld itself.

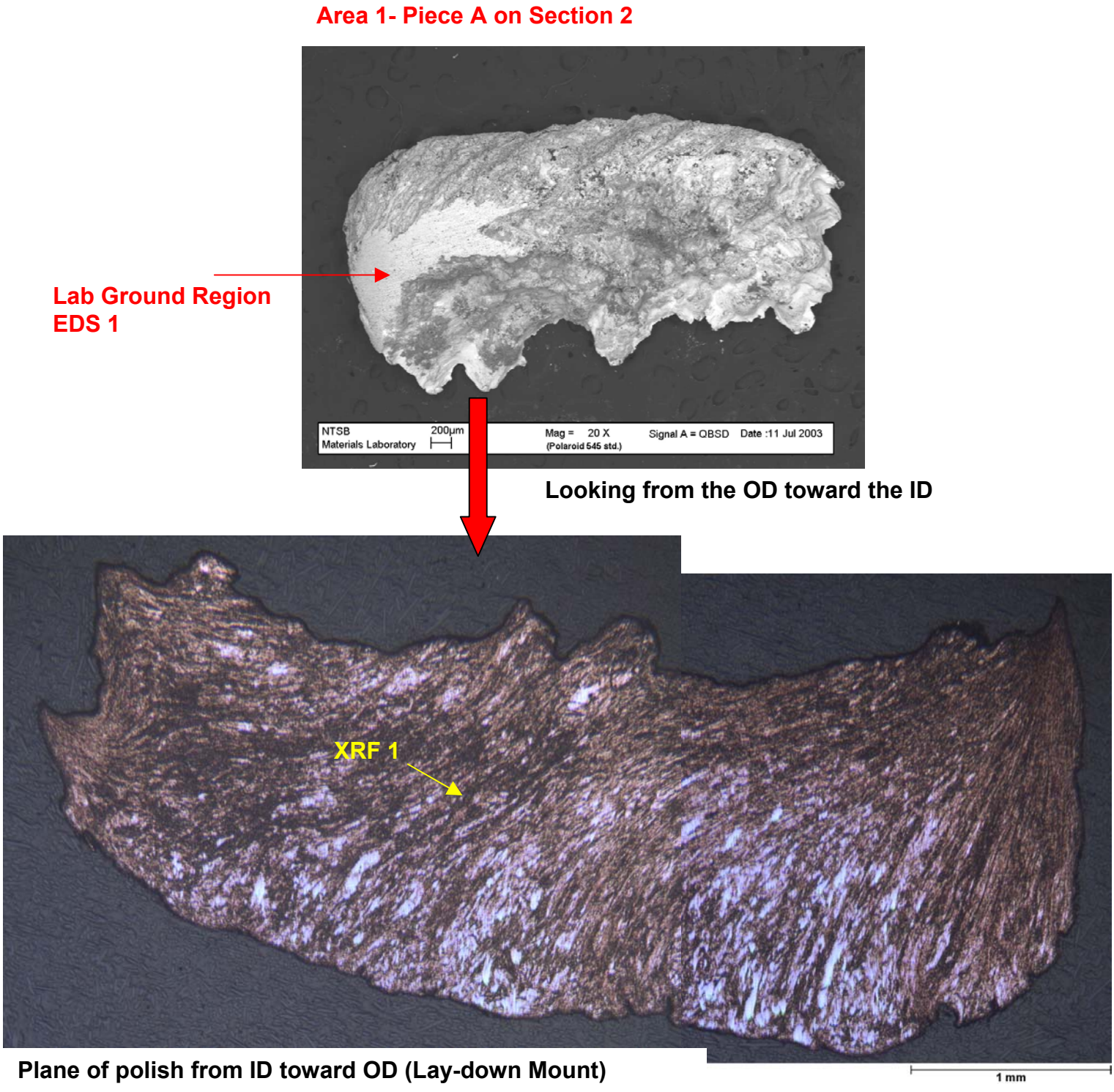

Figure 18: SEM view of the underside of copper nugget Piece A that was flaked off from Section 2 (upper image). The lower image is a lay-down etched micrograph of the nugget microstructure.

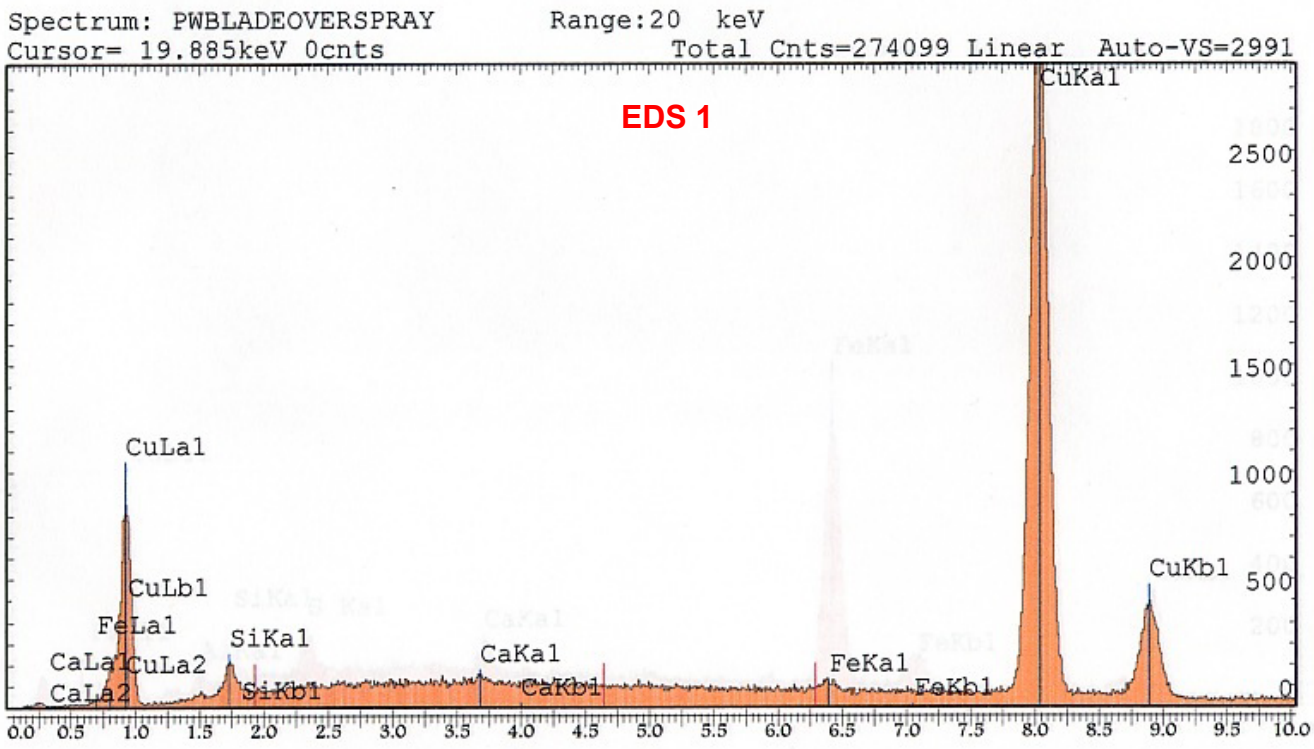

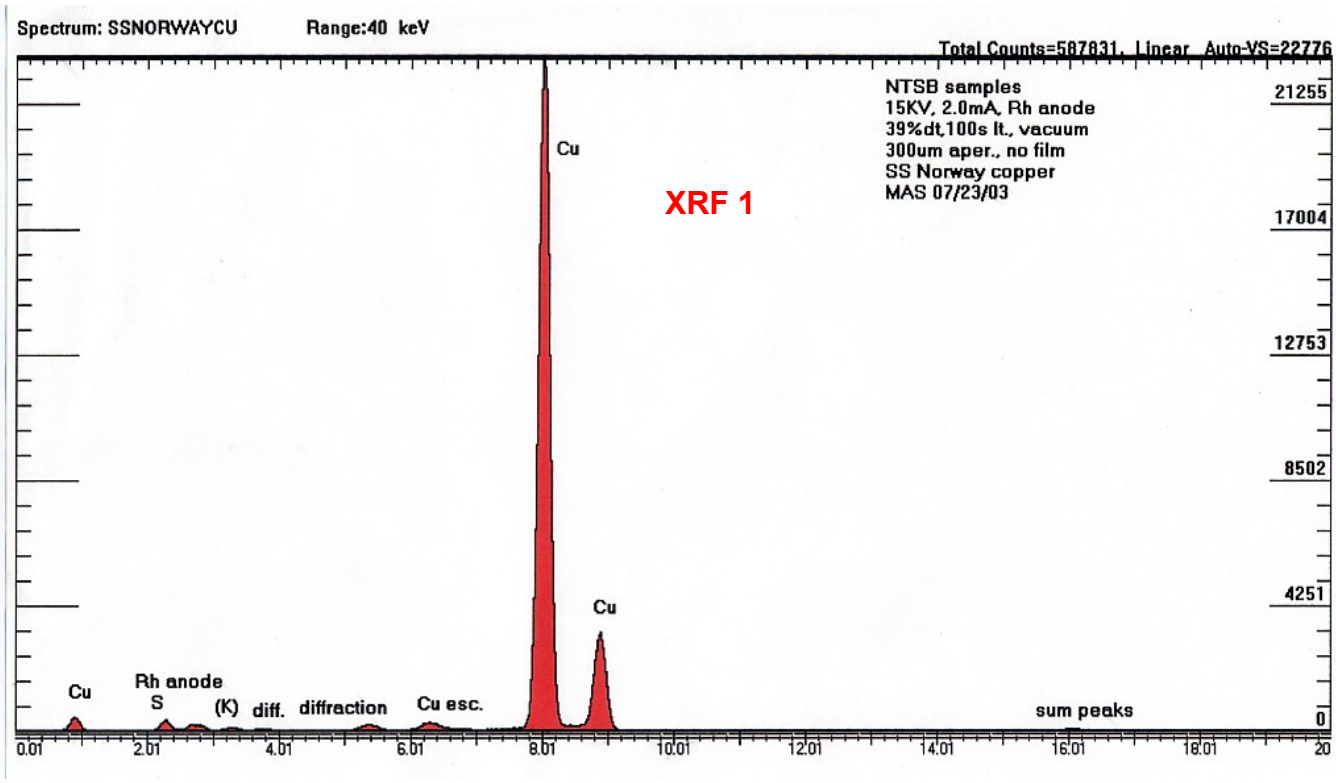

Figure 19: EDS (top) and XRF (bottom) spectra of the copper nugget shown in Figure 18.

Area 2 on Section 2- Near ID Surface

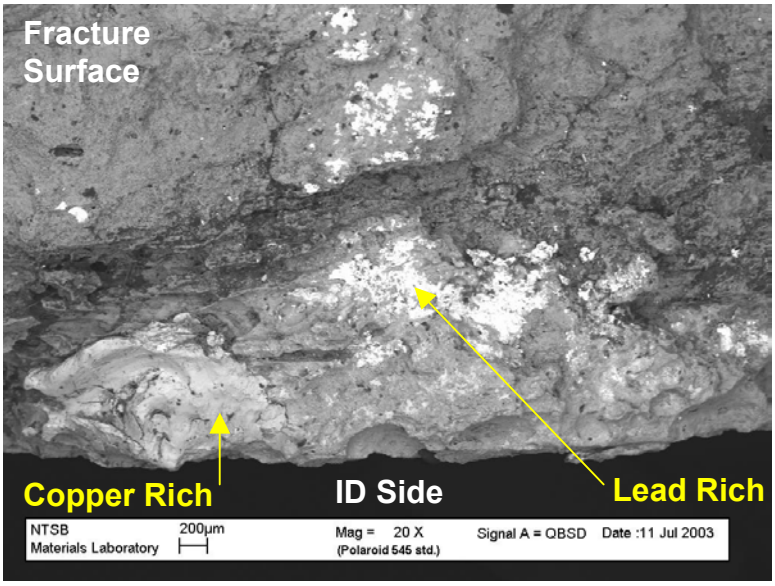

Area 3 on Section 2- Mid Depth

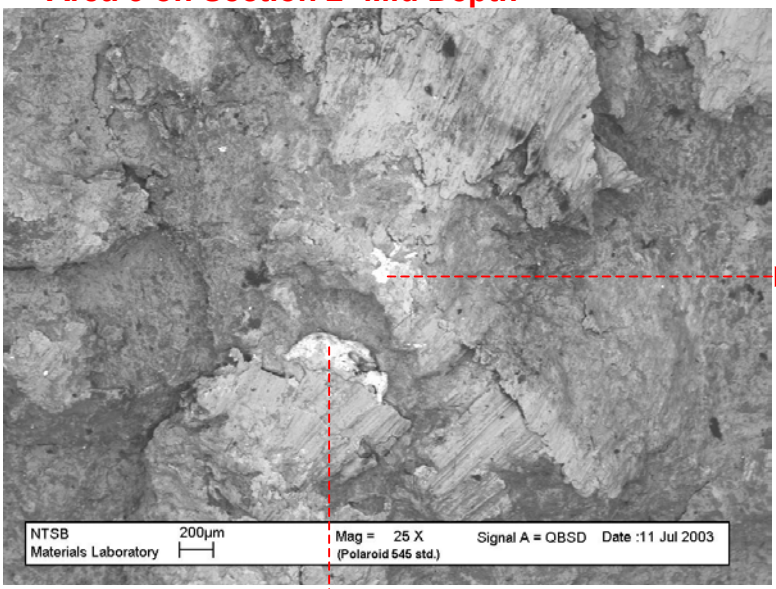

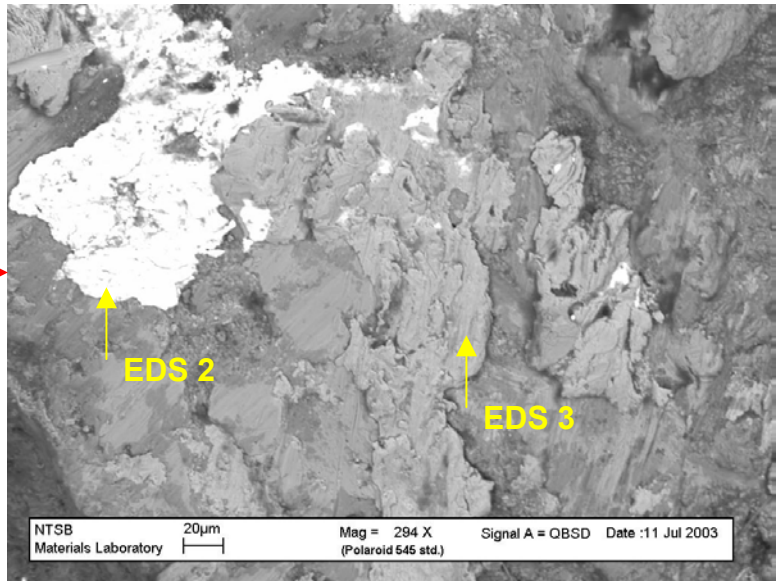

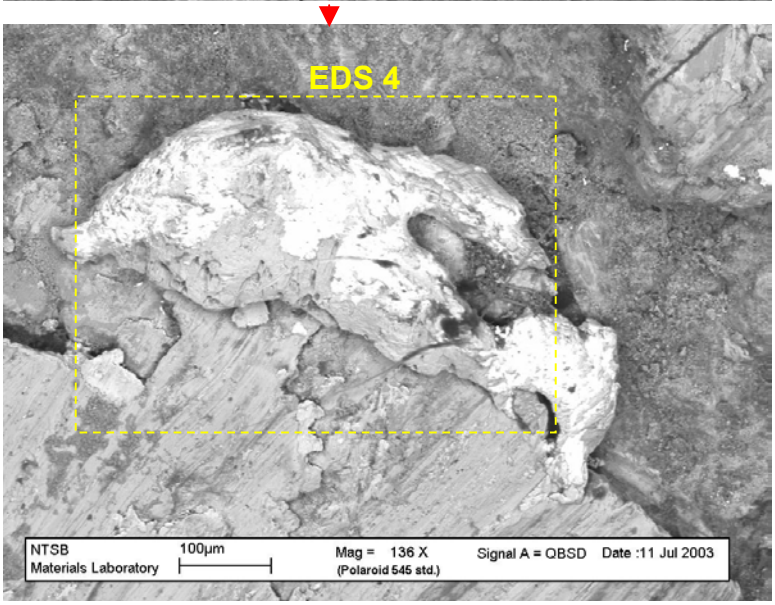

Figure 20: Varying magnification SEM views of additional location along the fracture surface of Section 2. In these locations EDS readings were taken as shown in Figure 21.

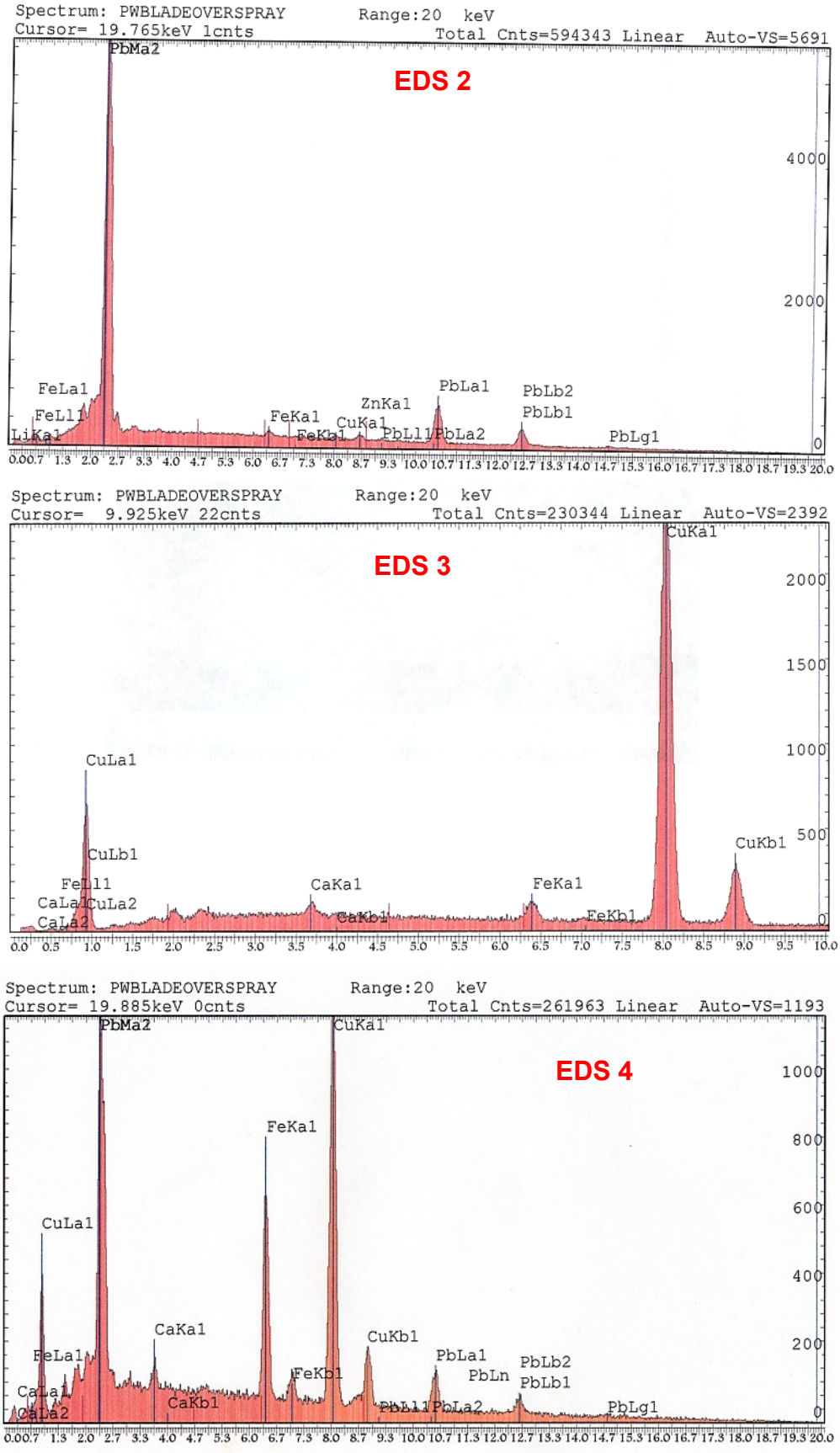

Figure 21: EDS spectra of the locations shown in Figure 20 on the fracture surface of Section 2.

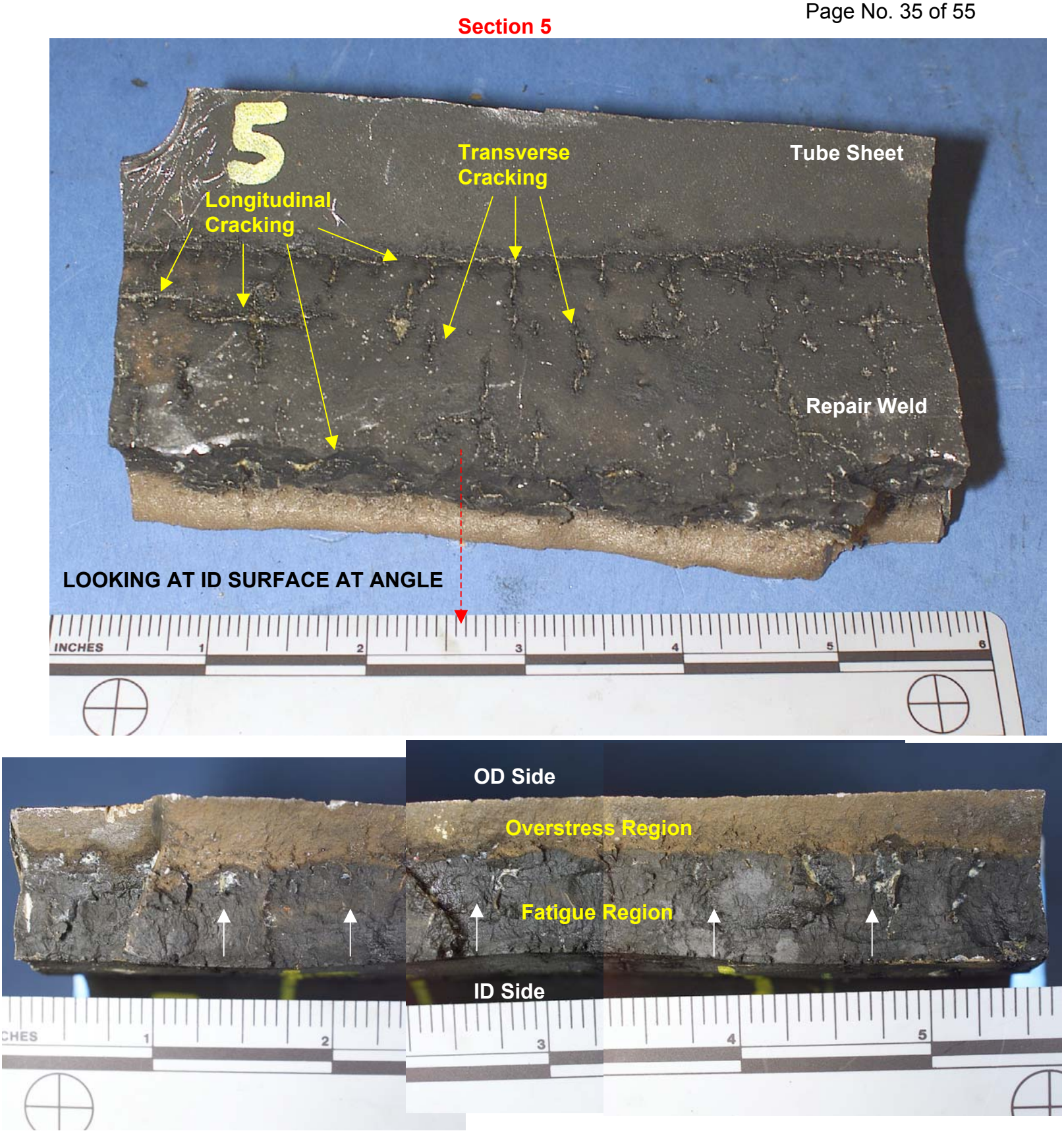

Figure 22: Views of the inner diameter surface (upper image) and fracture surface (lower montage) of Section 5 taken from the middle of the lower longitudinal weld of header 23.

Section 5

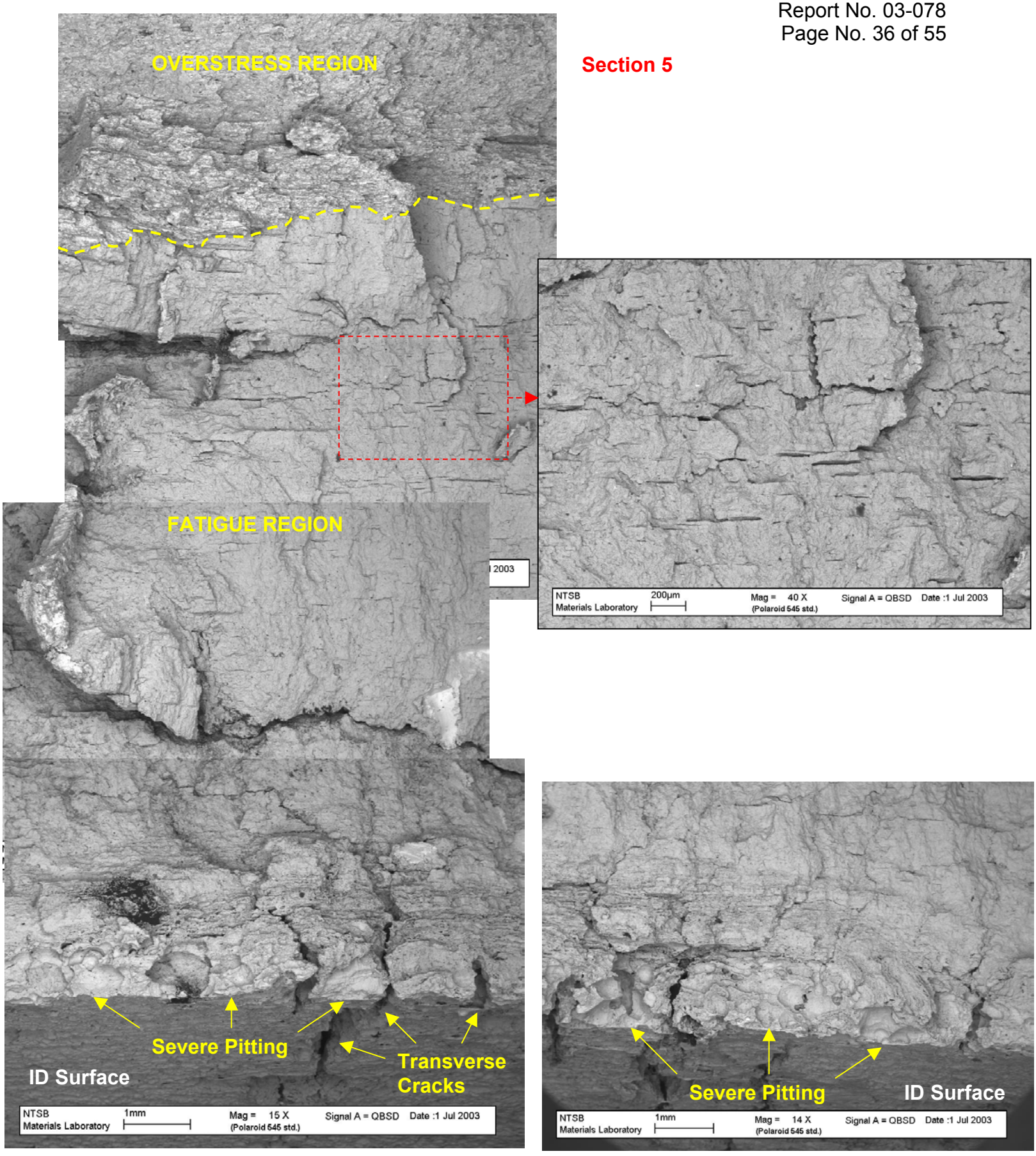

Figure 23: Varying magnification SEM views of the fracture surface of Section 5 at multiple locations.

Section 5

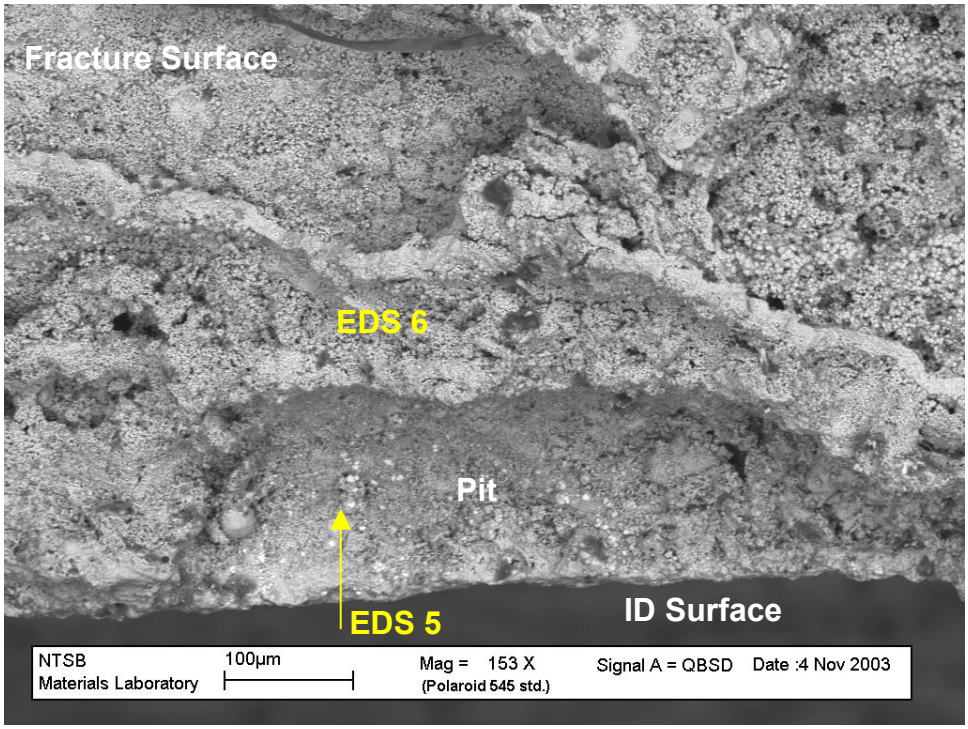

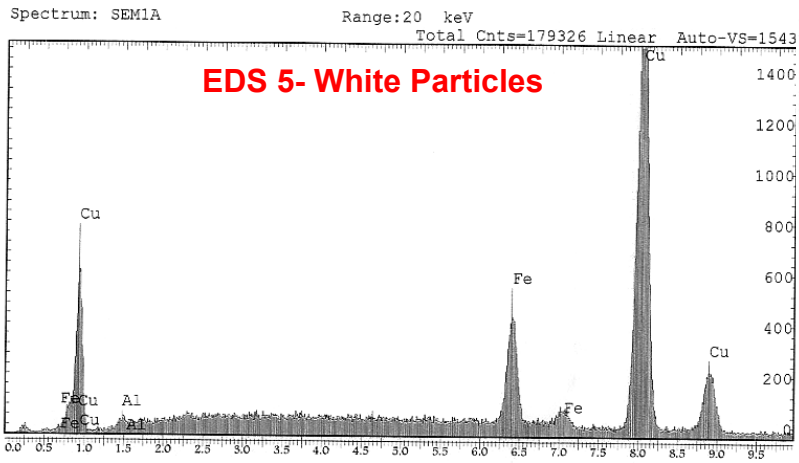

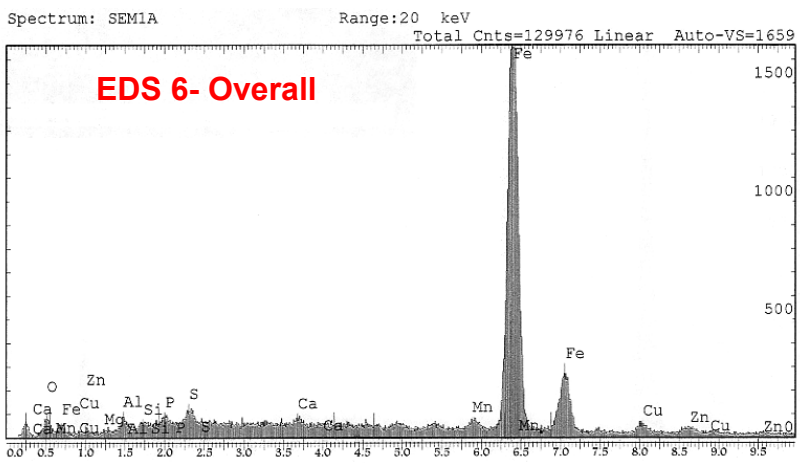

Figure 24: SEM image of the fracture surface of Section 5 near the ID surface (top image). The lower images are EDS spectra taken at the locations shown in the top image.

Section 5

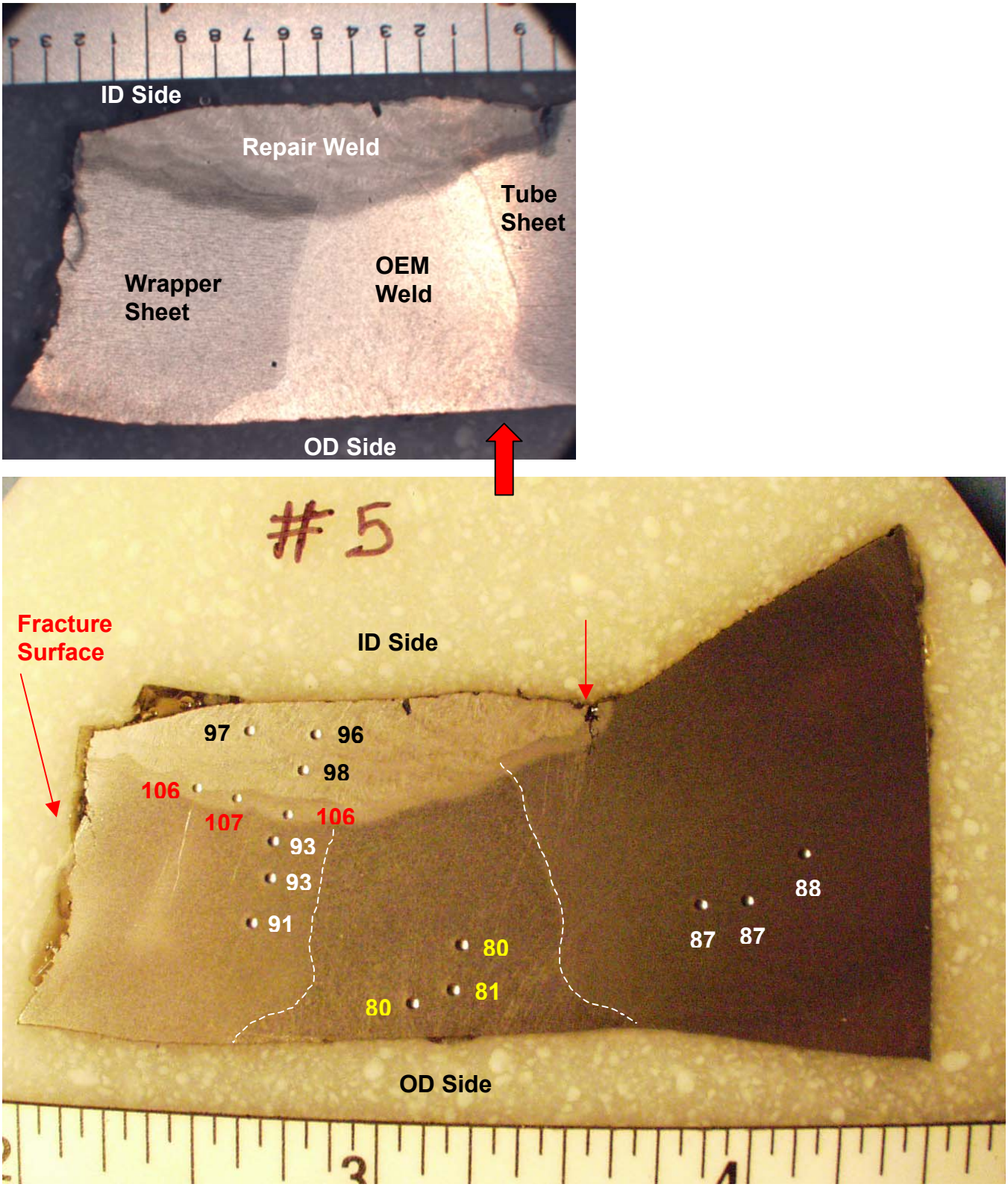

Figure 25: Transverse cross-sectional mounts through Section 5 at varying magnifications and lighting conditions. The lower image also shows the value and location where Rockwell B readings were taken.

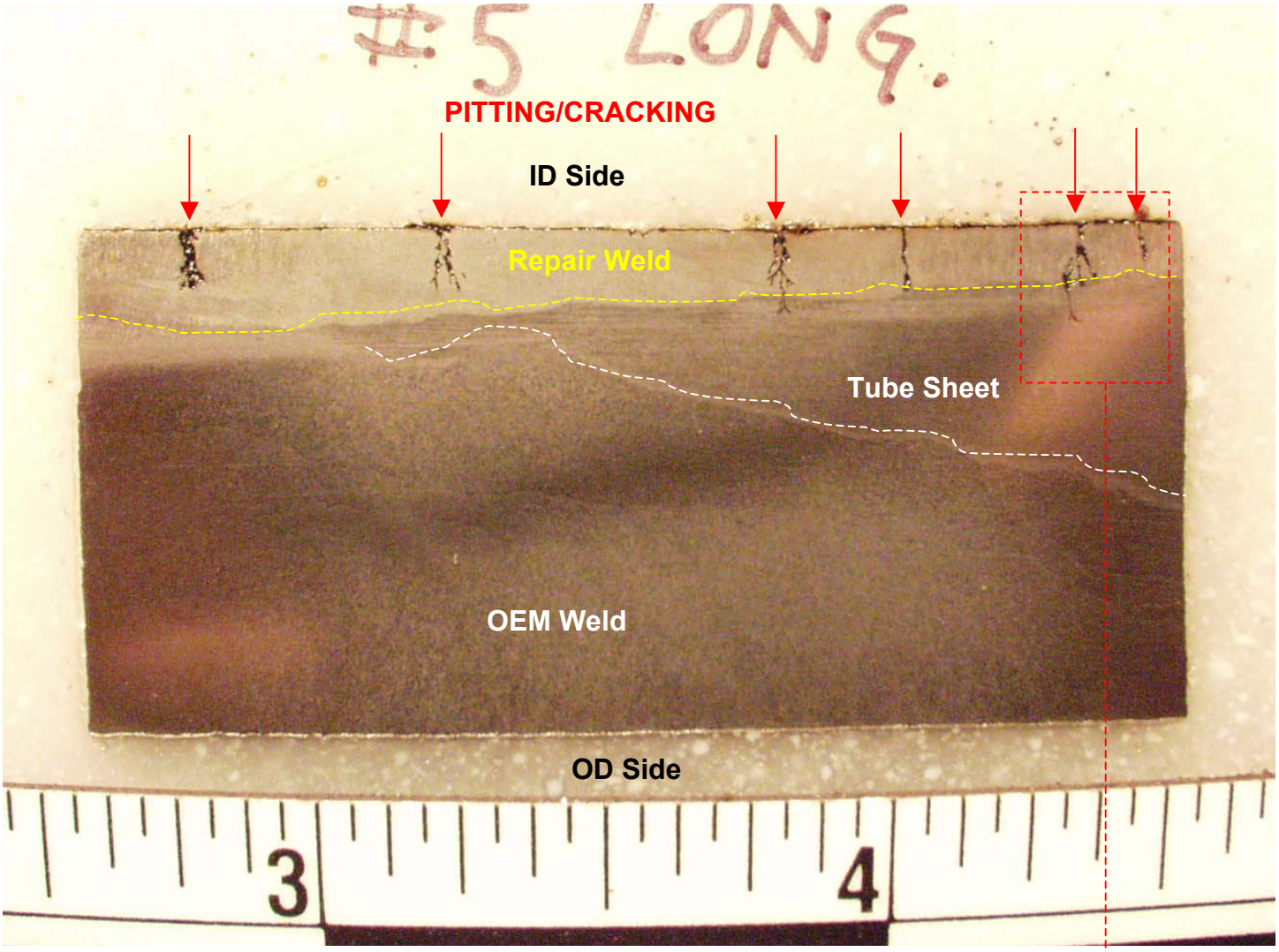

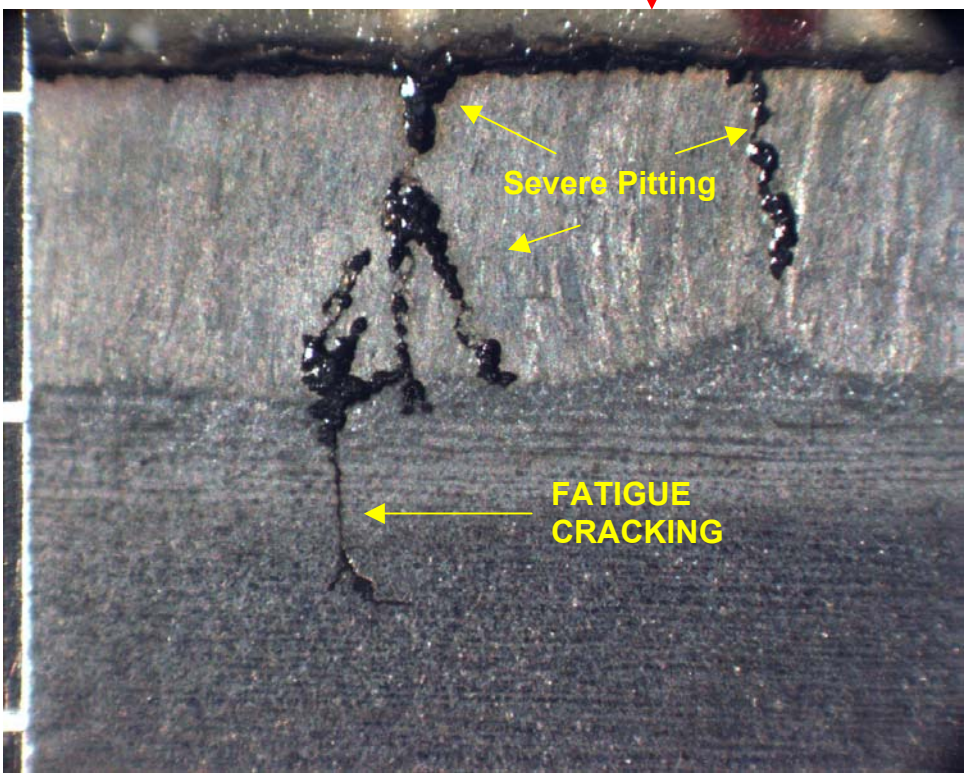

Figure 26: Longitudinal cross-sectional micrographs at varying magnifications through the longitudinal repair weld in Section 5.

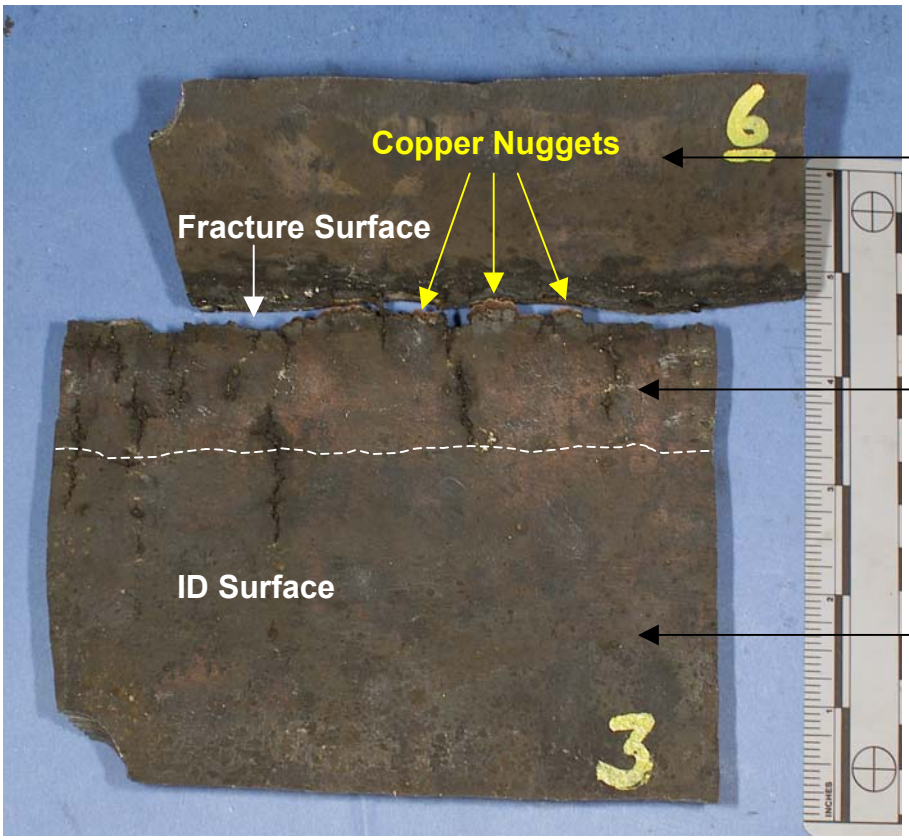

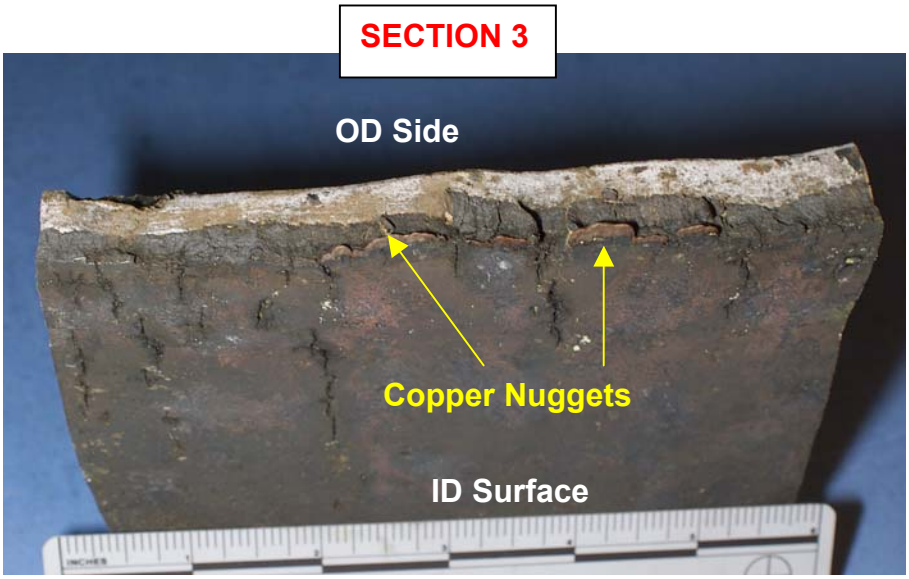

Figure 27: View of mating Sections 3 and 6 from the upper longitudinal weld of the header (upper image). The middle image is a view of the ID surface and fracture surface at an angle from Section 3 (weld and wrapper sheet side). The lower image is a straight-on view of the fracture surface of Section 3. The yellow arrows indicate where copper nuggets were observed and the white arrows in the lower image show the direction of propagation of the cracks.

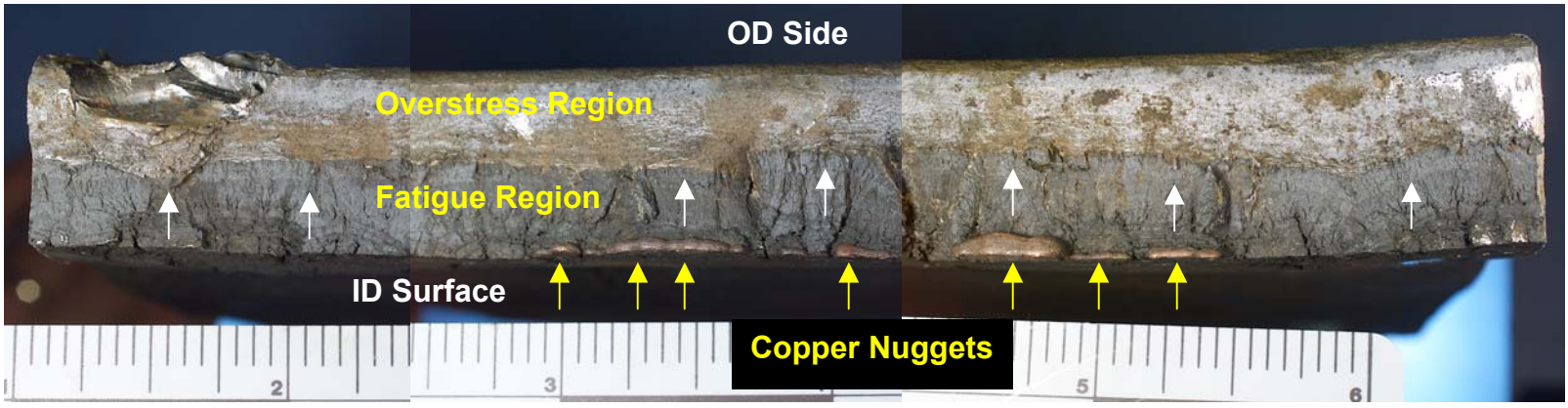

SECTION 6

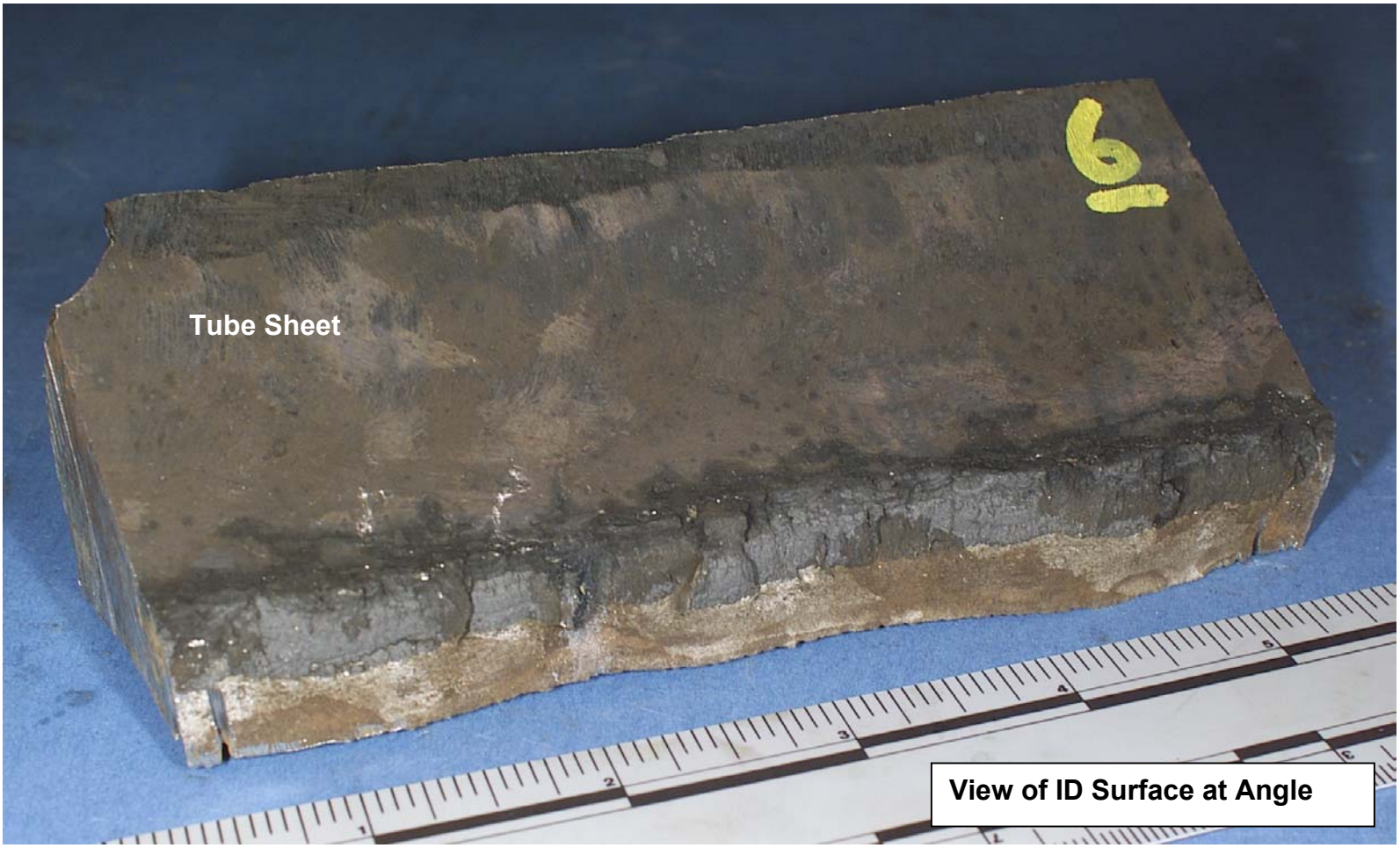

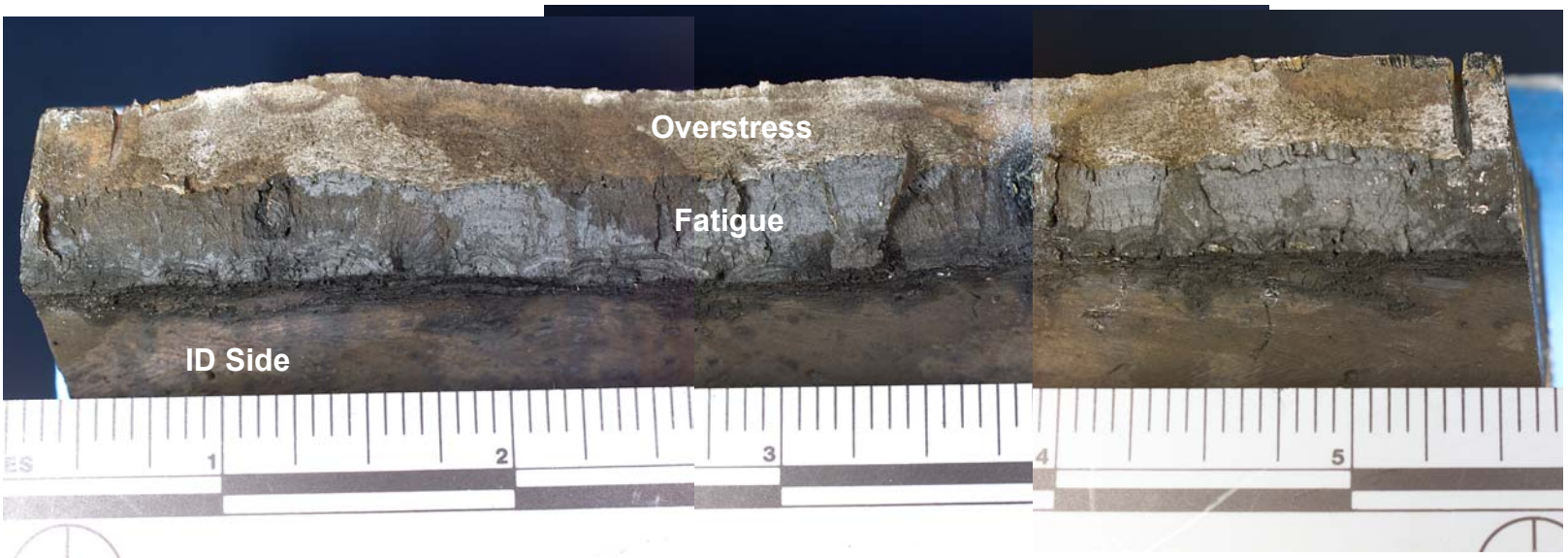

Figure 28: Views of the tube sheet fracture on Section 6 taken from the upper longitudinal weld of header 23. The upper image is a view of the fracture surface and ID surface at an angle, while the lower image is a more straight-on view of the fracture surface.

SECTION 3

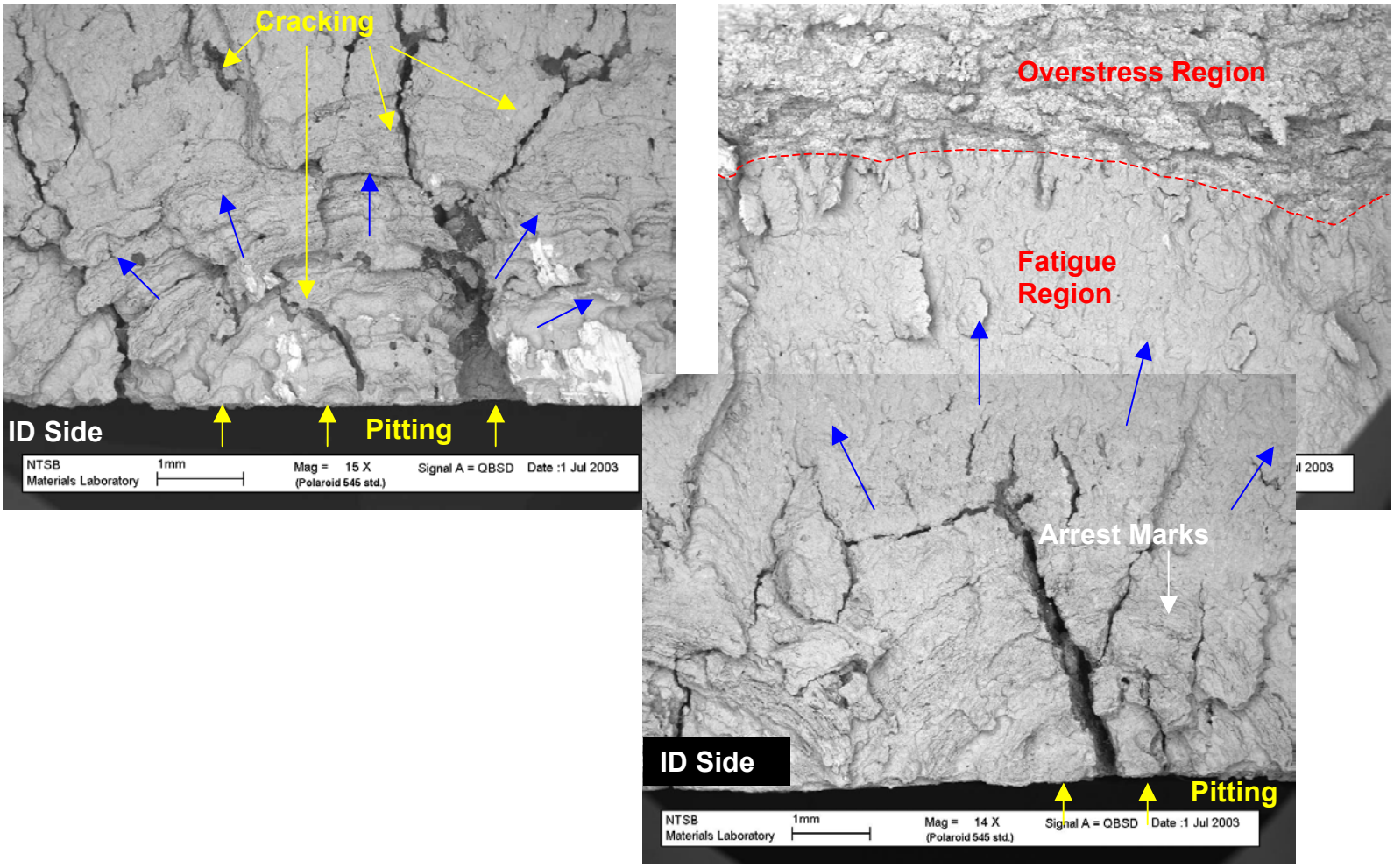

Figure 29: SEM images of the fracture surface of Section 3 near the ID surface.

SECTION 6

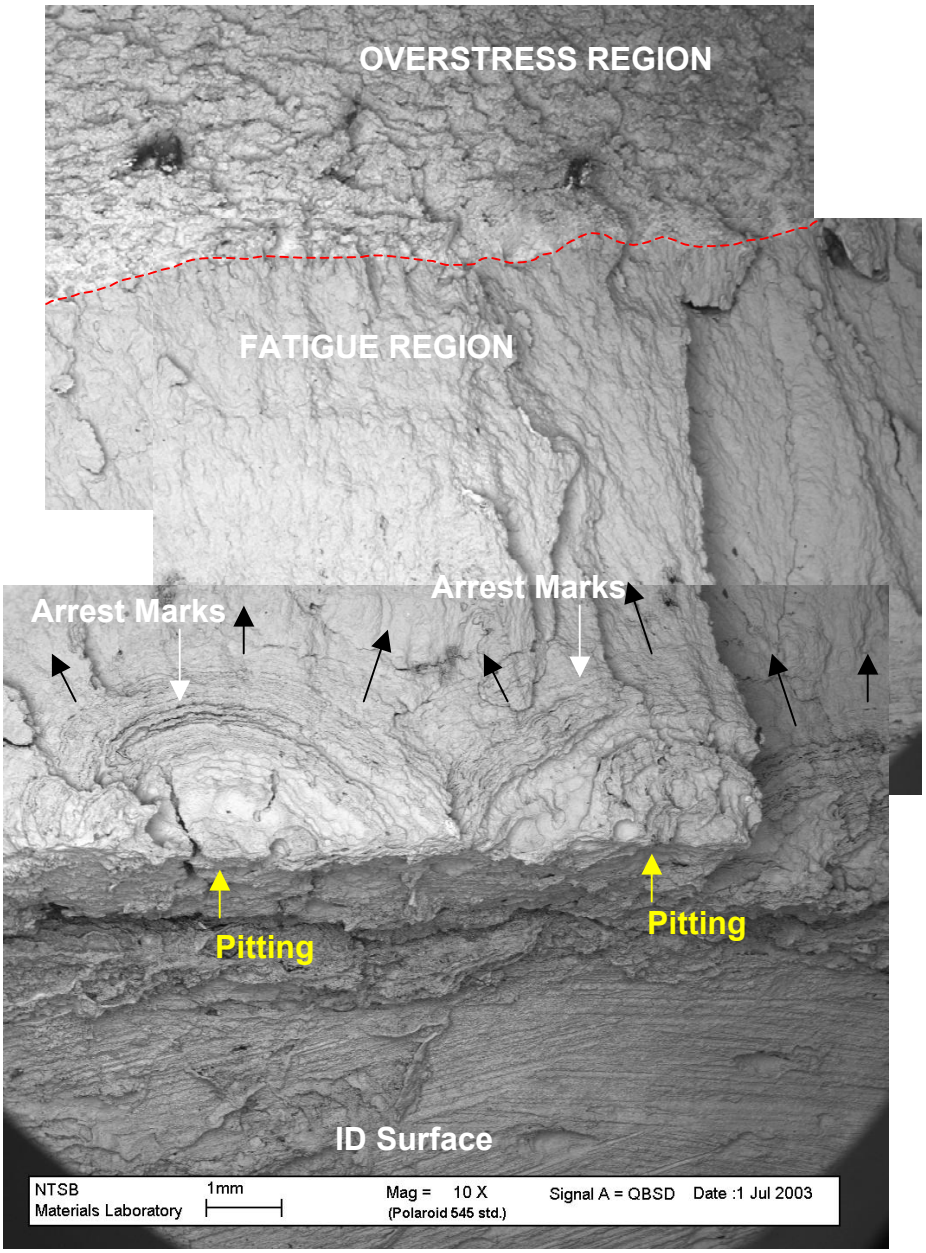

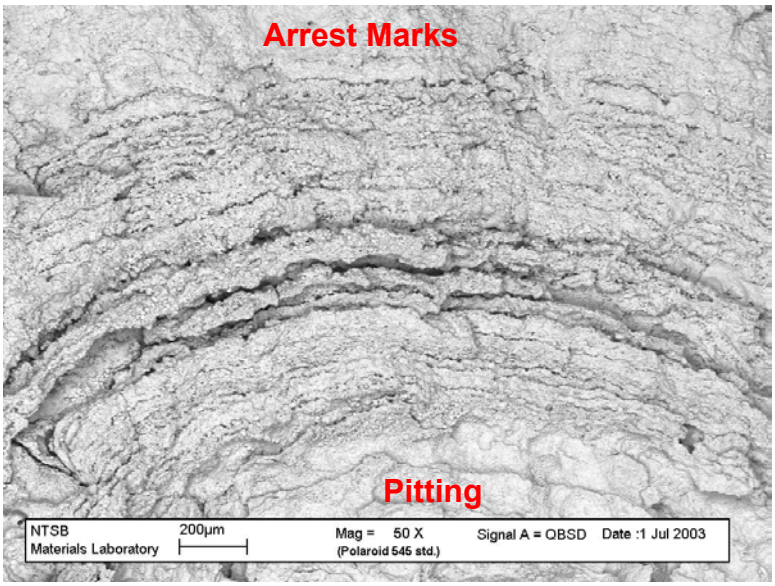

Figure 30: SEM montage of a region of the fracture surface from Section 6 (upper image). The lower image is a view of one of the origin areas near the ID surface at higher magnification.

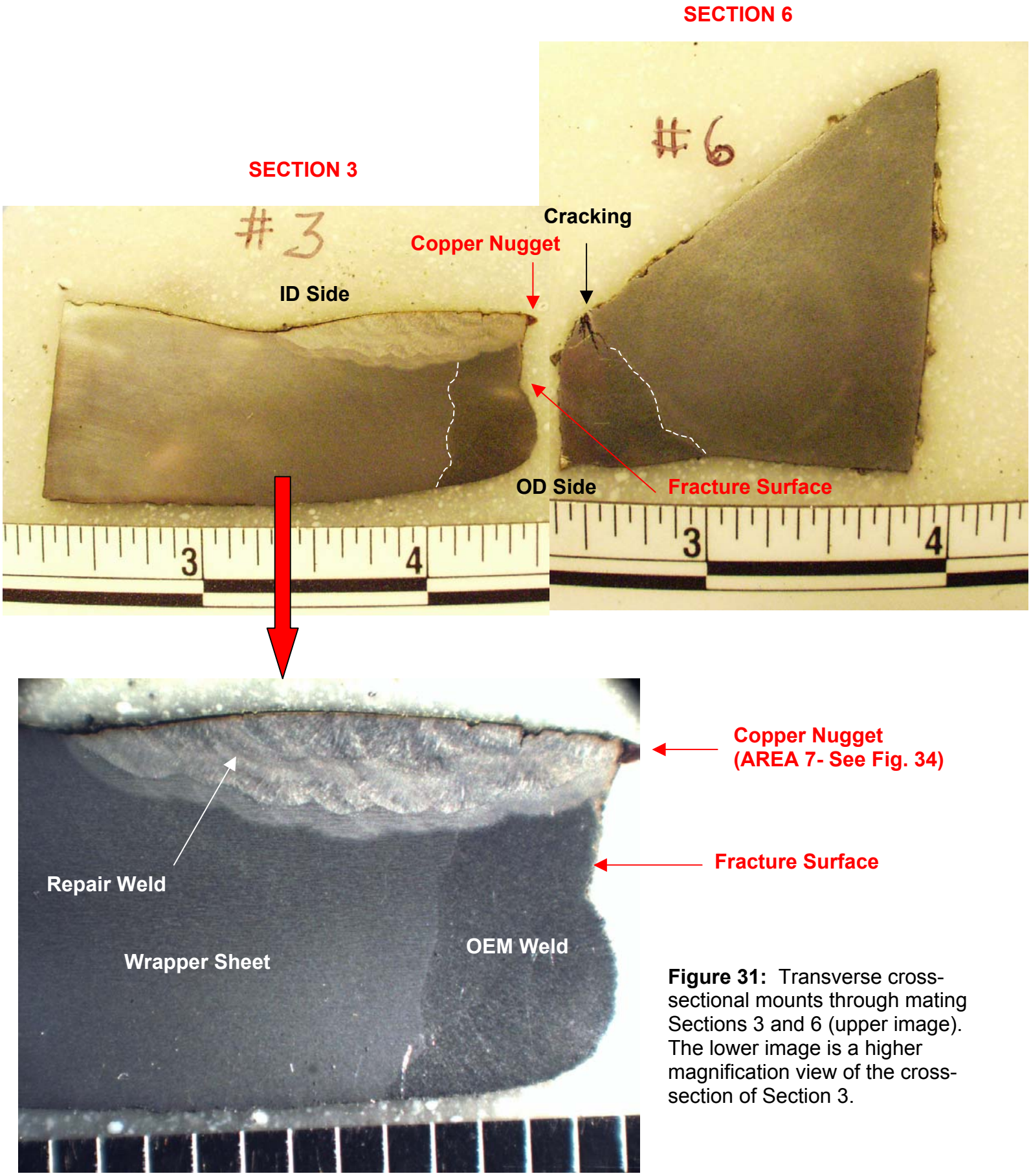

Figure 31: Transverse cross-sectional mounts through mating Sections 3 and 6 (upper image). The lower image is a higher magnification view of the cross-section of Section 3.

SECTIONS 3 & 6

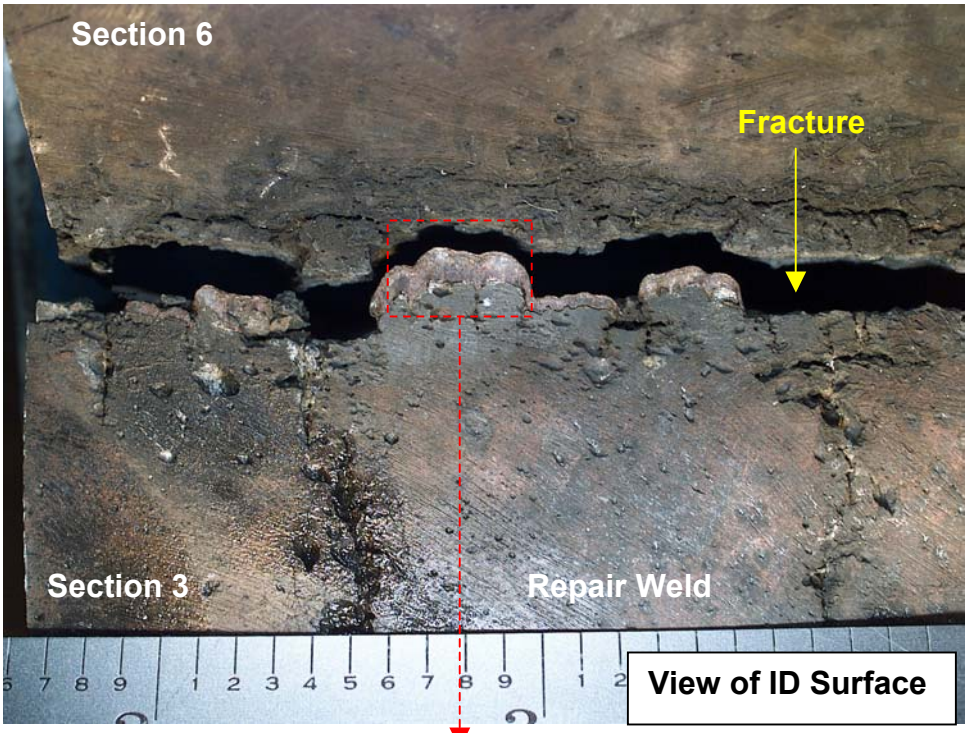

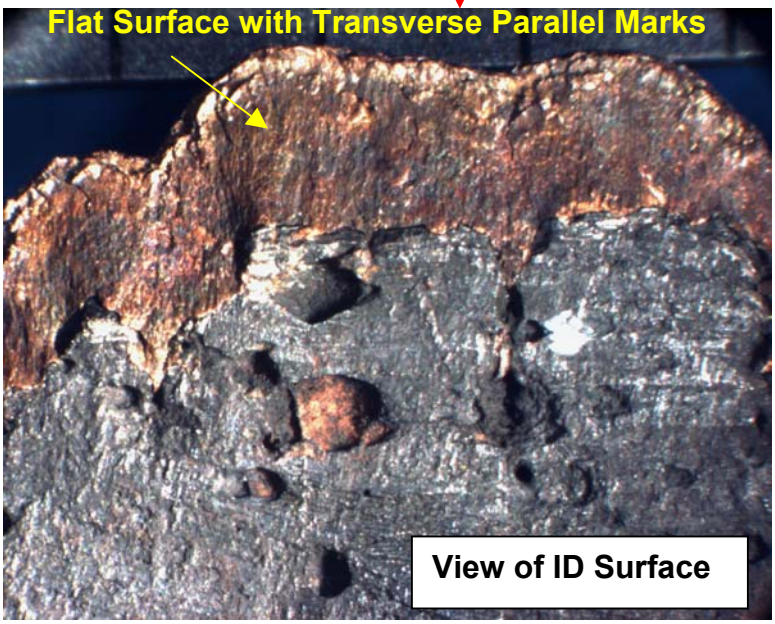

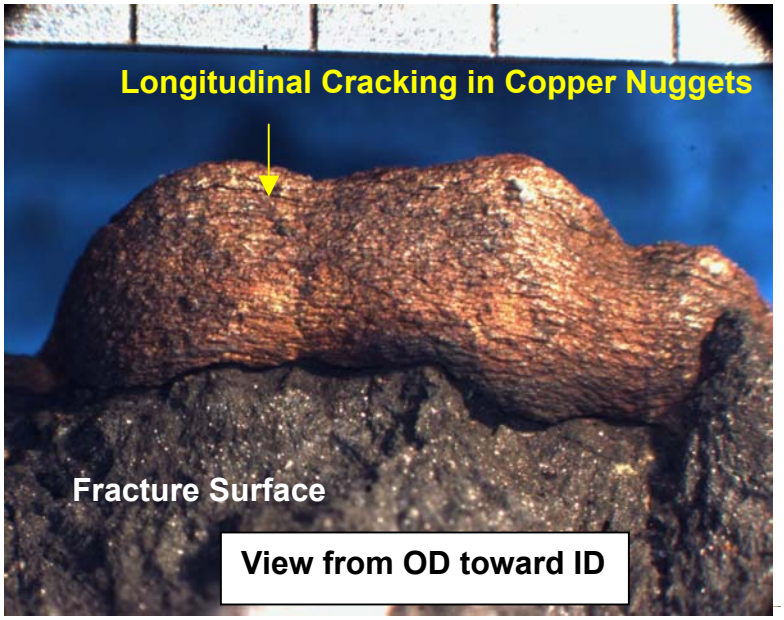

Figure 32: View of mating Sections 3 and 6 set next to each other as seen by looking at the ID surface (upper image). The middle left image is a view of the copper nuggets on the fracture as seen by looking at the ID surface. The middle right image is a view of the underside of the copper nuggets (interior to the crack) as seen by looking from the OD toward the ID. The lower image is a montage of the fracture surface of Section 3 in the area where copper nuggets were observed in Figure 27.

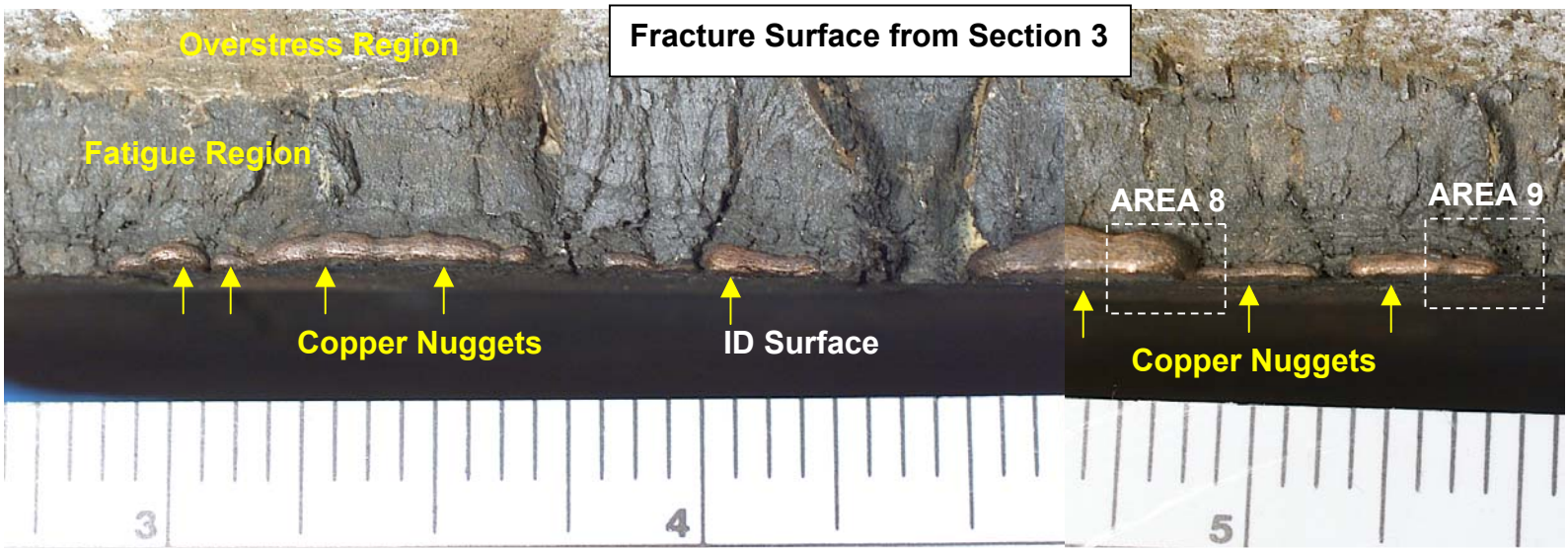

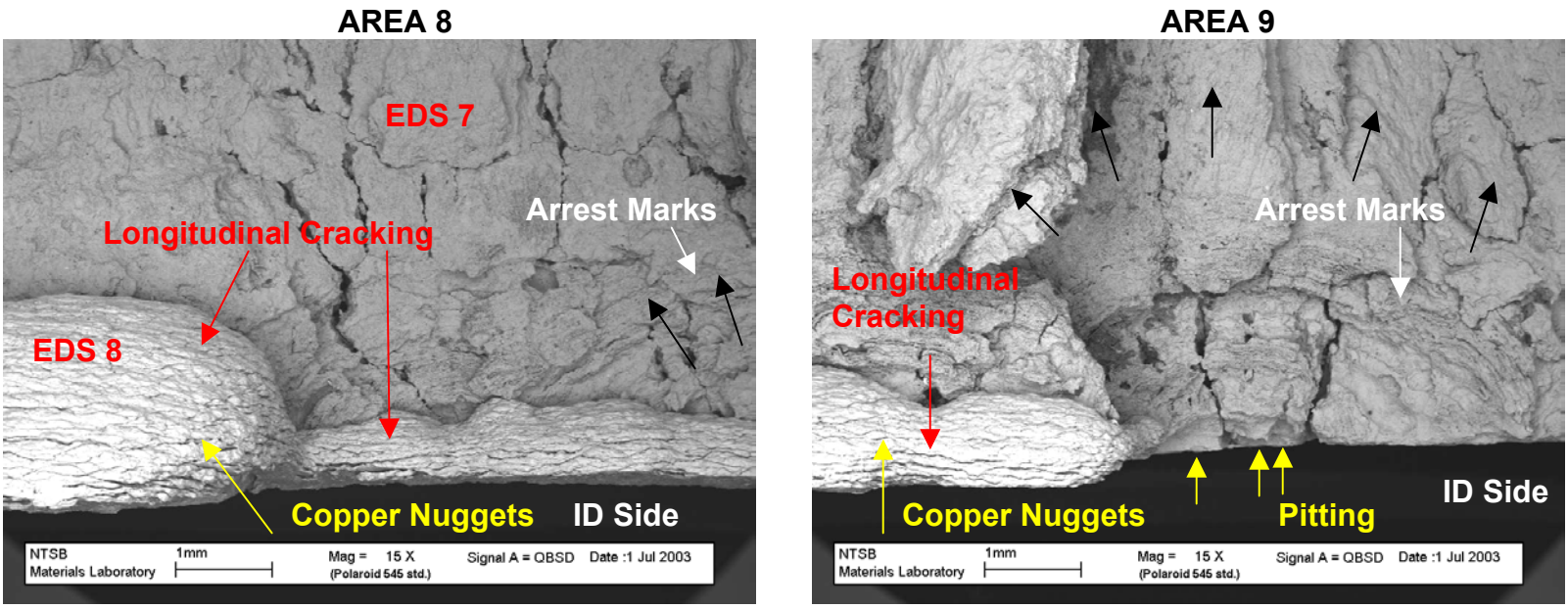

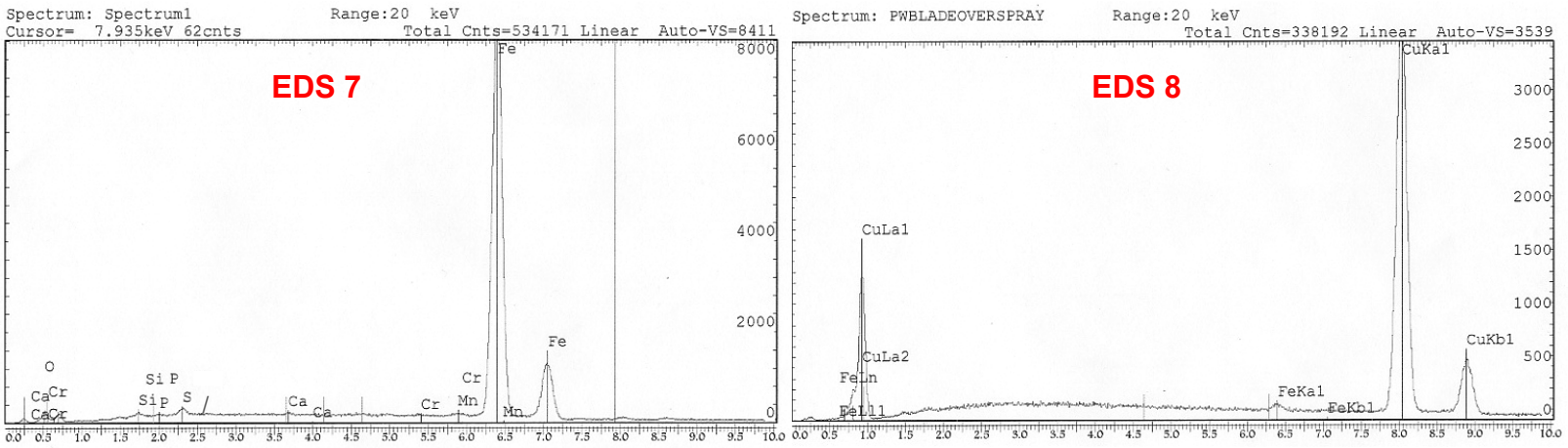

Figure 33: The top images are views of the copper nuggets on the fracture surface of Section 3 near the ID surface. The lower images are EDS spectra taken at the locations shown in the upper left image.

AREA 7- Copper Nugget from Section 3

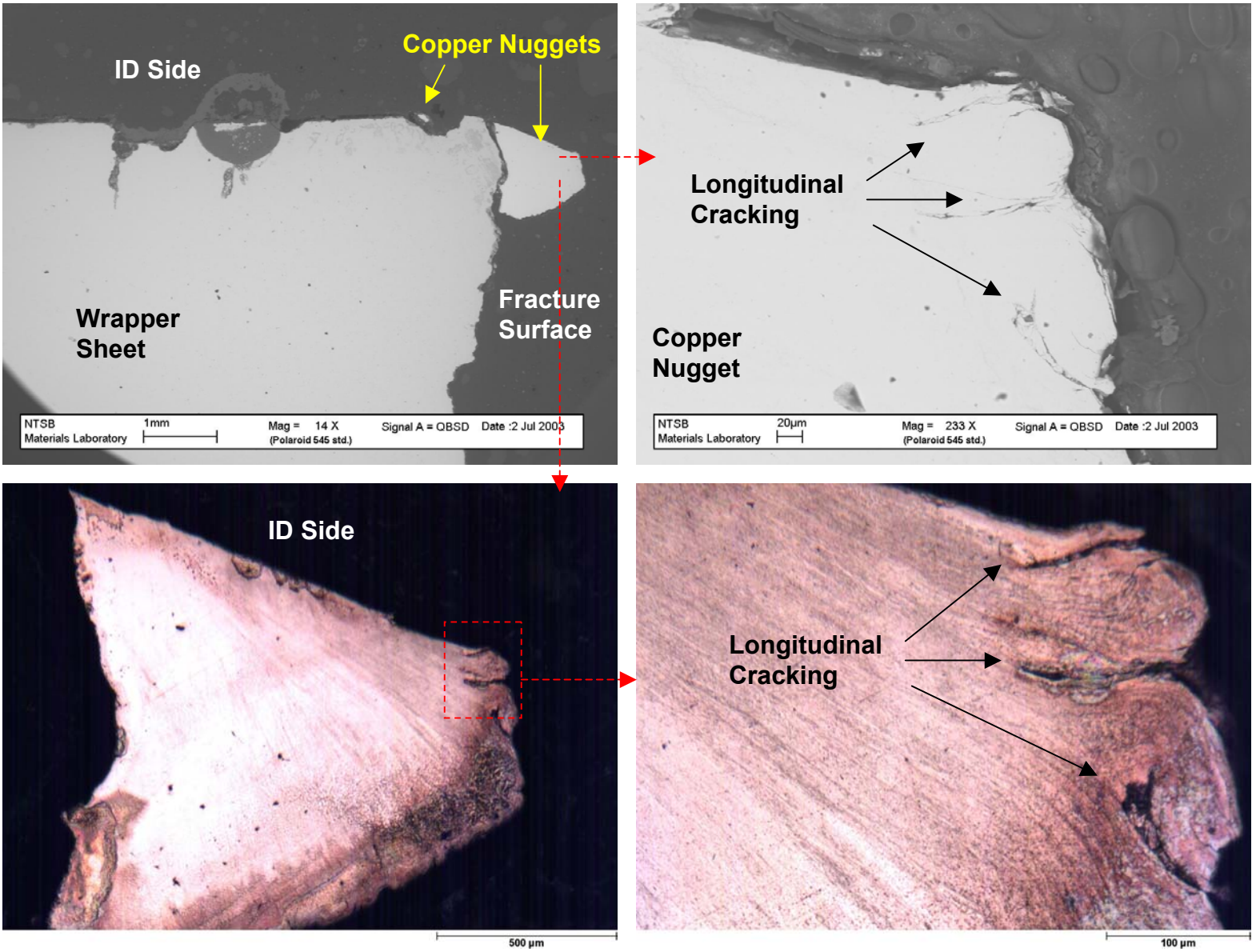

Figure 34: Varying magnification SEM views of the transverse cross-section of the copper nugget found on the fracture surface of Section 3 (top two images). The lower images are varying magnification optical micrographs of the same copper nugget.

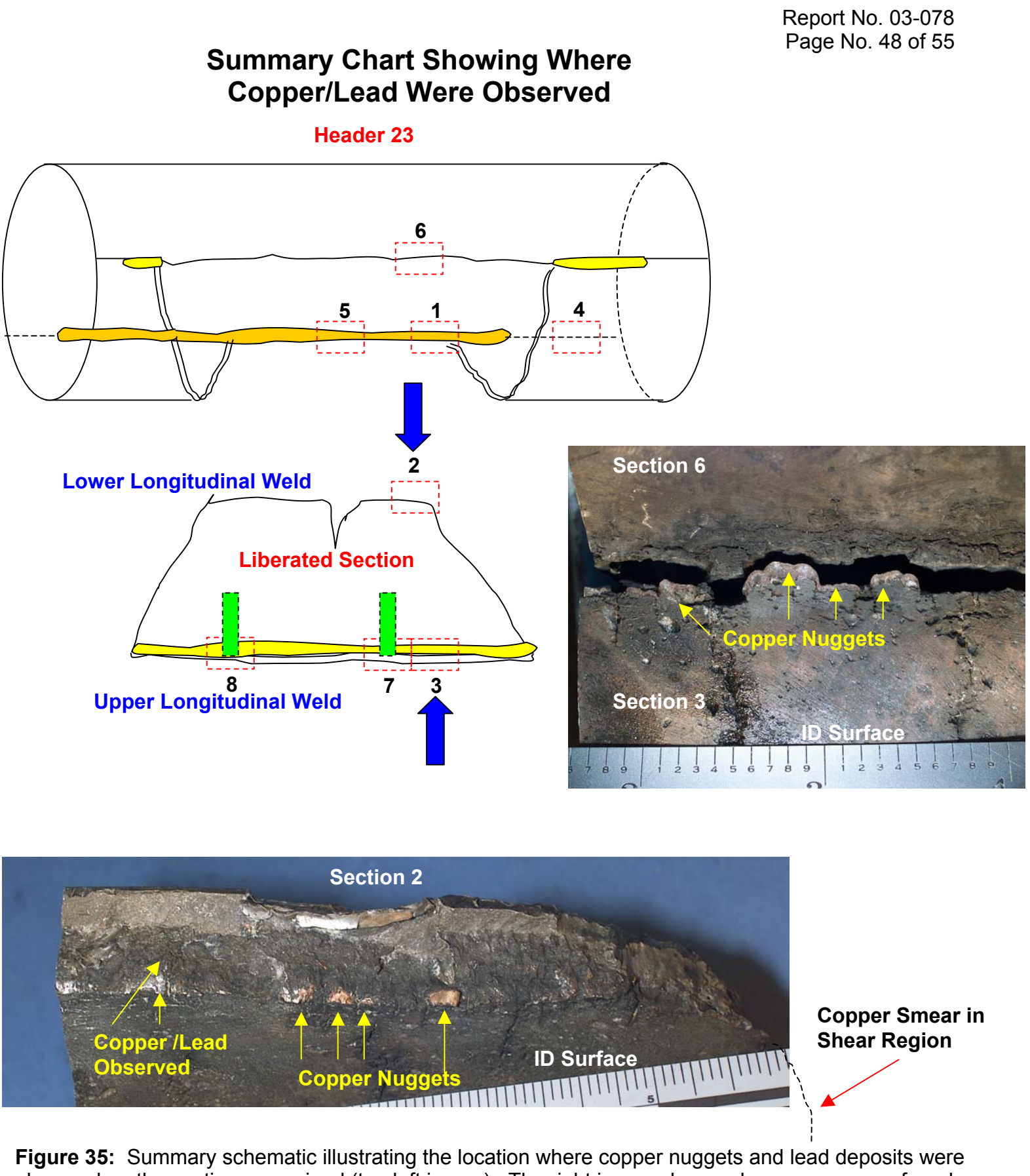

Figure 35: Summary schematic illustrating the location where copper nuggets and lead deposits were observed on the sections examined (top left image). The right image shows where copper was found on Section 3 and lower image shows where copper and lead were found on Section 2.

Laboratory Experiment

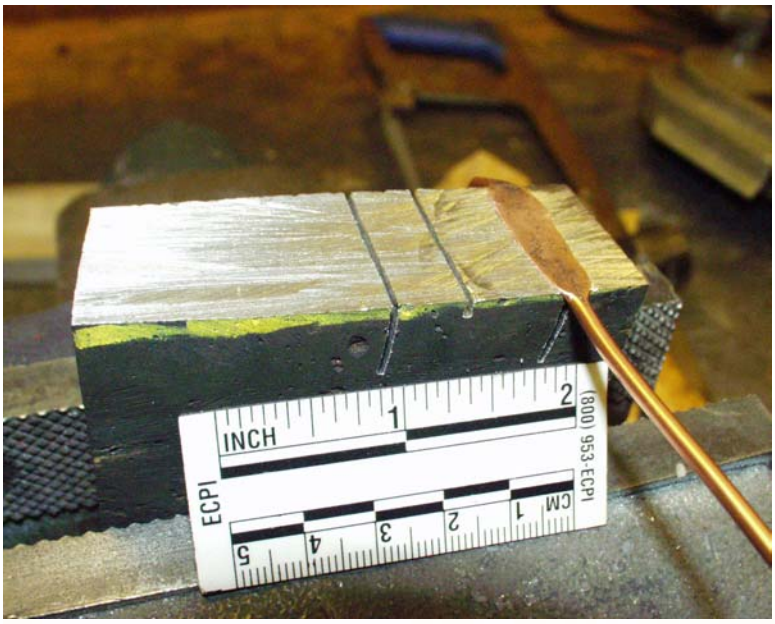

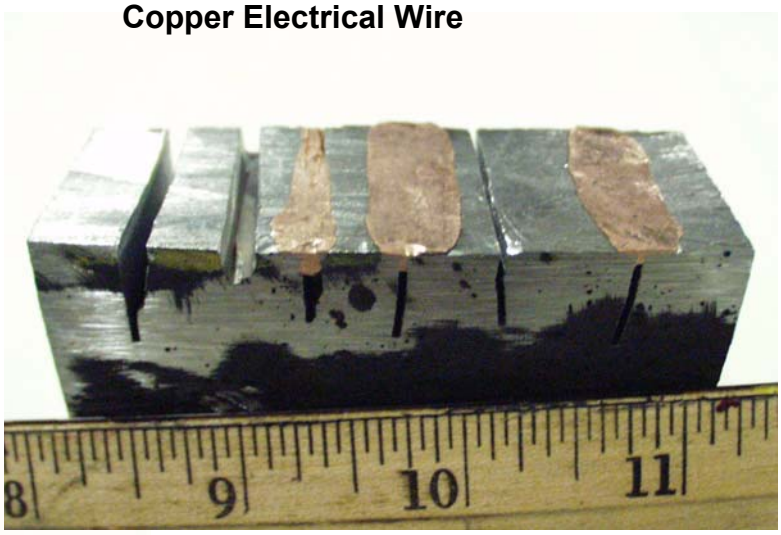

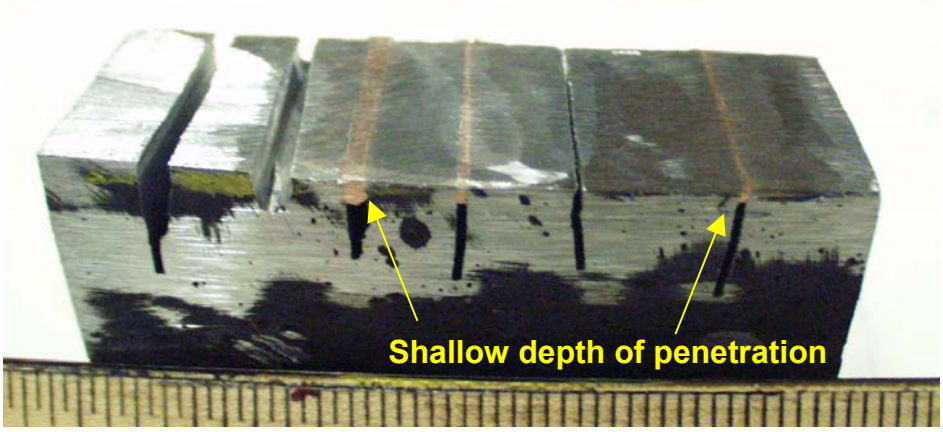

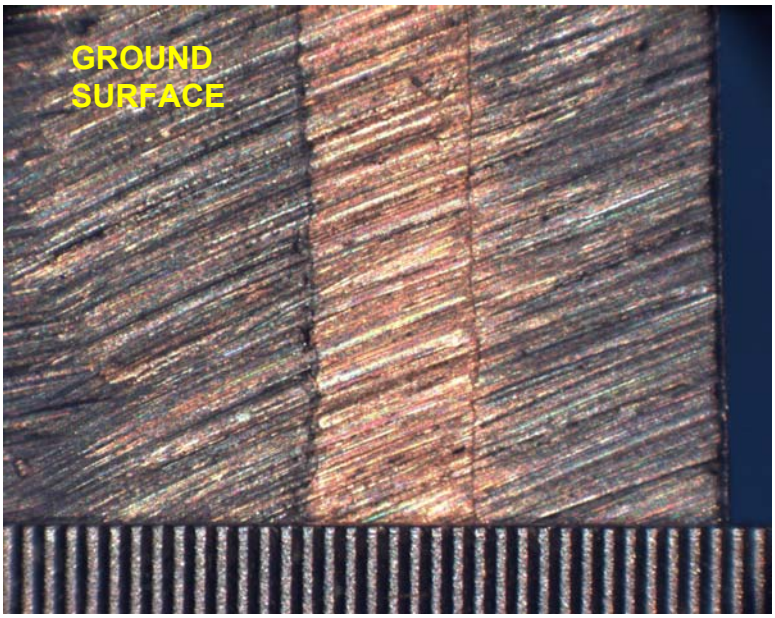

Figure 36: Images showing varying steps in an experiment performed in the lab. The top right images show how copper electrical wire looked after being hammered into a simulated crack. The middle image shows the profile of the cracks after hammering in the copper wire and grinding the surface flush. The lower image is a head-on view of one of the cracks filled with copper after grinding.

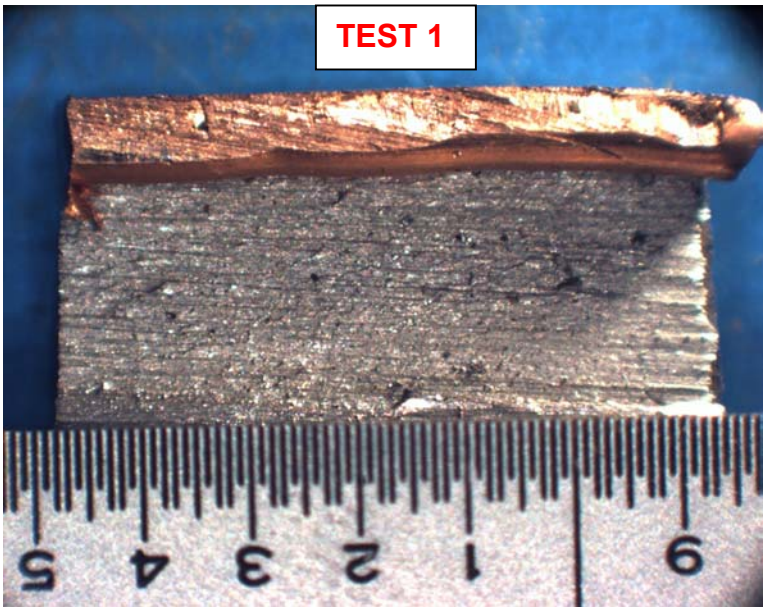

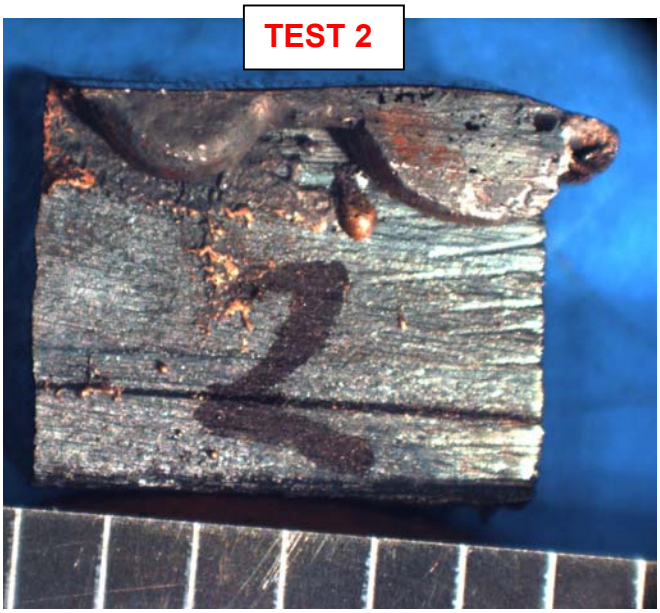

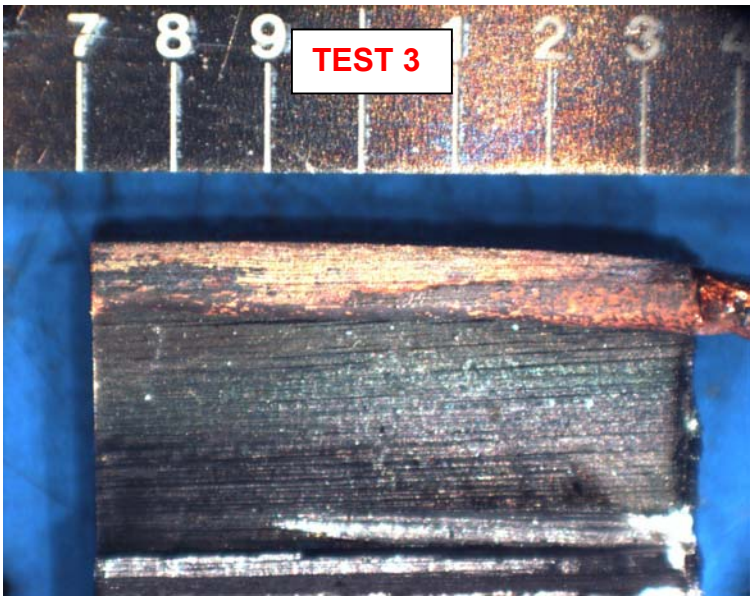

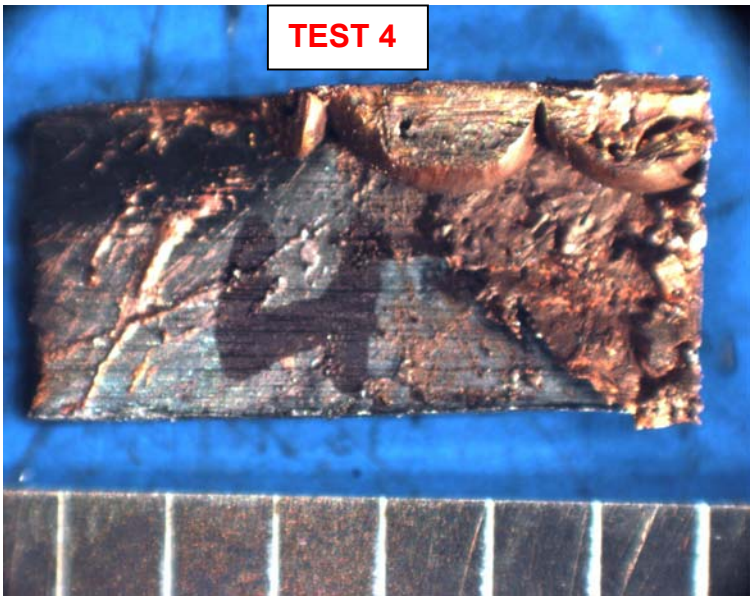

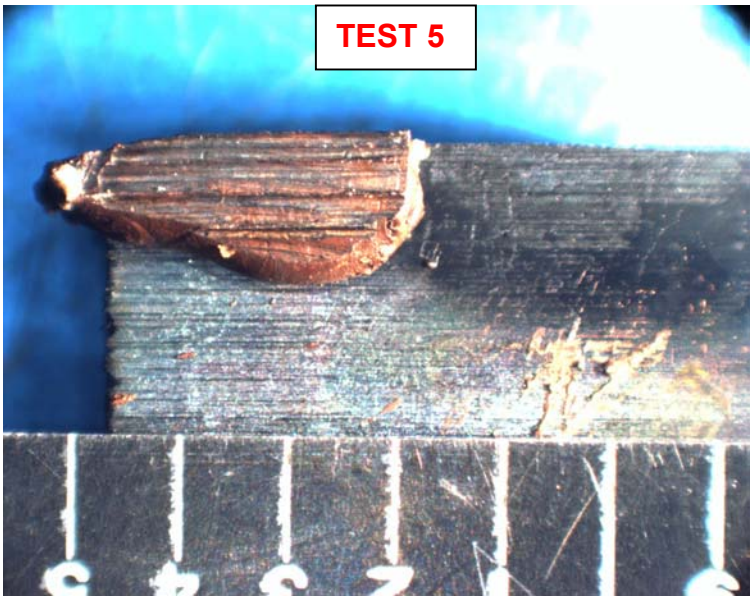

Figure 37: Copper wire forced into a simulated crack by varying methods. The images show the copper after the cracks were opened up in the lab. The following tests show how the copper was forced in to the simulated cracks:

Test 1- Hammered in copper wire (wrought)
Test 2- Heat base + melt in copper wire
Test 3- Hammered in copper wire + heat with torch
Test 4- Heat base metal, melt in copper wire + hammer copper when cool
Test 5- Heat base metal, melt in copper wire, and hammer copper while hot.

Wrought baseline and Test 1

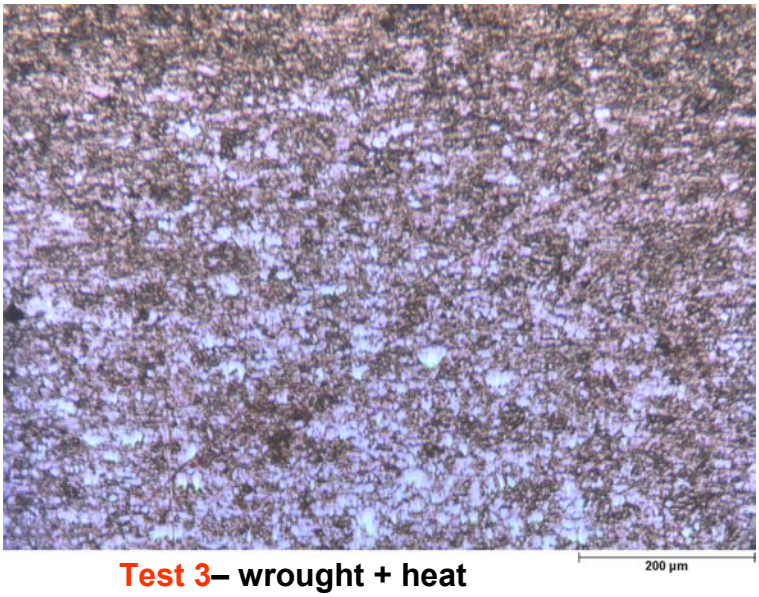

Test 2- Heat base + cast in

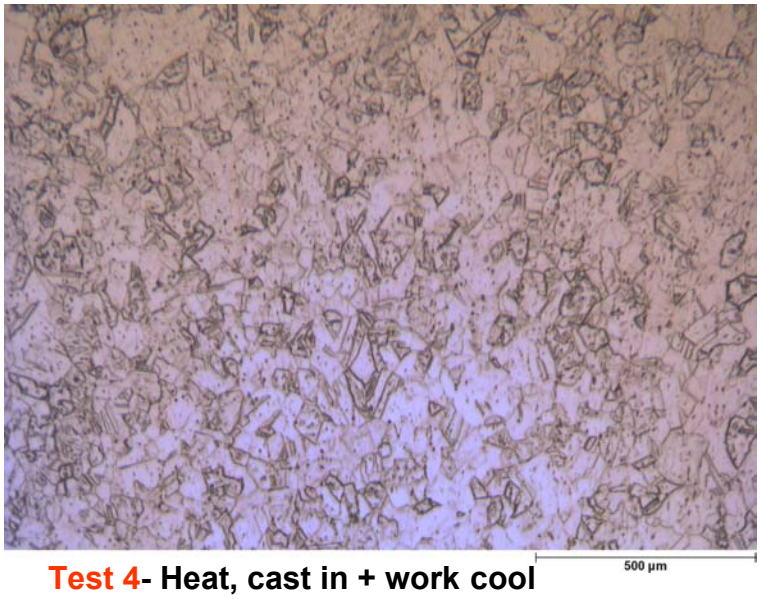

Test 3– wrought + heat

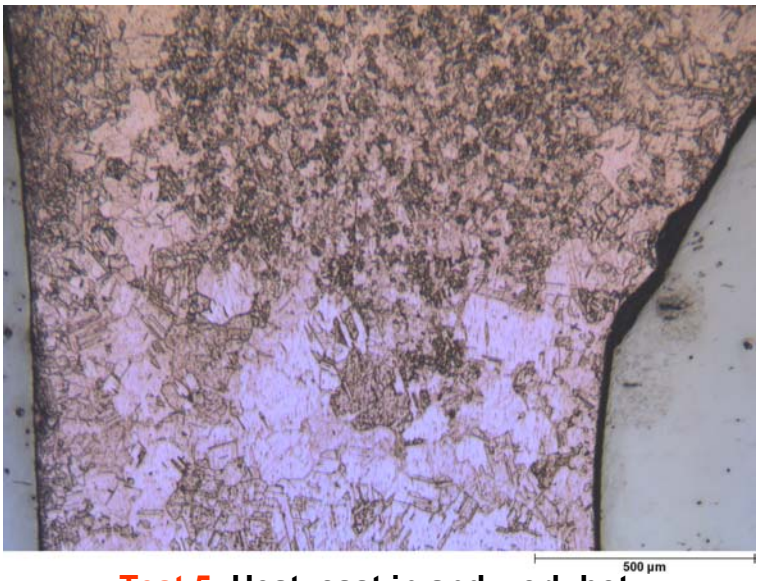

Test 4- Heat, cast in + work cool

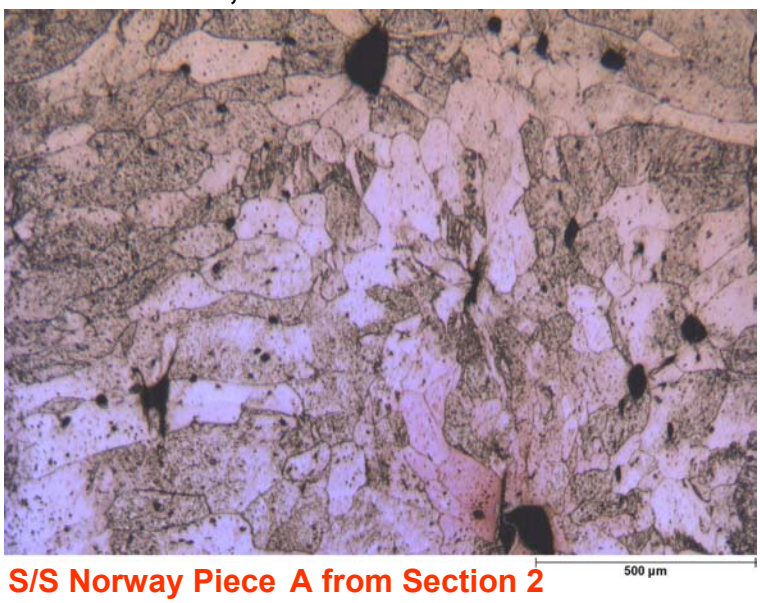

Test 5- Heat, cast in and work hot

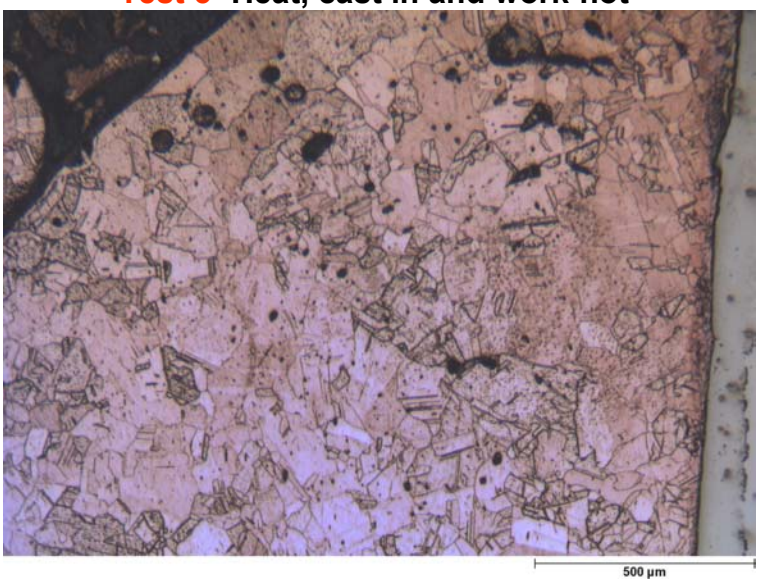

S/S Norway Piece A from Section 2

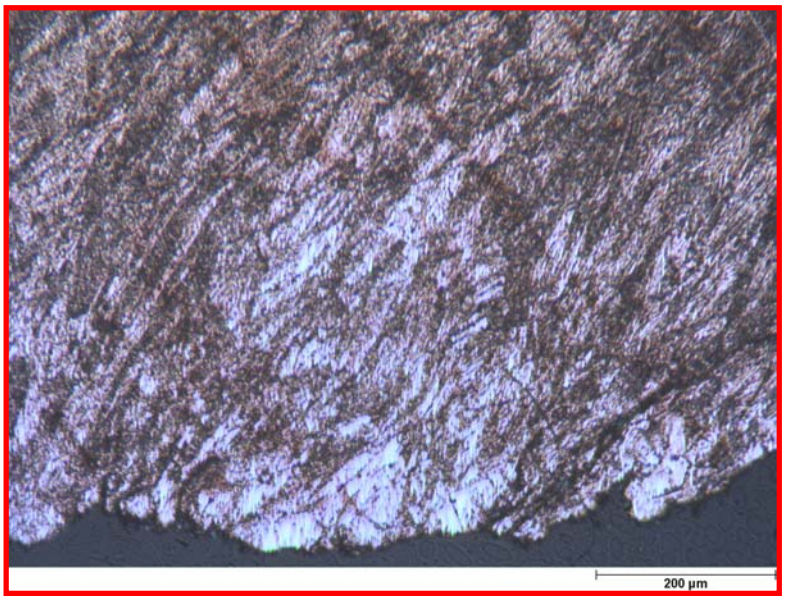

Figure 38: Laydown cross-sectional micrographs of the test specimens from Figure 37 and a comparison lay-down mount of Piece A from Section 2 from the S/S Norway.

Copper Refrigeration Line

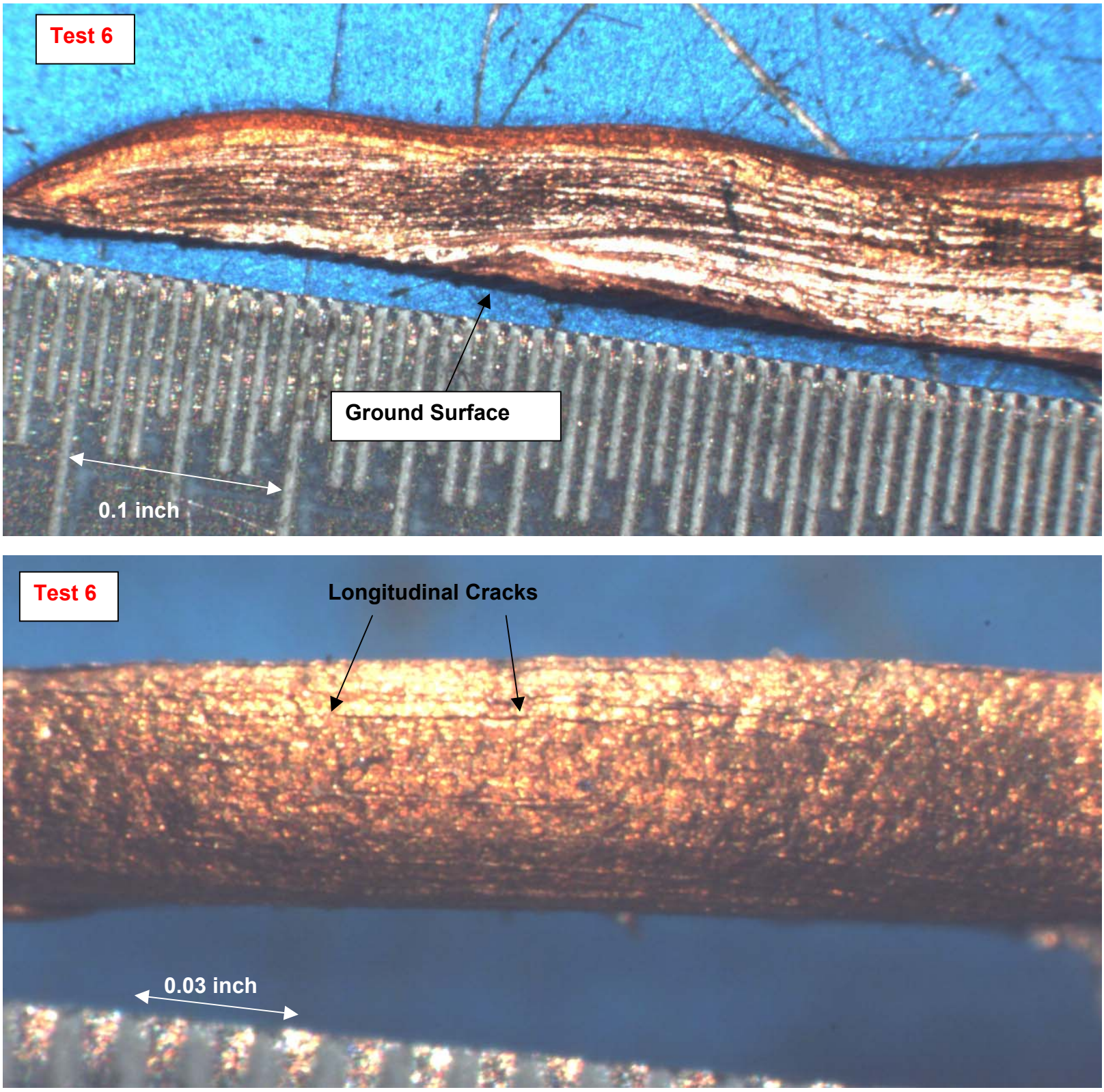

Figure 39: Varying magnification views of copper refrigeration line after having been hammered into a simulated crack, ground on the exposed surface, and removed from the crack.

Copper Refrigeration Line

Hammered Refrigeration Line

S/S Norway Piece A from Section 2

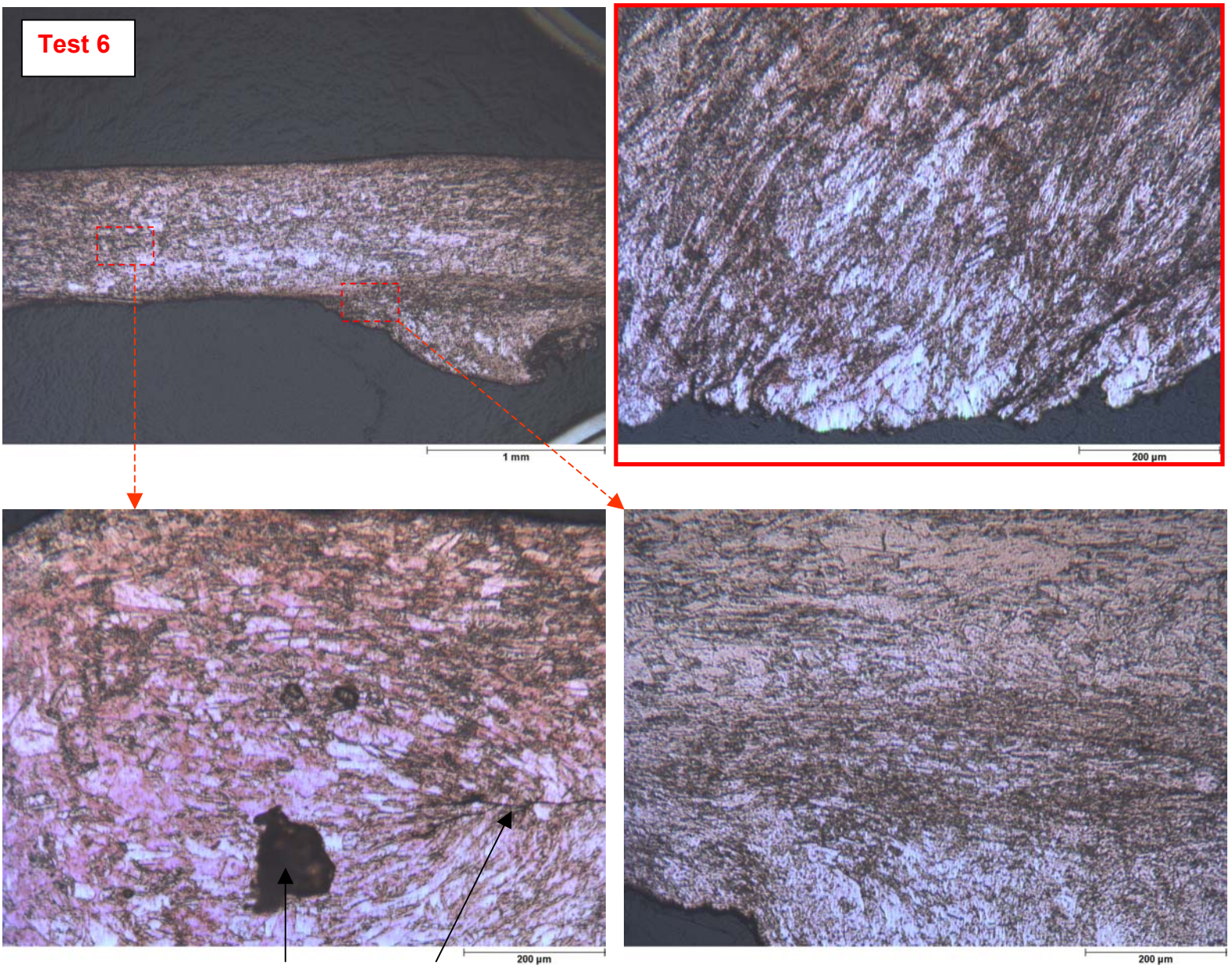

End of Lap, not Porosity

Lap from collapsing tube

Figure 40: Longitudinal micrographs at varying locations and magnifications of a section of copper refrigeration line that was hammered into a simulated crack (see Figure 39). A comparison microstructure from Piece A taken from Section 2 on the S/S Norway is shown in the top right image.

Appendix A

STORK® Materials Technology

Stork Materials Testing & Inspection

Material Testing and Non-Destructive Testing

15062 Bolsa Chica
Huntington Beach, CA 92649
USA

Telephone : (714) 892-1961
Telefax : (714) 892-8159
Website : www.storksmti.com

Contact: ROSSEY WILLIAM
National Transportation Safety
490 L'Enfant Plaza East, S.W.
WASHINGTON, DC 70594

Date: 7/30/2003 **P.O. No.:** PR44000246 **W/O No.:** NAT145-07-29-09850-1

TEST CERTIFICATE

*****ADDITIONAL TESTING 08/05/03*****

Desc.:	Steel Sample
Heat	N/S
Lot	N/S

CARBON STEEL

Element		repair weld	thin plate	original weld	thick plate
C	=	0.06	0.20	0.08	0.21
Mn	=	1.23	1.26	1.30	1.12
P	=	0.016	0.014	0.021	0.025
S	=	0.005	0.020	0.025	0.030
Si	=	0.32	0.19	0.42	0.23
Cr	=	0.03	0.11	0.04	0.09
Ni	=	0.04	0.15	0.08	0.12
Mo	=	0.51	0.66	0.18	0.46
Cu	=	0.04	0.15	0.10	0.14
V	=	0.016	0.077	0.024	0.074
Ti	=	0.016	0.002	0.005	0.029
H***	=	0.0001	0.0002	0.0002	0.0002
Fe	=	Balance	Balance	Balance	Balance

Chemical Analysis Performed by Optical Emission per SOP 2.02, Latest Revision

FOR INFORMATION ONLY

NADCAP NDT AND MATERIALS TESTING FASTENER TESTING

ACCREDITED CHEMICAL MECHANICAL FASTENERS

Respectfully submitted

Frank Nguyen
Chemical Laboratory Manager

REFERENCES

[1] Chantiers de L'Atlantique drawing number 930.381.1111.4.B (NTSB document D01).
[2] Documents covering the repairs of the boilers:
- Deutsche Babcock inspection report 18-8702-999 dated September 18, 1985 (NTSB D02).
- Lloyd Werft Bremerhaven working instructions written by Deutsche Babcock dated October 26, 1987 (NTSB D03).
- Bureau Veritas survey report covering period September 7 through 23, 1987 (NTSB D04).
- Kloster Cruise Limited interoffice memorandum dated October 8, 1987 (NTSB D05).
- Bureau Veritas survey report covering period November 7 through 21, 1987 (NTSB D06).
- Bureau Veritas survey report covering period September 3 through October 2, 1990 (NTSB D07).
- Deutsche Babcock repair document 18-9790-999, dated February 18, 1988 (NTSB D08).
- Deutsche Babcock repair document 94-8351-998, September 1990 (NTSB D09).
- Bureau Veritas survey covering the periods September 2 through 24, 1984 (NTSB D010).
- Bureau Veritas survey covering the periods April 14 through July 5, 1982 (NTSB D011).

[3] Water chemistry literature:
- "Metal Passivation," Bulletin MKB-001-01, form TP112870;1, Ashland Specialty Chemical Company-Drew Marine Division (NTSB D012).
- "Questions and Answers: Oxygen Scavengers," Nalco Chemical Company, Bulletin 116 (NTSB D013).
- Drew Marine Division, "Shipboard Water Treatment Manual," 4.1 Edition, document number TM-WT-1, dated 11/01, revision 7, page 16 (NTSB D014).
- Naval Ships' Technical Manual, Chapter 221, Boilers, Section 12- Corrosion, document S9086-GY-STM-010/CH-221R3

[4] Engineering & Inspections Unlimited, Inc. non-destructive testing inspection report FS-03-239 (NTSB D015).
[5] See NTSB document D010 listed above.
[6] Bureau Veritas e-mail/fax dated October 27, 1987(NTSB D016).
[7] NTSB document D09 in footnote, page 2
[8] 2001 American Society of Mechanical Engineers (ASME) Boiler and Pressure Vessel Code, Section 2, Part A: Ferrous Material Specifications, Specifications SA-20 (general specification for pressure vessel steels) and SA-516 (specification for pressure vessel plates, carbon steel, for moderate- and lower- temperature service). The maximum molybdenum content is contained in Table 1 of specification SA-20.